

UNCLASSIFIED

AD NUMBER
AD802419
NEW LIMITATION CHANGE
TO Approved for public release, distribution unlimited
FROM Distribution: Further dissemination only as directed by Army Engineer Research and Development Lab., Fort Belvoir, VA 22060, AUG 1966, or higher DoD authority.
AUTHORITY
USAMERDC ltr, 11 Jul 1993

THIS PAGE IS UNCLASSIFIED

Each transmittal of this document outside the agencies of the U. S. Government must have prior approval of Commanding Officer, Army Engineer Research & Development Labs, Fort Belvoir, Va. 22090  
Cu

## HIDDEN OBJECT DETECTION BY MAGNETOABSORPTION AND INDUCTION METHODS

John P. Claassen  
William L. Rollwitz

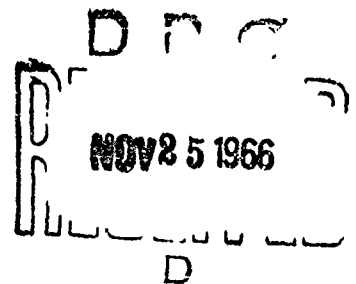
**FINAL TECHNICAL REPORT**  
Contract No. DA-44-009-AMC-1205(T)  
Period Covered: June 1965 - June 1966

Prepared for

**Barrier and Intrusion Detection Division**  
**U. S. Army Engineer Research and Development Laboratories**  
**Fort Belvoir, Virginia**

Sponsored by

**Advanced Research Projects Agency**  
**Washington, D. C.**  
**ARPA Order No. 688**



**SOUTHWEST RESEARCH INSTITUTE**  
SAN ANTONIO HOUSTON

802419

SOUTHWEST RESEARCH INSTITUTE  
8500 Culebra Road, San Antonio, Texas 78206

Department of Instrumentation Research

HIDDEN OBJECT DETECTION BY MAGNETOABSORPTION  
AND INDUCTION METHODS

John P. Claassen  
William L. Rollwitz

FINAL TECHNICAL REPORT  
Contract No. DA-44-009-AMC-1205(T)  
Period Covered: June 1965-June 1966

Prepared for

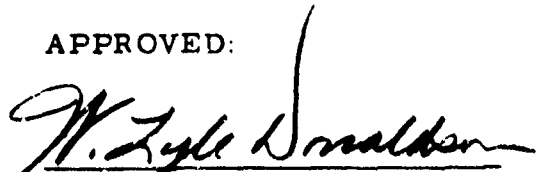
Barrier and Intrusion Detection Division  
U. S. Army Engineer Research and Development Laboratories  
Fort Belvoir, Virginia

Sponsored by

Advanced Research Projects Agency  
Washington, D. C.  
ARPA Order No. 688

Program Code No. 5730  
Contract Date: 23 June 1965  
Contract Amount: \$49,973  
Expiration Date: 22 August 1966  
Project Engineers: John P. Claassen and  
William L. Rollwitz, 512-OV 4-2000

APPROVED:



W. Lyle Donaldson, Director  
Department of Instrumentation  
Research

## NOTICE PAGE

When Government drawings, specifications or other data are used for any purpose other than in connection with a definitely related Government procurement operation, the United States Government thereby incurs no responsibility nor any obligation whatsoever; and the fact that the Government may have formulated, furnished, or in any way supplied the said drawings, specifications, or other data is not to be regarded by implication or otherwise as in any manner licensing the holder or any other person or corporation, or conveying any right or permission to manufacture, use or sell any patented invention that may in any way be related thereto.

**DDC Availability Notice:** U. S. Military Agencies may obtain copies of this report directly from DDC. Other qualified DDC users should request through Commanding Officer, USAERDL, Fort Belvoir, Virginia.

## PREFACE

This report was prepared by John P. Classen and William L. Rollwitz, Project Engineers, of the Electronics and Electrical Engineering Division of Southwest Research Institute. The research was supported by the Advanced Research Projects Agency, Washington, D. C., and was monitored by the U. S. Army Research and Development Laboratories under Contract DA-44-009-AMC-1205(T). The project was administered under the direction of the Electrical Department of the Barrier and Intrusion Detection Division, USAERDL with Guy F. Origlio serving as the contract representative.

## SUMMARY

The work of this contract was: (1) to design, develop, and test a detector for buried nonmetallic objects using the magnetoabsorption detection method, and (2) to adapt the magnetoabsorption detection head so as to give both magnetoabsorption and induction signals useful for detection and identifying the composition of hidden objects. Consequently, the largest part of the effort was directed toward the design and construction: (1) of the detection head to be used for both problems, (2) the magnetoabsorption detection system with sufficient sensitivity for both soils and small objects, and (3) the electronic systems for obtaining the amplitude and phase of the desired harmonics.

These components were assembled in a laboratory test facility for mine detection studies. In the mine detector, the fundamental of the magnetoabsorption signal from the soil is coherently detected using as a reference signal the second harmonic of the magnetic bias. The usefulness of this method and the capability of the system, to detect mines buried 2 inches with a detector height of 1-3/4 inches, was demonstrated by a 35-percent decrease in signal when the detector crossed a mine buried in a box of soil in the laboratory. The percentage decrease in the detected signal, caused by the void made in the soil by the nonmetallic mine, remained constant as the height of the detection head varied from 2-1/2 inches down to zero. In this system, the direct induction signal was rejected by using a

double-D configuration in the detection coil and a high-pass filter in the marginal oscillator (Robinson Circuit) used for the magnetoabsorption detector. A frequency of 500 kilocycles was used for the marginal-oscillator, and the magnetic bias field was at a frequency of 55 cycles.

To obtain the magnetoabsorption and induction signals simultaneously, the double-D type of detection head was used with the marginal oscillator previously mentioned. Since the magnetoabsorption signal is a modulation of the amplitude of the radiofrequency (500 kc) marginal oscillator and the direct induction signal is at 55 cycles, the two signals were separated by filters. The high-pass filter mentioned previously made the detected output of the marginal oscillator the magnetoabsorption signal at a fundamental of 110 cycles. The low-pass filter gave the induction signal at a fundamental of 55 cycles. Lissajous patterns were made with the magnetoabsorption or direct induction signals on the vertical axis and the 55-cyclic bias field on the horizontal axis of the oscilloscope. Harmonic amplitudes were also made for each signal. A total of twenty-one objects were used which varied in sizes from a volume of 1 cubic foot to 1/32 cubic foot. The comparison of the Lissajous signals plus the harmonic analyses of each signal demonstrated that the combination of the amplitudes and phases of the harmonics of the magnetoabsorption and direct induction signals can be used both to detect the presence of hidden objects and to identify their composition.

## TABLE OF CONTENTS

	<u>Page</u>
LIST OF ILLUSTRATIONS	vii
LIST OF TABLES	xi
I. INTRODUCTION	1
II. SUMMARY OF RESULTS	3
A. Equipment	5
B. Magnetic-Void Buried-Object Detection	7
C. Discrete Object Detection and Identification	19
D. Influence of Object to Detector Distance	60
III. DISCUSSION	63
A. Electromagnetic Studies on Magnetic-Void and Discrete Object	63
B. Detection Head Assembly	70
C. Marginal Oscillators	80
D. Equipment for the Magnetic-Void Detection in Soils	88
E. Equipment for Discrete Object Detection and Identification	90
F. Equipment Development	94
IV. CONCLUSIONS	105
A. Magnetic-Void Detector	105
B. Discrete Object Detection and Identification	106
V. RECOMMENDATIONS	108
A. Magnetic-Void Detection	108
B. Discrete-Object Detection and Identification	108
REFERENCES	109



## LIST OF ILLUSTRATIONS

<u>Figure</u>		<u>Page</u>
1	Block Diagram of the Equipment Developed for the Magnetic-Void, Buried-Object Magnetoabsorption System	4
2	Powered Dolly with Detector Mounted, Solid-State System Shown in Background	5
3	Soil Magnetoabsorption Signals Obtained: (a) at the Surface and (b) with 1.5 Inches Separation	7
4	One Scan Cycle of the Box When No Mine Is Present. The Detector Is Mounted 1-Inch above the Soil.	9
5	One Scan Cycle over a Mine Flush with the Surface. The Detector Height Is 1-Inch above the Top of the Soil.	10
6	One Scan Cycle with Mine Buried One Inch. The Detector Height Is 1-Inch above the Soil.	11
7	One Scan Cycle with Mine Buried Two Inches. The Detector Height Is 1-Inch above the Soil Surface	12
8	Linear Graph of the Signal Amplitude as a Function of Detector Coil Height with No Buried Object	14
9	Semilog Graph of the Signal Amplitude as a Function of Detection Coil Height with No Buried Object	15
10	Graph of the Percentage Change in the Amplitude of the Magnetoabsorption Signal Caused by a Buried Magnetic Void. Data Are Shown for Detection Head Heights of 1/2, 3/4, 1, 1-1/4, 1-1/2, and 1-3/4 Inches	16
11	Variations of Percent Signal Deviation with Detection Head Height for Magnetic-Void Depths of 2, 1 and Zero Inches (Level with Surface)	18

## LIST OF ILLUSTRATIONS (CONT'D)

<u>Figure</u>		<u>Page</u>
12	Block Diagram of the Discrete Object Detection and Identification Laboratory Test System	20
13a	Channel Iron	22
13b	Harmonic Amplitudes from Channel Iron	23
14a	Angle Iron	24
14b	Harmonic Amplitudes for Angle Iron	25
15a	Copper Tubing	27
15b	Harmonic Amplitude Curves for Copper Tubing	28
16a	BX Electrical Cable	29
16b	Harmonic Amplitudes from Type BX Electrical Conduit	30
17a	Thin-Wall Electric Conduit	31
17b	Harmonic Amplitudes for Thin-Wall Electric Conduit	32
18a	Standard Electrical Outlet Box Switch	34
18b	Harmonic Amplitudes for an Electrical Outlet Box	35
19a	Toggle Bolt	36
19b	Harmonic Amplitudes for a Toggle Bolt	37
20a	Standard Single Pole Switch	39
20b	Harmonic Amplitudes for a Standard Electrical Switch	40
21	Star Bolt (Brass Bolt, Lead Sheath)	41
22	Lead Tubing	41

LIST OF ILLUSTRATIONS (CONT'D)

<u>Figure</u>		<u>Page</u>
23a	Plaster Metal Lath	42
23b	Harmonic Amplitudes for Metal Lath	43
24a	Microphone (Aluminum Encased)	45
24b	Harmonic Amplitudes for an Aluminum-Encased Microphone	46
25a	Microphone (Knowles Electronic Model BE 1530)	48
25b	Harmonic Amplitudes for a Knowles Microphone	49
26a	Ferrite Rod	50
26b	Harmonic Amplitude for a Ferrite Rod	51
27a	Miller Choke Ferrite Core (4200 Series)	52
27b	Harmonic Amplitudes for an Iron Core Choke	53
28a	Solid-State Preamplifier	55
28b	Harmonic Amplitudes for a Transistorizer Preamplifier	56
29	Mercury Cell	57
30a	PC Oscillator	58
30b	Harmonic Amplitudes for a Printed Circuit Oscillator	59
31	The Variations of the Magnetoabsorption Signal with Object Height	62
32	Magnetic Bias Field Coil Form	72
33	11-1/2-Inch Double-D RF Coil Form	74
34	Quality Factor Variations with Frequency for 11-1/2- Inch Double-D Coil	74

## LIST OF ILLUSTRATIONS (CONT'D)

<u>Figure</u>		<u>Page</u>
35	A Demonstration Model Mone Detector Head with Mounting Bracket	76
36	The Relative Field Variation of Horizontal and Vertical Components at and above 11-1/2 Inch Double-D Coil	76
37	10-5/8-Inch Double-D RF Coil Form	78
38	Quality Factor Variations with Frequency for 10-5/8-Inch Double-D Coil	78
39	Detector Head with Shielding Exposed	79
40	The Rollins' Circuit for Magnetoabsorption Detection	80
41	Robinson Marginal-Oscillator Employing a Bipolar Transistors Limiter	84
42	Solid-State Robinson Type Marginal-Oscillator Employing a Diode Limiter	84
43	First Harmonic Output as a Function of Input for a Limiter	86
44	Block Diagram of the Magnetoabsorption Magnetic- Void Detector	89
45	Basic Block Diagram of the Hidden Object Detector Composed of a Magnetoabsorption and an Induction Detector	91
46	Schematic Representation of the Outputs Available for Obtaining a Fingerprint or Identifying Signal for Hidden Objects	93
47	Detector-Amplifier	96
48	Amplifier	96

## LIST OF ILLUSTRATIONS (CONT'D)

<u>Figure</u>		<u>Page</u>
49	Low-Pass Filter with Amplifier	98
50	Phase Detector	98
51	Frequency Discriminator	100
52	Frequency Doubler	103
53	Phase Shifter	104

## LIST OF TABLES

<u>Table</u>		<u>Page</u>
I	Magnetic Bias Coil Characteristic	72
II	Electrical Properties of the 11-1/2-Inch Radio-frequency Coil	73
III	Electrical Characteristics of the 10-5/8-Inch Radiofrequency Coil	77
IV	Equipment by Channels	94

## I. INTRODUCTION

Earlier effort at Southwest Research Institute under Contract DA-44-009-ENG-4678, Problem 11, as reported in the final report dated 19 April 1962, demonstrated that magnetoabsorption signals were derivable from soils typical to the immediate San Antonio area and that explosives gave no magnetoabsorption signals. Work on other projects had greatly increased the understanding of the phenomenon and had indicated detection systems with increased sensitivity. On the basis of these and other observations, this investigation was undertaken to design, fabricate, and test a device for (1) the detection, by means of the magnetoabsorption signals from the soil, the presence of a magnetic void caused by a buried nonmagnetic nonconductor, and (2) the description of the composition of the material in buried objects by combining the direct induction and magnetoabsorption detection in one detection head but with separate electronics and display. To these objectives, the program was separated into the following parts:

- (1) To conduct a search of the literature for studies in electromagnetic topics that might be readily adaptable for a suitable electromagnetic model for design guidance in the detection of discrete and dispersed objects.
- (2) To investigate the geometry and performance required from a double-D type of detection head to give the maximum magnetoabsorption signals from large volumes of material, with a dispersed ferromagnetic or ferrimagnetic component, such as soils in a flat geometry.

- (3) To design, construct, and test a completely solid-state marginal-oscillator type of magnetoabsorption detector with a high sensitivity when used with the detection head.
- (4) To determine the operational characteristics of the system composed of the marginal-oscillator and the detection head and, in particular, to measure:
  - (a) the sensitivity of the system to mine depth;
  - (b) the effects of detector height;
  - (c) the effects of moisture;
  - (d) the effects of scanning rate;
  - (e) the effects of the frequency of the marginal-oscillator;
  - (f) the effects of the frequency of the magnetic bias field.
- (5) To design, construct, and test a solid-state laboratory type model of the magnetic-void buried-object detector based upon the results from (4).
- (6) To test the above system to determine its characteristics as a detector of buried nonmagnetic nonconducting objects.
- (7) To study the character and requirements of a discrete, magnetic, conducting object detection system using the detection head of (2), the detector of (3) and a combination of the direct induction and magnetoabsorption signals.
- (8) To add to the designs of (5) the detection of the direct induction signal and to determine the differences, in the shapes and harmonic content, between the direct induction and magnetoabsorption signals from various discrete objects.
- (9) To determine the characteristics of the discrete object detector in differentiating between nonmagnetic conductors, unmagnetized magnetic conductors, magnetized magnetic conductors, magnetic nonconductors, magnetized magnetic nonconductors and permanent magnets.

The manner in which these tasks were conducted and results obtained are described in the remainder of the report.

## II. SUMMARY OF RESULTS

### A. Equipment

The block diagram of the equipment developed for the laboratory tests of the magnetic-void buried-object magnetoabsorption detection system is shown in Figure 1. The photograph of the equipment as it was used in the laboratory is shown in Figure 2.

The strong magnetic bias field at 55 cps is produced by the bias coil which is fed from the 55-cps generator through a power amplifier. With 20 watts of power, a magnetic field of 36-oersteds peak intensity at 55 cps can be obtained.

The radiofrequency magnetoabsorption detection coil,  $L_1$ , has the double-D configuration so that the amount of the 55-cycle voltage is minimized which is directly induced from the bias coil to the radiofrequency coil. By proper geometrical adjustment of the double-D coil, the amount of 55-cycle voltage induced can be reduced to a value below 50 microvolts. The double-D radiofrequency coil is tuned to approximately 500 kilocycles by capacitor  $C_1$ .

The amount of 55-cycle voltage induced in the double-D coil will be increased when the detection head is placed near or on the ground. Therefore, the high-pass filter is used to reject the 55-cycle voltage and prevent it from reaching the amplifiers. The 500-kilocycle voltage as well as the 110-cycle magnetoabsorption modulation is passed by the high pass filter to the amplifier.



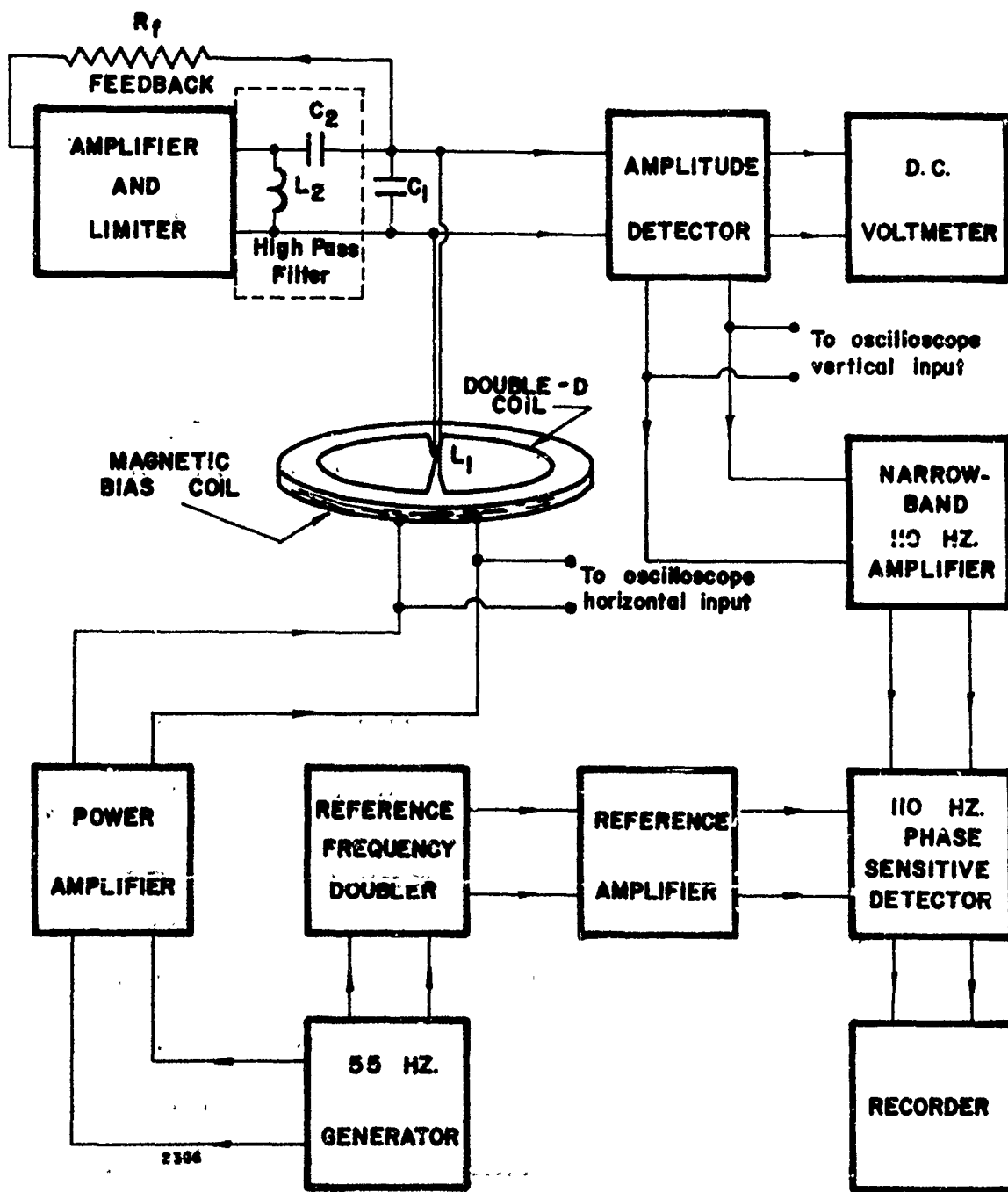


FIGURE 1. BLOCK DIAGRAM OF THE EQUIPMENT DEVELOPED FOR THE MAGNETIC-VOID, BURIED-OBJECT MAGNETOABSORPTION SYSTEM

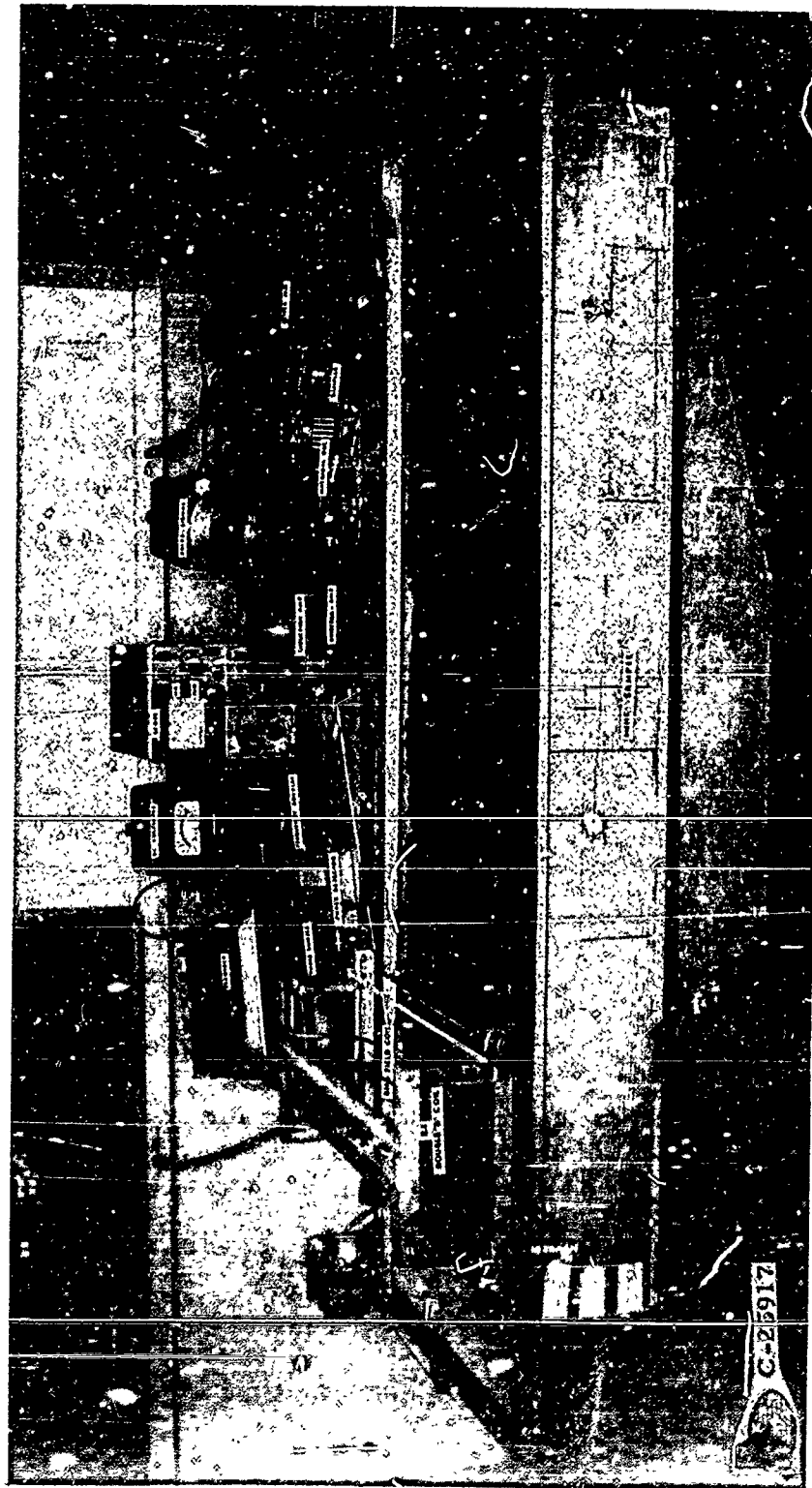


FIGURE 2. POWERED DOLLY WITH DETECTOR MOUNTED.  
SOLID-STATE SYSTEM SHOWN IN BACKGROUND

The amplifier increases the amplitude of the 500-kilocycle signal and passes it through a limiter to control the oscillation level and to strip the 110-cps magnetoabsorption signal off of the radiofrequency to be fed back. The output of the limiter is fed back to the radiofrequency coil through the feedback resistor,  $R_f$ , so that a sustained oscillation is obtained whose level is controlled by the limiter.

The output of the resulting marginal-oscillator at A is a radiofrequency voltage whose amplitude is modulated with the magnetoabsorption signal. The magnetoabsorption signal itself is obtained by passing the marginal-oscillator output through an amplitude detector which in this case is an infinite-impedance type using a Field Effect Transistor. The output of the detector feeds a dc voltmeter to measure the oscillator level, and an amplifier phase-detector system to improve signal/noise ratios. The signal/noise ratio at the output of the amplitude detector varied from a low of 2/1 to a value greater than 10/1. Figure 3 gives two representative magnetoabsorption Lissajous figures (magnetoabsorption signal on the vertical and magnetic bias on horizontal) taken with the detection head on the surface of the soil and spaced 1.5 inches.

The signal/noise improvement, required for a good measurement, was obtained by reducing the bandwidth. Thus, the output of the amplitude detector is passed through a narrow-band amplifier whose center frequency is at 110 cycles and whose bandwidth is 10 cycles. To further reduce the bandwidth, the signal is fed through a 110-cycle amplitude-sensitive phase detector.



(a)  
At Soil Surface



(b)  
1-1/2 Inches  
above Soil

FIGURE 3. SOIL MAGNETOABSORPTION SIGNALS  
OBTAINED: (a) AT THE SURFACE AND  
(b) WITH 1.5 INCHES SEPARATION

The 110-cycle reference for the phase-detector is obtained from the 55-cycle generator through a frequency doubler and a power amplifier. The output of the phase-detector is a dc voltage which is passed through a low-pass filter of 1/6-cycles bandwidth. Thus, the bandwidth has been reduced from about 1,000 cycles to 1/6 cycles, and the signal/noise ratio has been improved by seventy-times. The output of the phase detector is applied to a recorder for laboratory measurements and to a meter for field measurements.

B. Magnetic-Void Buried-Object Detection

The laboratory test system used for the magnetic-void buried-object detection system is shown in Figure 2. In order to easily, continuously and linearly traverse the test box of soil with the detection head, the mechanical

traversing mechanism, driven by a reversible motor with reversing limit switches, was used as shown on the box in Figure 2. The test box is 72 inches long, 24 inches wide and 6 inches deep. A type M-19 mine case was buried at its center at varying depths. A scan was then made over the length of the box and back with the output of the phase detector applied to the recorder.

The recorded amplitude of the magnetoabsorption signal is large when no buried object is present, and it decreases when the detection head is directly over a buried object which is a magnetic void. Figure 4 shows one scan cycle from one end, A, to the other end, B, and return with no mine buried for a 1-inch detector height. The variations shown are those to be expected from the magnetic variations of the soil. When a M-19 mine casing is buried flush with the surface and the detector is held 1 inch above the surface, the signal variation shown in Figure 5 is obtained for one scan cycle. The magnetoabsorption signal decreases by more than 175 millivolts. When the M-19 mine casing is buried with its top 1 inch below the surface and when the detection head is kept at 1 inch above the surface of the soil, the variation in amplitude shown in Figure 6 was obtained for one scan cycle. Thus, for a 1-inch depth, the amplitude changes by over 100 millivolts as the magnetic void is traversed. When the mine is buried at a depth of 2 inches, a variation larger than 25 millivolts is obtained as shown in Figure 7. For all of these measurements, the bottom of the detection head is 1 inch from the top of the soil. The radiofrequency coil itself is  $11/16$  inch from the bottom

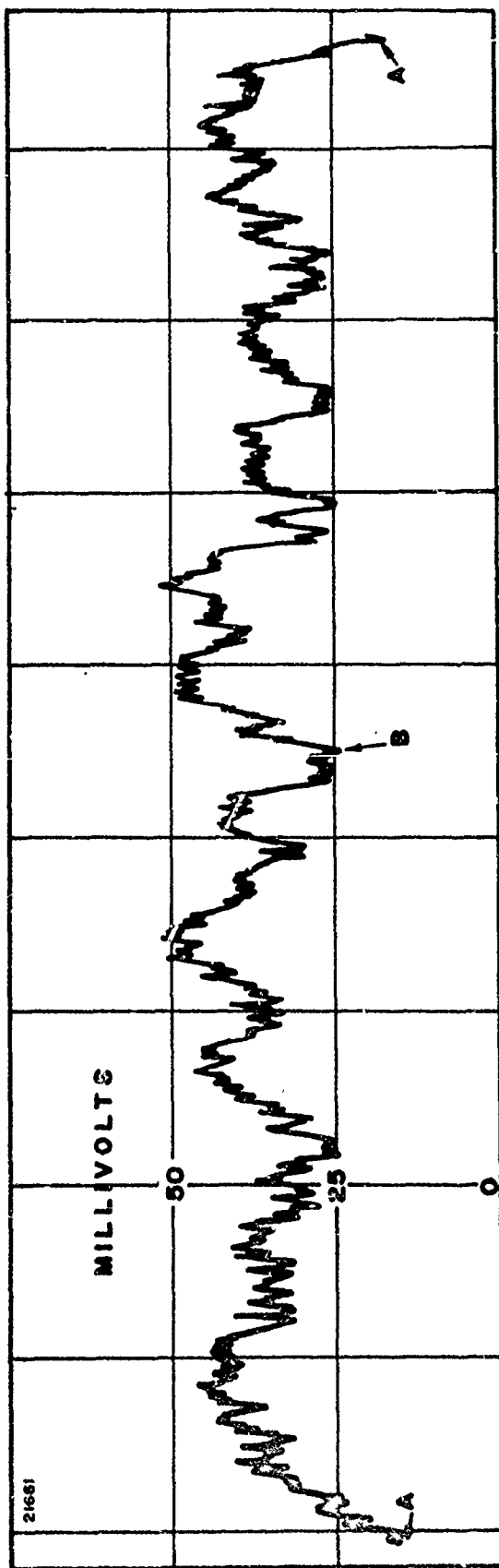


FIGURE 4. ONE SCAN CYCLE OF THE BOX WHEN NO MINE IS PRESENT.  
 THE DETECTOR IS MOUNTED 1-INCH ABOVE THE SOIL.

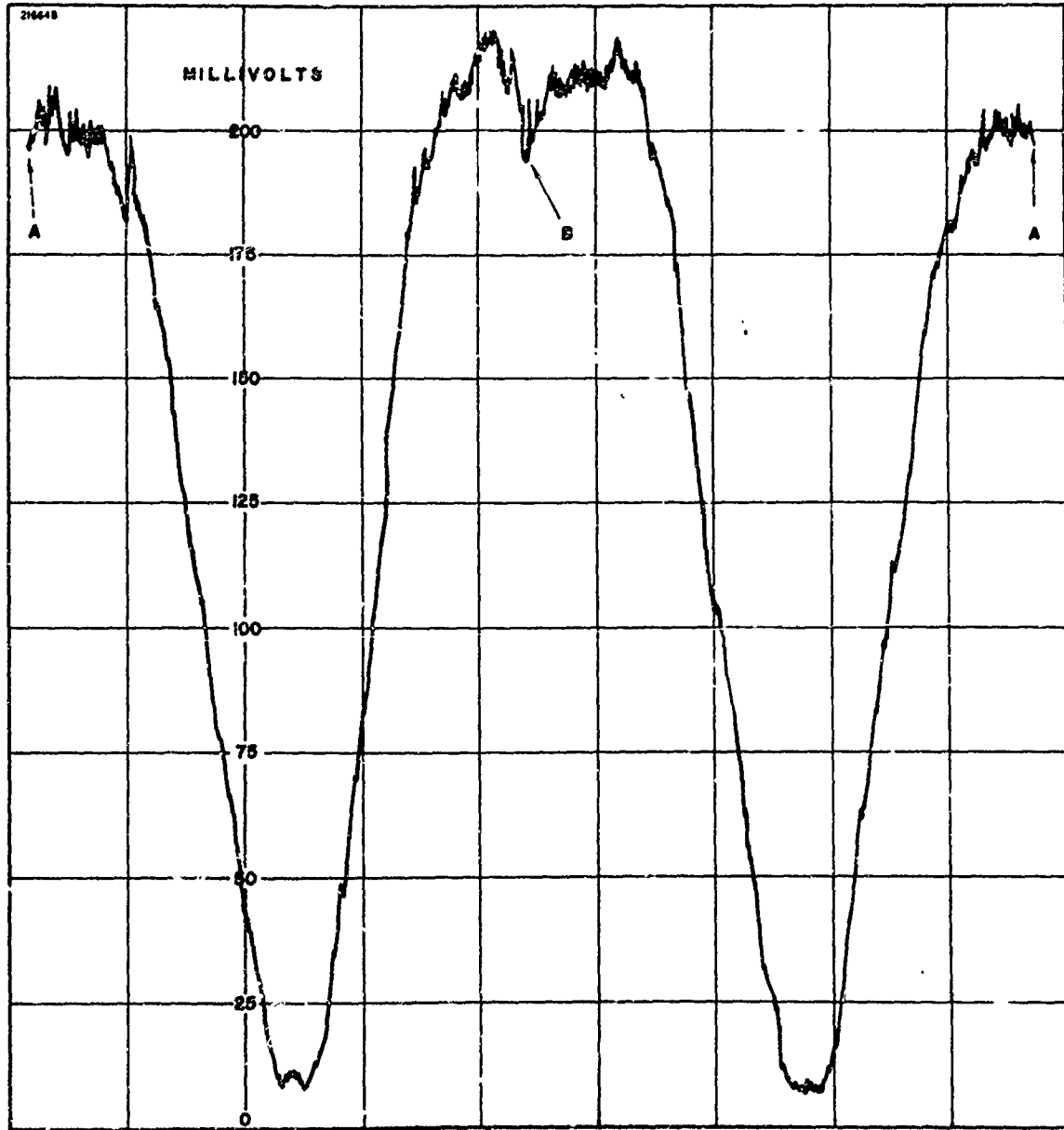


FIGURE 5: ONE SCAN CYCLE OVER A MINE FLUSH WITH THE SURFACE. THE DETECTOR HEIGHT IS 1-INCH ABOVE THE TOP OF THE SOIL.

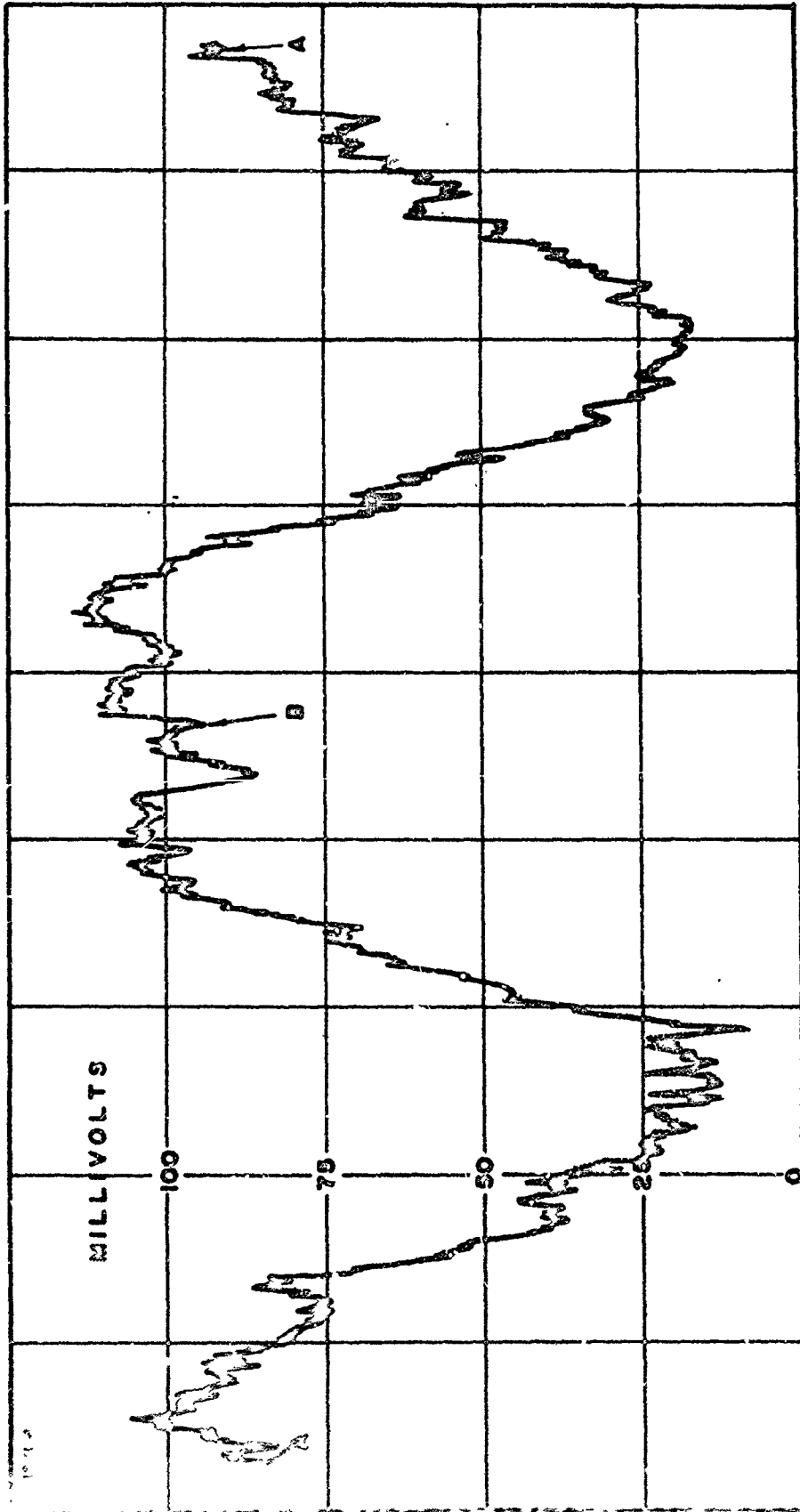


FIGURE 6. ONE SCAN CYCLE WITH MINE BURIED ONE INCH.  
THE DETECTOR HEIGHT IS 1-INCH ABOVE THE SOIL.



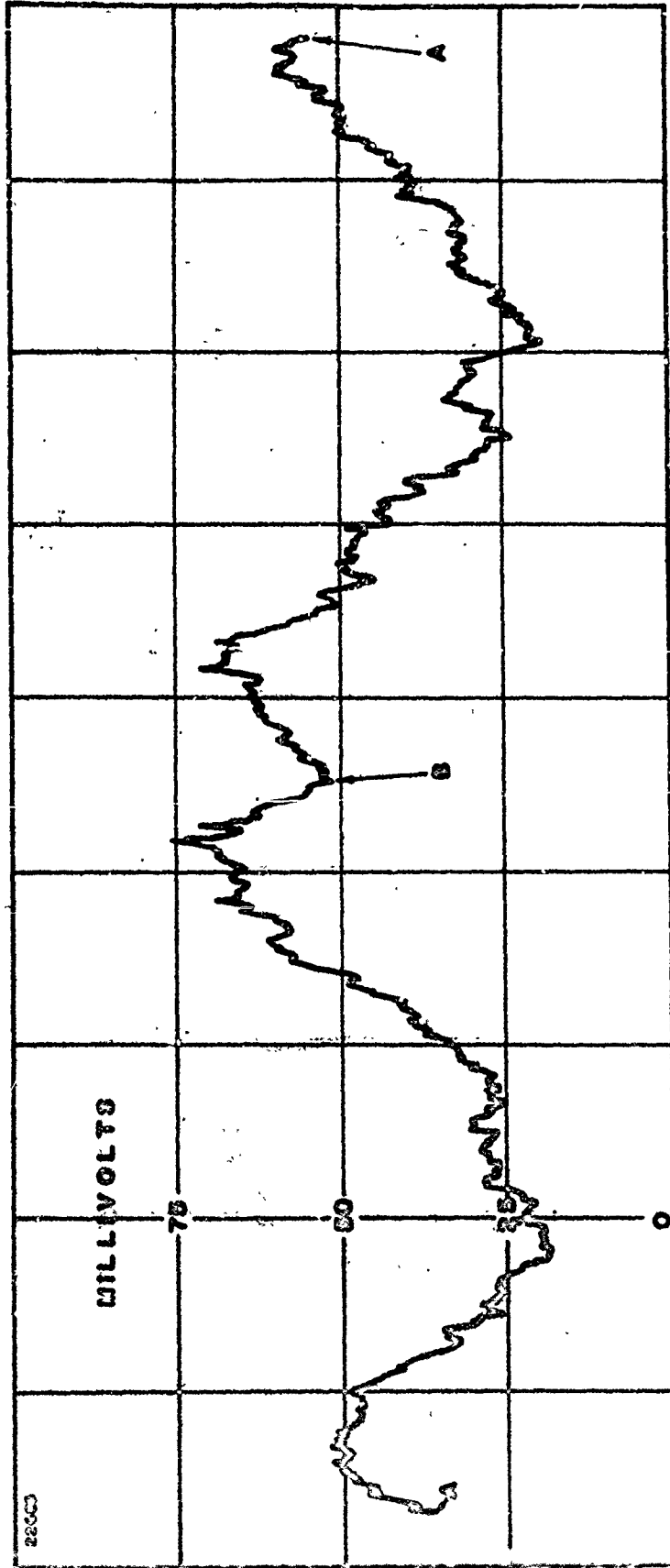


FIGURE 7. ONE SCAN CYCLE WITH MINE BURIED TWO INCHES.  
THE DETECTOR HEIGHT IS 1-INCH ABOVE THE SOIL SURFACE.

of the detection head so that the actual soil-to-coil height is nearly 1-3/4 inches.

The variation of the amplitude of the magnetoabsorption signal as a function of the height of the detection coil with no buried object is plotted on the linear graph of Figure 8. When the output is plotted on semilog paper, the straight line of Figure 9 is obtained. This straight line indicates that the amplitude varies as the height to some power. The field from two mutually-coupled current-loops would vary as the height to the fourth power. If the graph of Figure 8 is plotted on log-log paper, a fit of height to the 3.3 power is obtained. Time and effort were not expended to attempt to determine the reasons for the difference obtained. It should be remembered, however, that the magnitude of the magnetoabsorption signal depends upon a combination of the strength of radiofrequency field and the strength of the magnetic bias field.

The percent change in the magnetoabsorption signal amplitude, caused by the presence of the magnetic void from the M-19 mine casing, as a function of the mine depth, is shown in the graph of Figure 10 for detection head heights of 1/2, 3/4, 1, 1-1/4, 1-1/2 and 1-3/4 inches. The data graphed in Figure 10 show that the percentage change in signal amplitude is independent of detector height. Figure 10 also shows that buried magnetic voids buried with their tops 2 inches below the surface of the soil can be detected with the detection coil 2-1/2 inches above the soil surface.

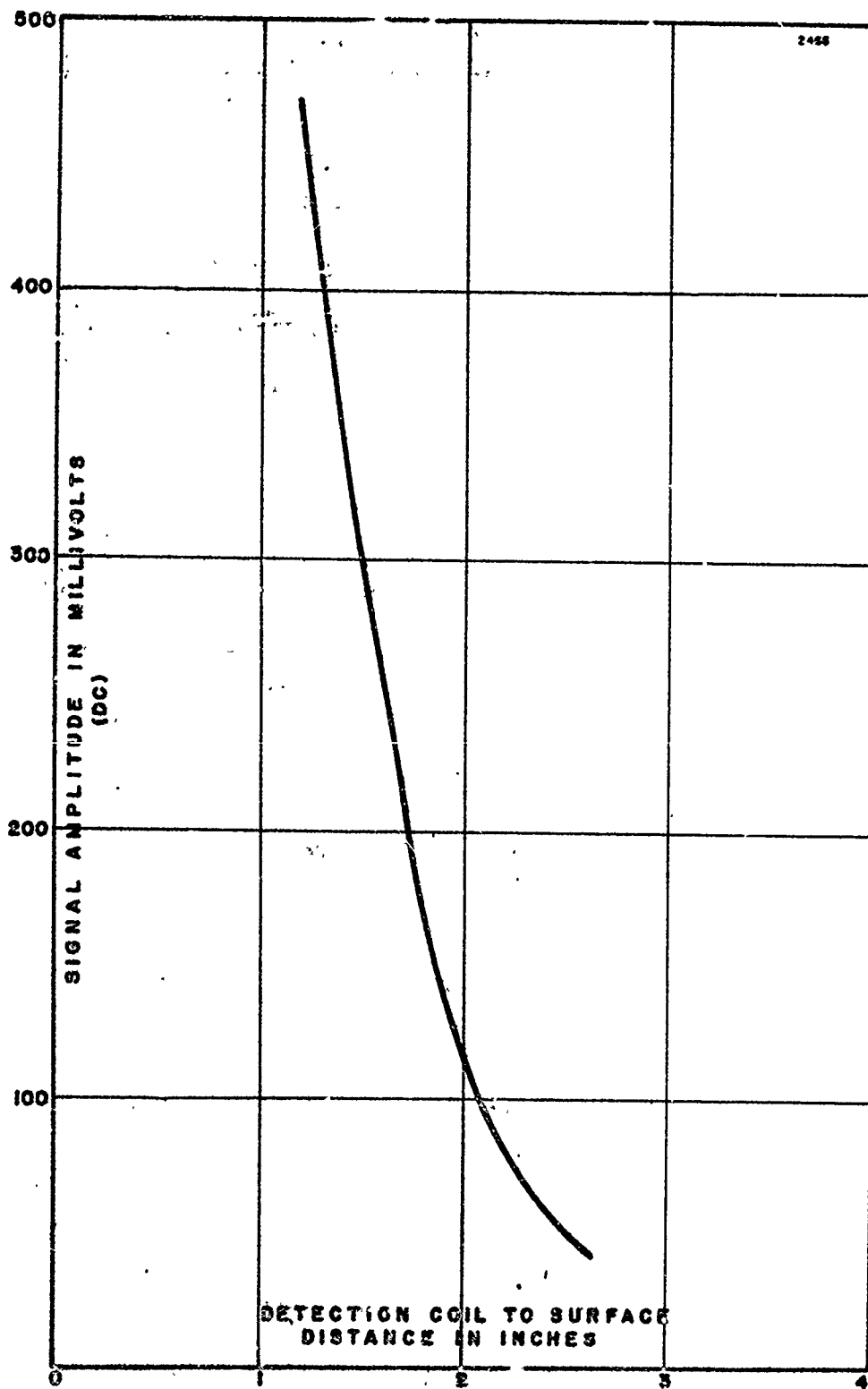


FIGURE 8. LINEAR GRAPH OF THE SIGNAL AMPLITUDE AS A FUNCTION OF DETECTOR COIL HEIGHT WITH NO BURIED OBJECT

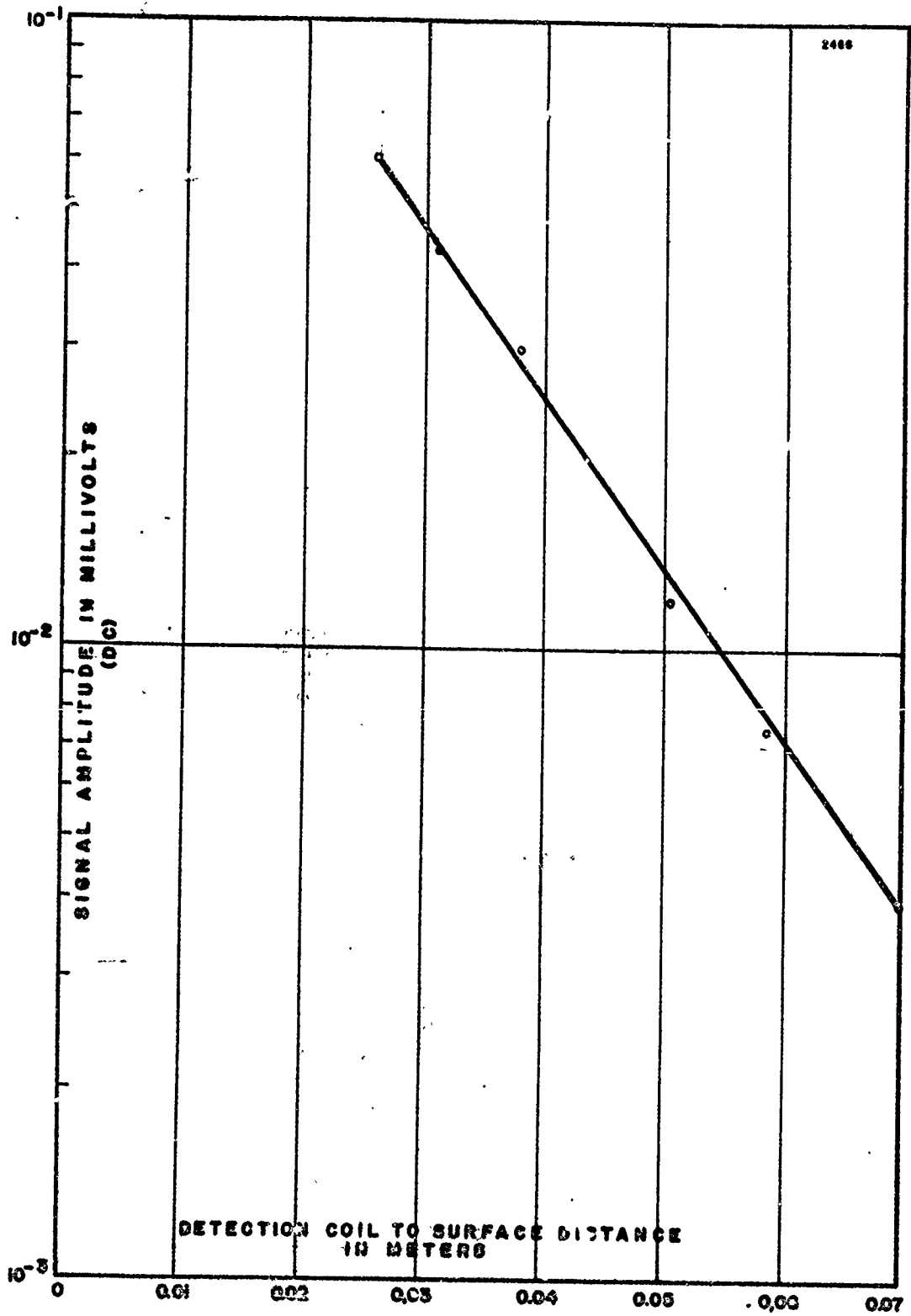


FIGURE 9. SEMILOG GRAPH OF THE SIGNAL AMPLITUDE AS A FUNCTION OF DETECTION COIL HEIGHT WITH NO BURIED OBJECT

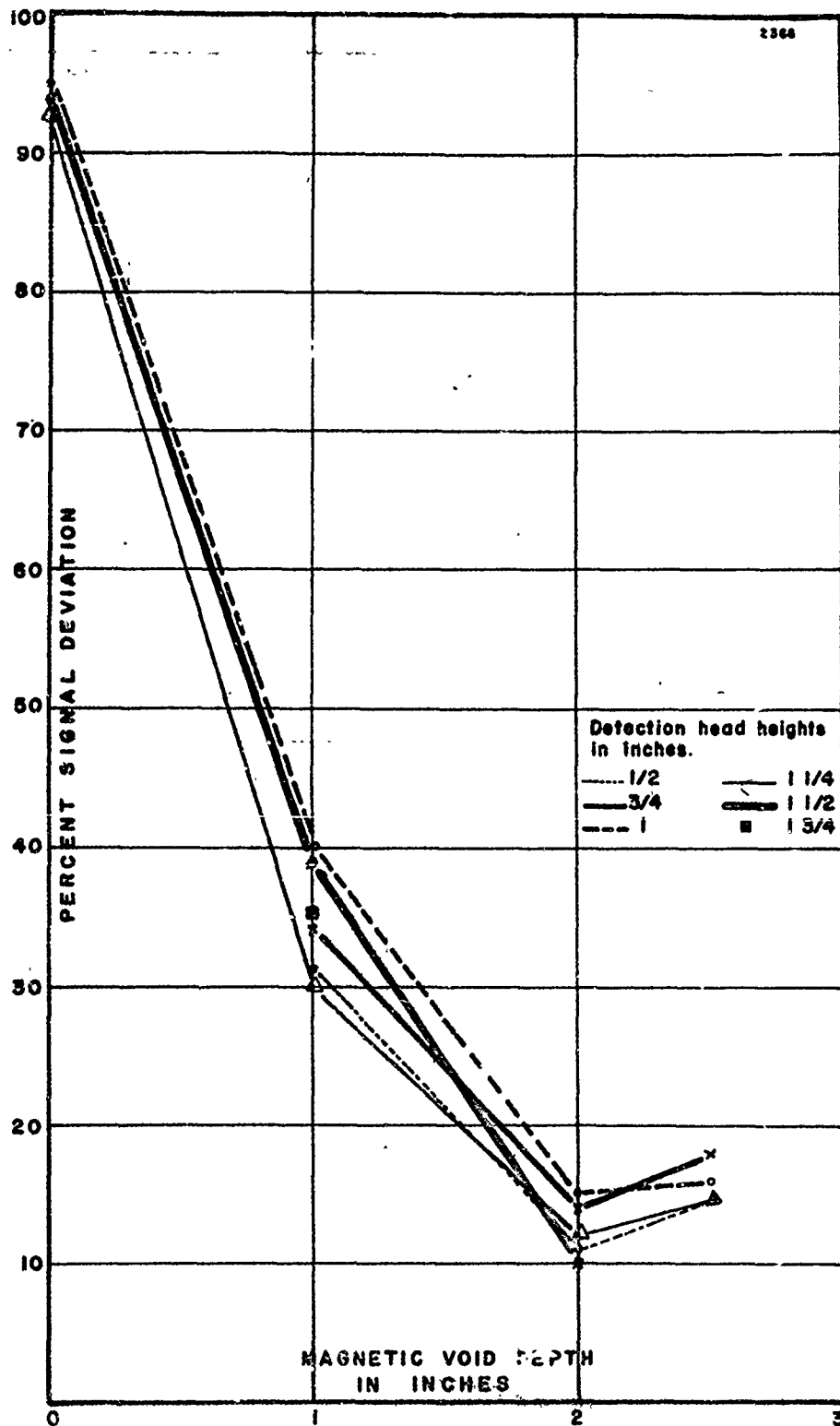


FIGURE 10. GRAPH OF THE PERCENTAGE CHANGE IN THE AMPLITUDE OF THE MAGNETOABSORPTION SIGNAL CAUSED BY A BURIED MAGNETIC VOID. DATA ARE SHOWN FOR DETECTION HEAD HEIGHTS OF 1/2, 3/4, 1, 1-1/4, 1-1/2, AND 1-3/4 INCHES

When the data of Figure 10 are plotted as the percentage change, for a family of curves at void depths of 2, 1, and 0 inches, as a function the height of the detection head, the constant-percent with detection-head-height characteristic is shown as in Figure 11.

The results shown in Figures 4 through 11 demonstrate that the amplitude of the fundamental of the magnetoabsorption signal at 110 cycles can be used to detect the presence of a magnetic void buried in soils. The results further show that the percentage change in the amplitude of the magnetoabsorption signal caused by a magnetic void is independent of the height of the detection head while it varies exponentially with the depth of the magnetic void. Thus, if an automatic gain control system is used, the time constant,  $T$ , of the system and the feedback characteristic,  $B$ , must be adjusted so that

$$\frac{T}{1+AB} > \frac{d}{S} \quad (1)$$

where

$A$  is the gain of the controlled amplifier;

$d$  is the diameter of the magnetic void;

$S$  is the speed of the detection head over the ground.

Such an adjustment will make the detection system less sensitive to variations in detection-head heights and more sensitive to variations caused by buried magnetic voids.

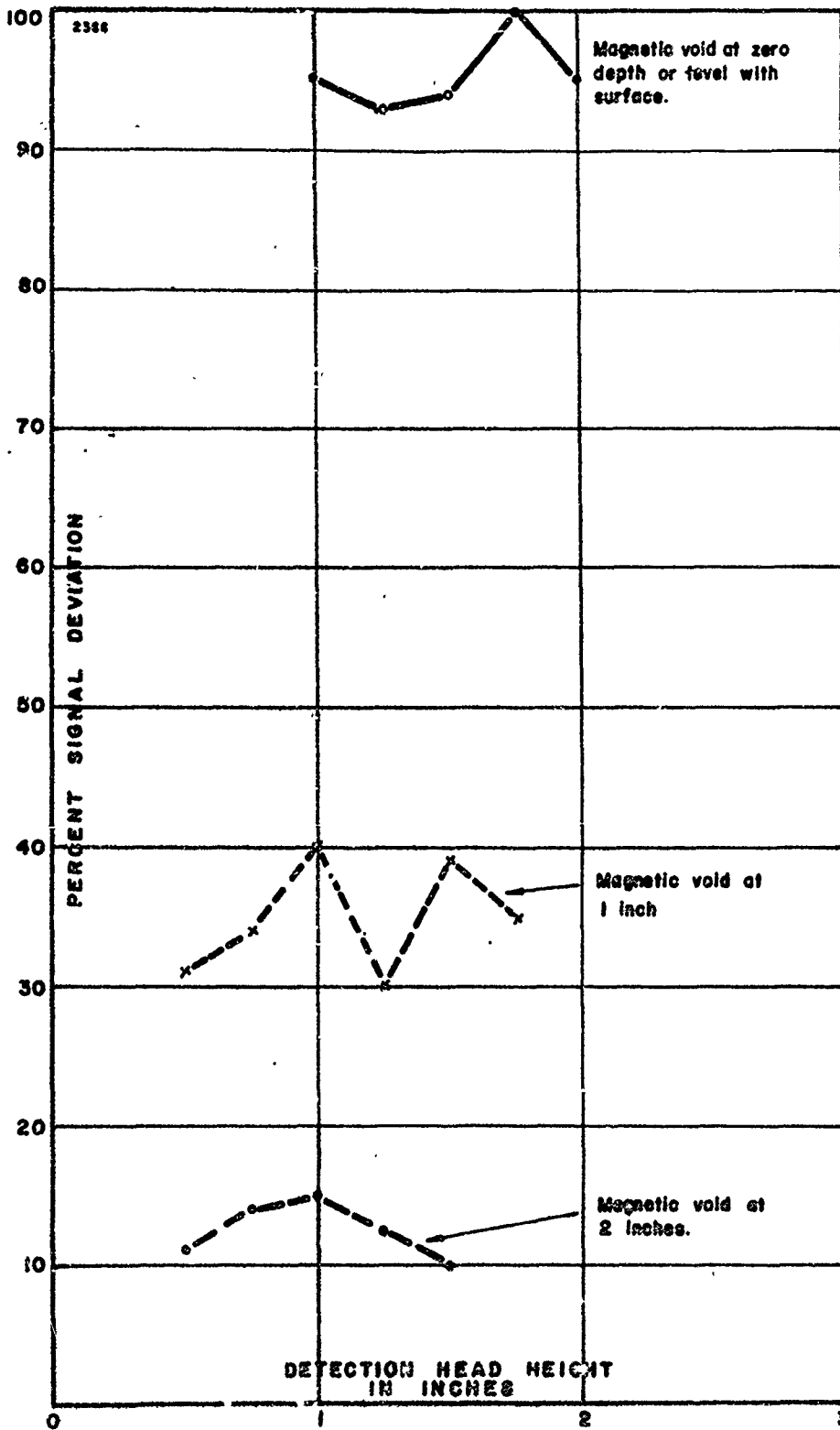


FIGURE 11. VARIATIONS OF PERCENT SIGNAL DEVIATION WITH DETECTION HEAD HEIGHT FOR MAGNETIC-VOID DEPTHS OF 2, 1 AND ZERO INCHES (LEVEL WITH SURFACE)

### C. Discrete Object Detection and Identification

To obtain the ability to both detect and identify the composition of discrete objects, the amplitude and phase of both the direct induction and the magnetoabsorption signals must be used. The double-D radiofrequency coil type of detection head had been designed to provide both signals, and, thus, it can be used without modification. Since the shapes (Lissajous Figures) and the amplitudes of the harmonics of the magnetoabsorption signals were to be compared, only the high-pass filter, the amplifier-limiter and the amplitude detector components of the magnetic-void detector (Fig. 1) were used for the magnetoabsorption part of the discrete object detector tests for object signatures. (The 55-cycle generator and power amplifier were also necessary.)

Because the direct induction signals in the double-D radiofrequency detection coil are at 55 cycles, they could be separated from the magnetoabsorption signal at point A in Figure 1 by a low-pass filter. Therefore, the block diagram of Figure 12 was used for a laboratory test system to make the determinations of: (1) the shape of the Lissajous figures for the magnetoabsorption signals, (2) the amplitudes of the harmonics of the magnetoabsorption signals, (3) the shape of the Lissajous figures for the direct induction signals, and (4) the amplitudes of the harmonics of the direct induction signals. The test setup in the laboratory would look similar to that of Figure 2 except that the detection head is turned upside down and the discrete objects are placed on top of it.



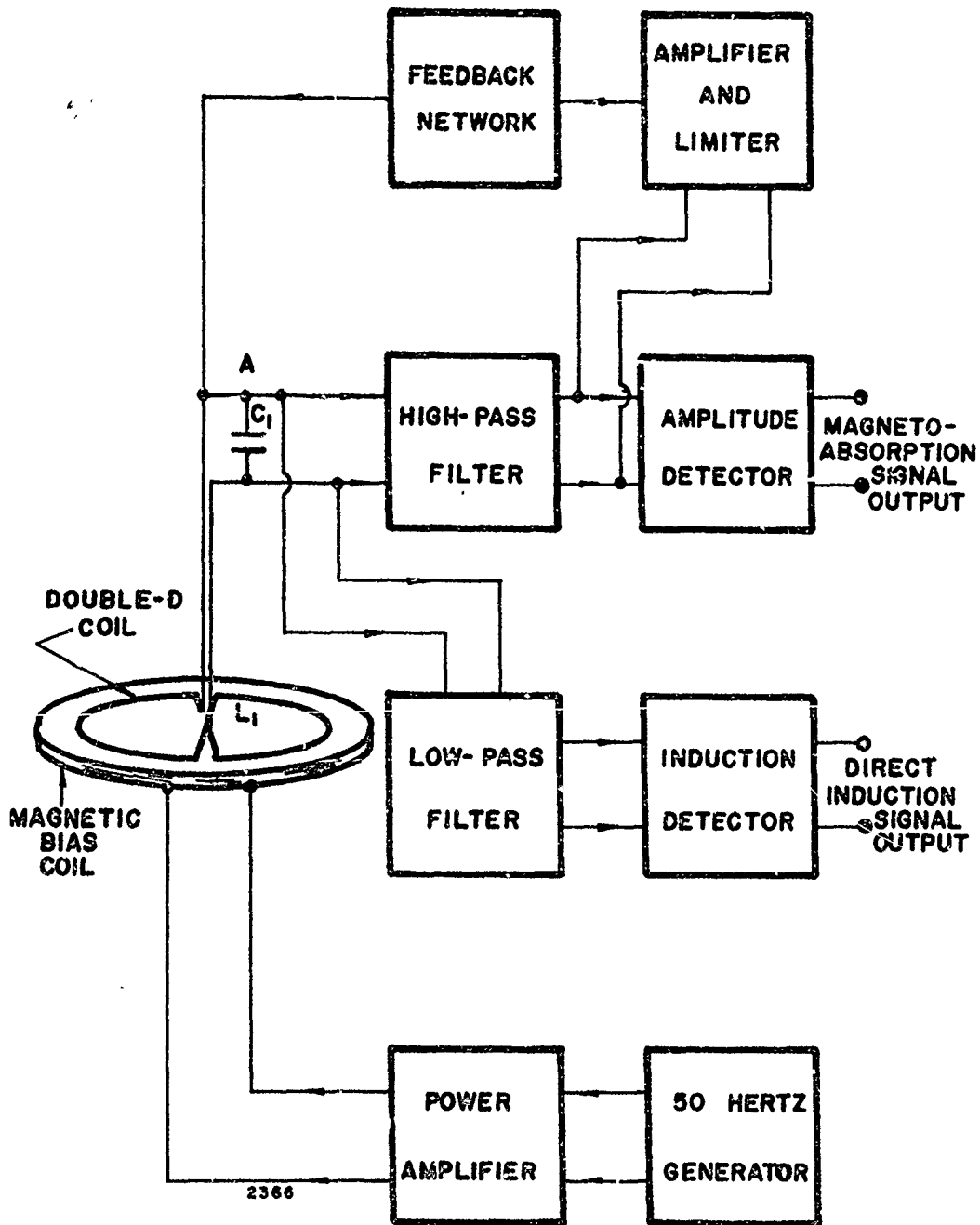


FIGURE 12. BLOCK DIAGRAM OF THE DISCRETE OBJECT DETECTION AND IDENTIFICATION LABORATORY TEST SYSTEM

The results shown by the two Lissajous figures and the two harmonic analyses for each of the twenty-one discrete objects will be given in the following paragraphs. Pictures are also given showing the object being measured and its relation to the detection head. A total of eleven (11) construction type materials and ten (10) electronic components is used.

I. Measurements on Construction Materials

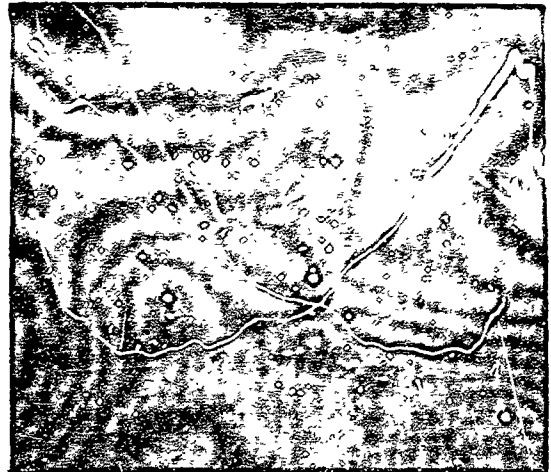
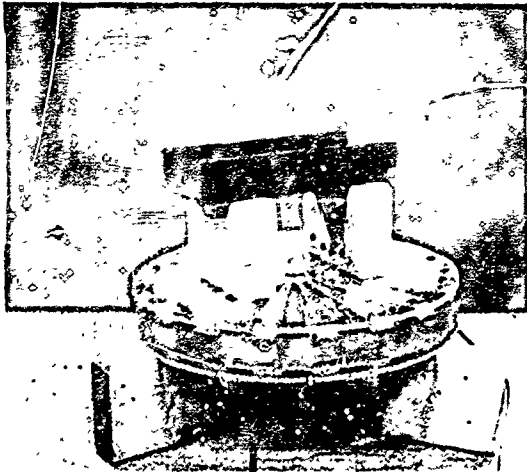
a. Channel Iron

The Lissajous patterns obtained from a large piece of channel iron and the mounting pictures are shown in Figure 13a. It has both a magnetoabsorption and a direct induction signal since it is a ferromagnetic conductor. In addition, the induction signal is nearly  $90^\circ$  out of phase with the magnetic bias. The harmonic amplitudes are shown in Figure 13b. The magnetoabsorption signal has a strong second-harmonic component with only two higher harmonics. The direct induction signal has its fundamental at 50 cycles, a small 100-cycle component and a third-harmonic component at 150 cycles indicating that the material is a ferromagnetic conductor.

b. Angle Iron

The results for a piece of angle iron are shown in Figures 14a and 14b. The presence of a higher harmonic in the magnetoabsorption signal shows the angle iron to be made from different material than the channel iron or to have had different treatment. However, the magnetoabsorption and direct induction results are very similar to those obtained with the channel iron.

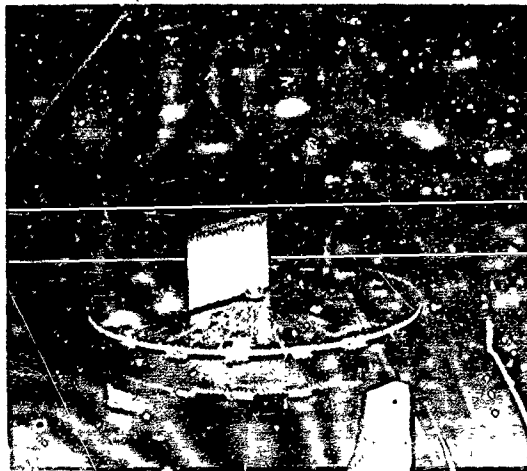
**MAGNETOABSORPTION SIGNAL**



**OBJECT LOCATION:** 3-5/8"

**VERTICAL SEN:** 0.5 V/cm  
2.5 vpp

**INDUCTION SIGNAL**



**OBJECT LOCATION:** 3-5/8"

**PHASE INDICATION**

**OBJECT DESCRIPTION:** CHANNEL IRON

**CHARACTERISTIC DIMENSIONS:** 1" x 4" x 10"

**FIGURE 13a**

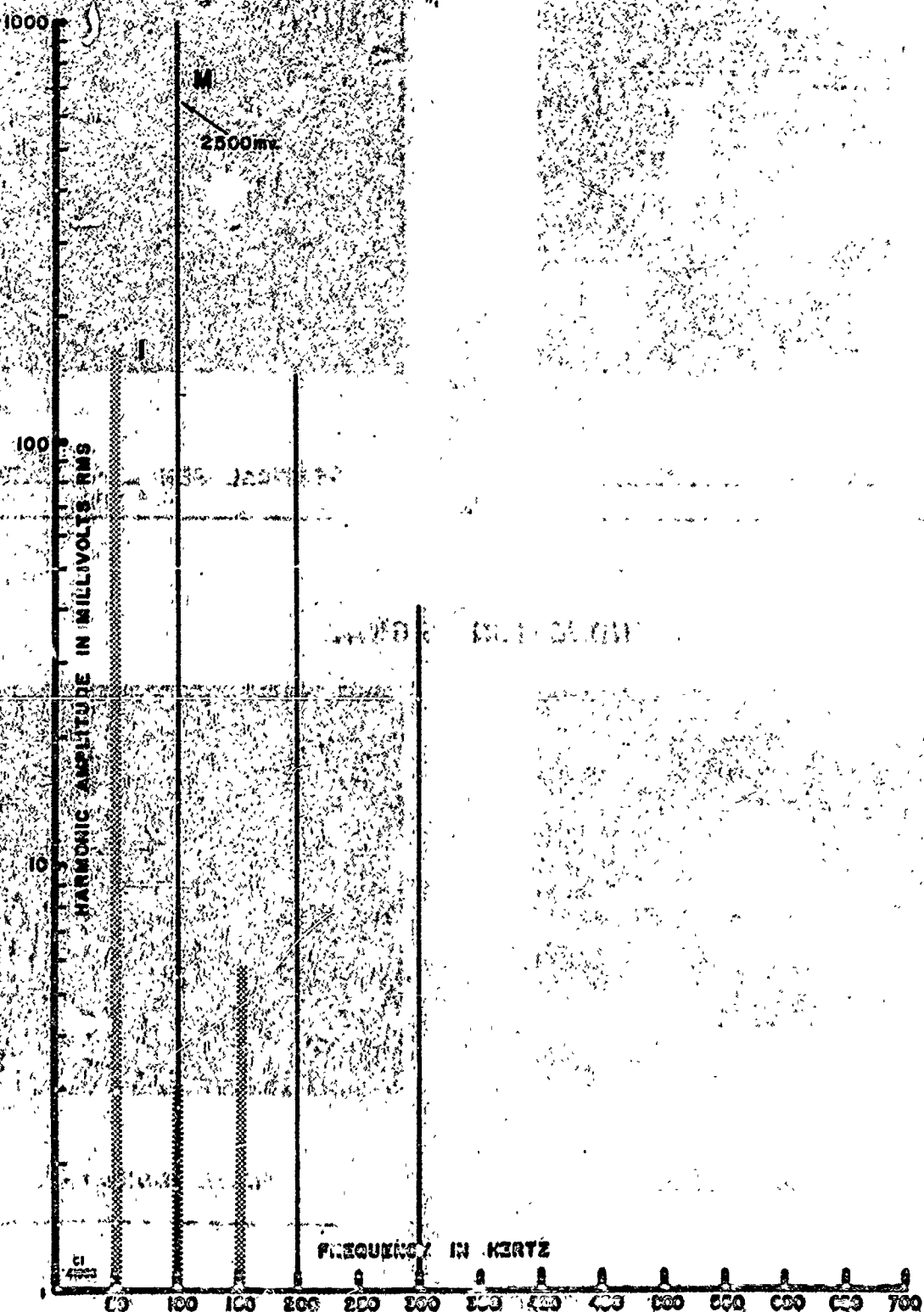
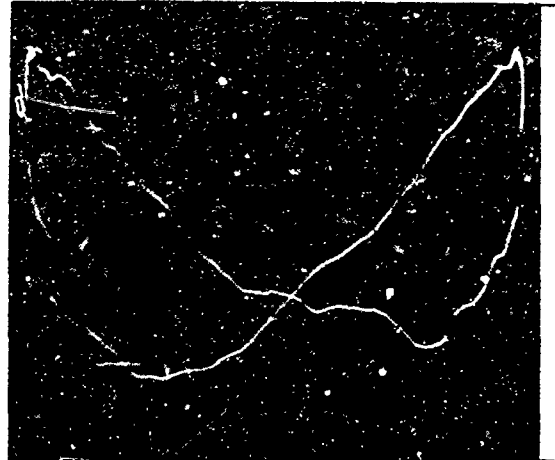
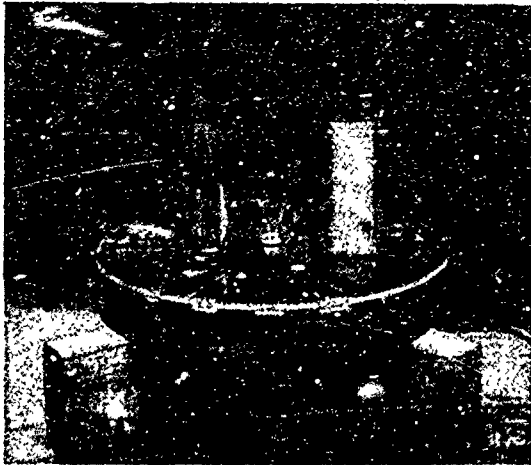


FIGURE 13b. HARMONIC AMPLITUDES FROM CHANNEL IRON

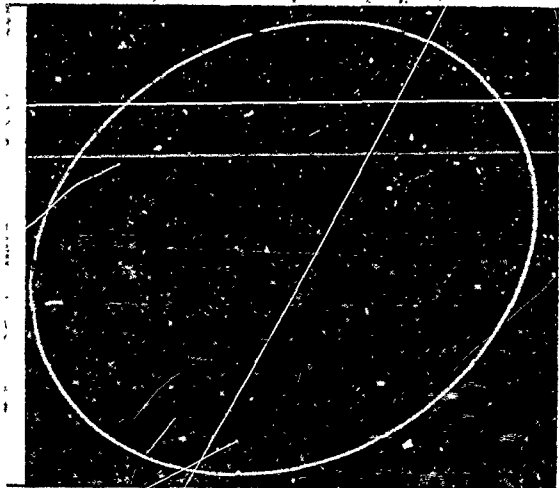
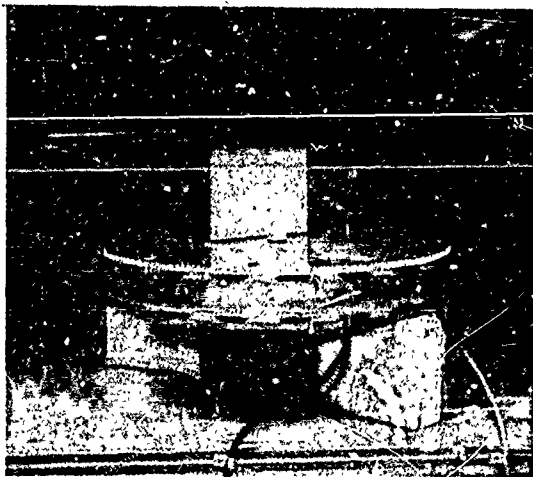
## MAGNETOABSORPTION SIGNAL



OBJECT LOCATION: 4-3/4"

VERTICAL SEN: 0.5 V/cm  
2.4 vpp

## INDUCTION SIGNAL



OBJECT LOCATION: 3-5/8"

PHASE INDICATION

OBJECT DESCRIPTION: ANGLE IRON

CHARACTERISTIC DIMENSIONS: 3" x 3" x 15-1/2"

FIGURE 14a

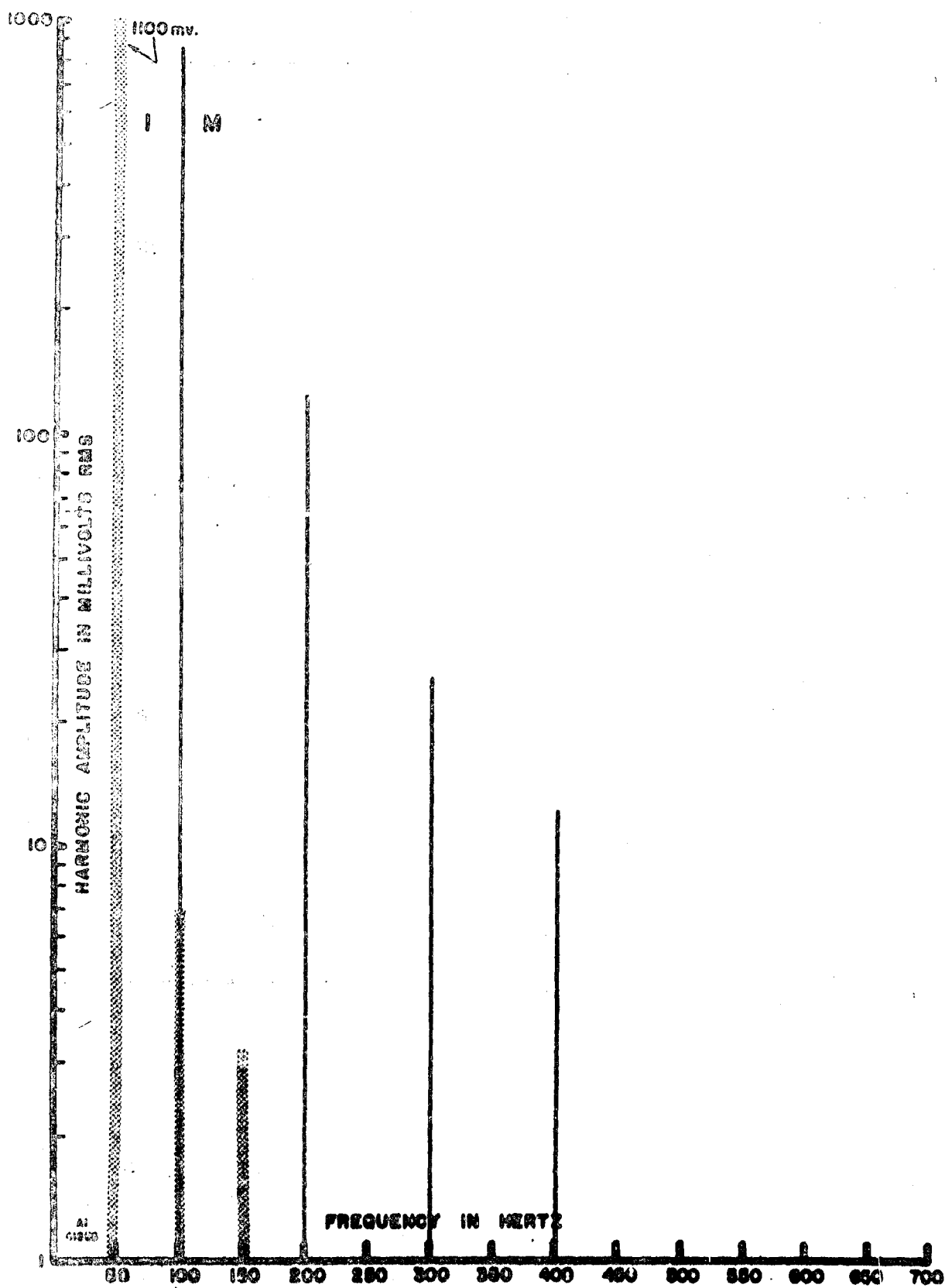


FIGURE 14b. HARMONIC AMPLITUDES FOR ANGLE IRON

Best Available Copy

c. Copper Tubing

The copper tubing gave no magnetoabsorption signal as shown in Figure 15a. The induction signal was strong and had a phase angle close to zero as characteristic of nonmagnetic conductors. The harmonic amplitudes of Figure 15b show no magnetoabsorption data and only the harmonics present from the direct induction as expected from a nonmagnetic conductor.

d. Type BX Electrical Conduit

The magnetoabsorption signal from a 4-foot length of type BX electrical conduit is shown in Figure 16a. Its shape indicates that it is from a piece of hardened or cold-worked steel. The presence of higher harmonic amplitudes, as shown in Figure 16b, also indicates this characteristic. The phase angle induction signal of Figure 16a also is that to be expected if the sample is a magnetic conductor. The high amplitude of the third harmonic on the induction signal also indicates a magnetic conductor.

e. Thin-Wall Electrical Conduit

The magnetoabsorption signal from thin-wall electrical conduit, Figure 17a, shows that it is made from a magnetic material that has been cold-worked or work hardened. This is further indicated by the large amplitude of the higher harmonics of the magnetoabsorption signal in Figure 17b. That it is a magnetic conductor is shown by the direct induction signal, phased  $90^\circ$  relative to the bias field, of Figure 17a. The harmonic

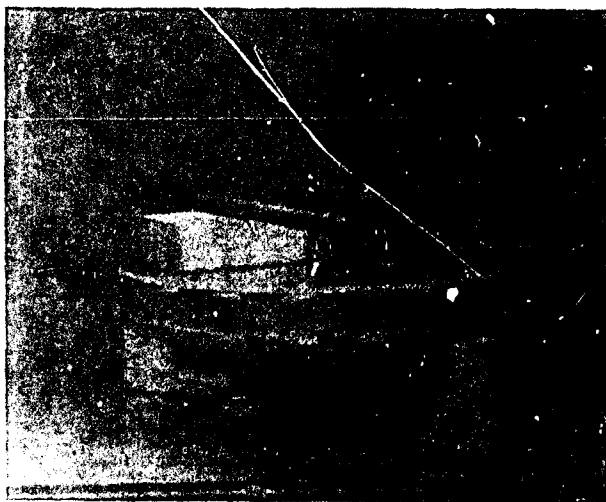
MAGNETOABSORPTION SIGNAL

NONE

OBJECT LOCATION: \_\_\_\_\_  
\_\_\_\_\_

VERTICAL SEN: \_\_\_\_\_  
\_\_\_\_\_

INDUCTION SIGNAL



OBJECT LOCATION: 1-3/4"  
\_\_\_\_\_

PHASE INDICATION  
\_\_\_\_\_

OBJECT DESCRIPTION: COPPER TUBING  
\_\_\_\_\_

CHARACTERISTIC DIMENSIONS: 1/2" O.D. x 12"  
\_\_\_\_\_

FIGURE 15a



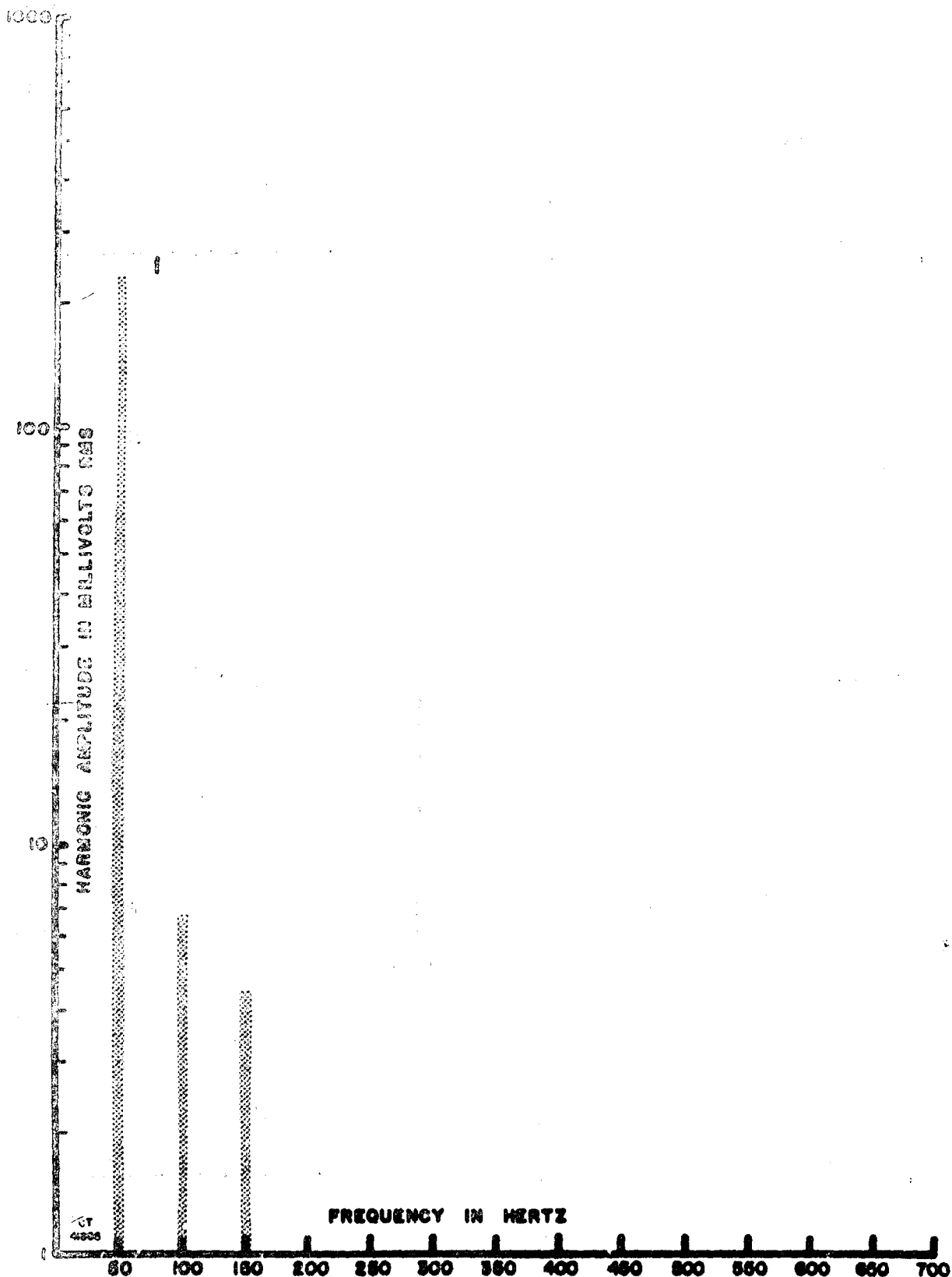
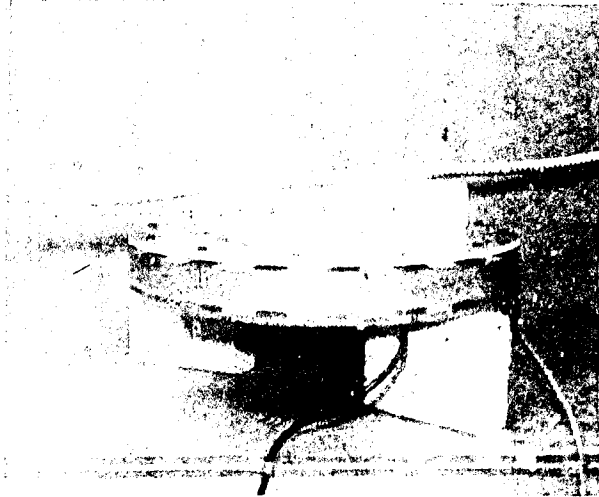


FIGURE 15b. HARMONIC AMPLITUDE CURVES FOR COPPER TUBING

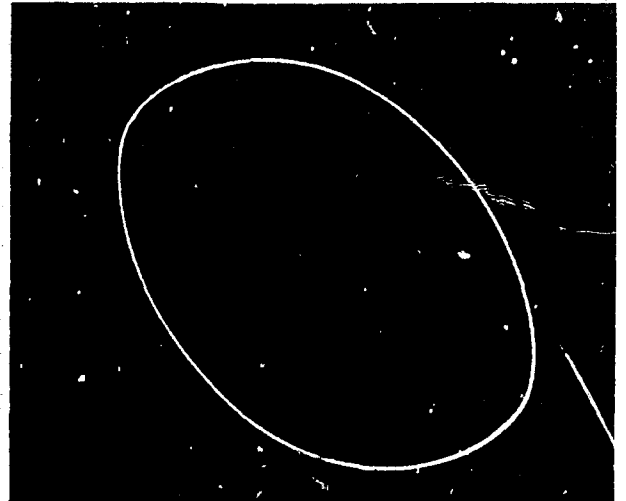
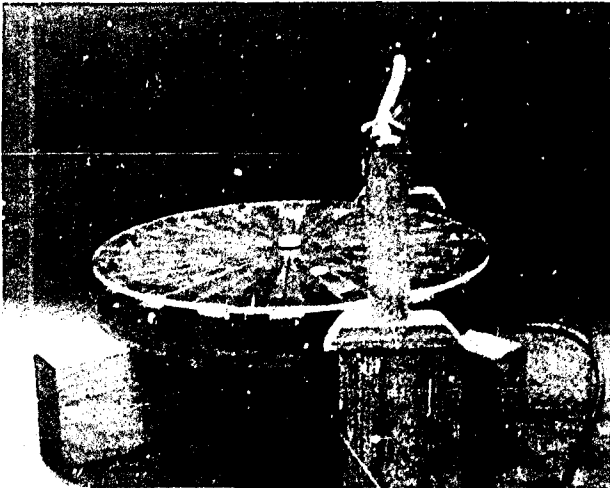
MAGNETOABSORPTION SIGNAL



OBJECT LOCATION: 1-3/4"

VERTICAL SEN: 0.5 V/cm  
2.0 vpp

INDUCTION SIGNAL



OBJECT LOCATION: 6"

PHASE INDICATION

OBJECT DESCRIPTION: BX ELECTRICAL CABLE

CHARACTERISTIC DIMENSIONS: 1/2" O. D. x 4'

FIGURE 16a

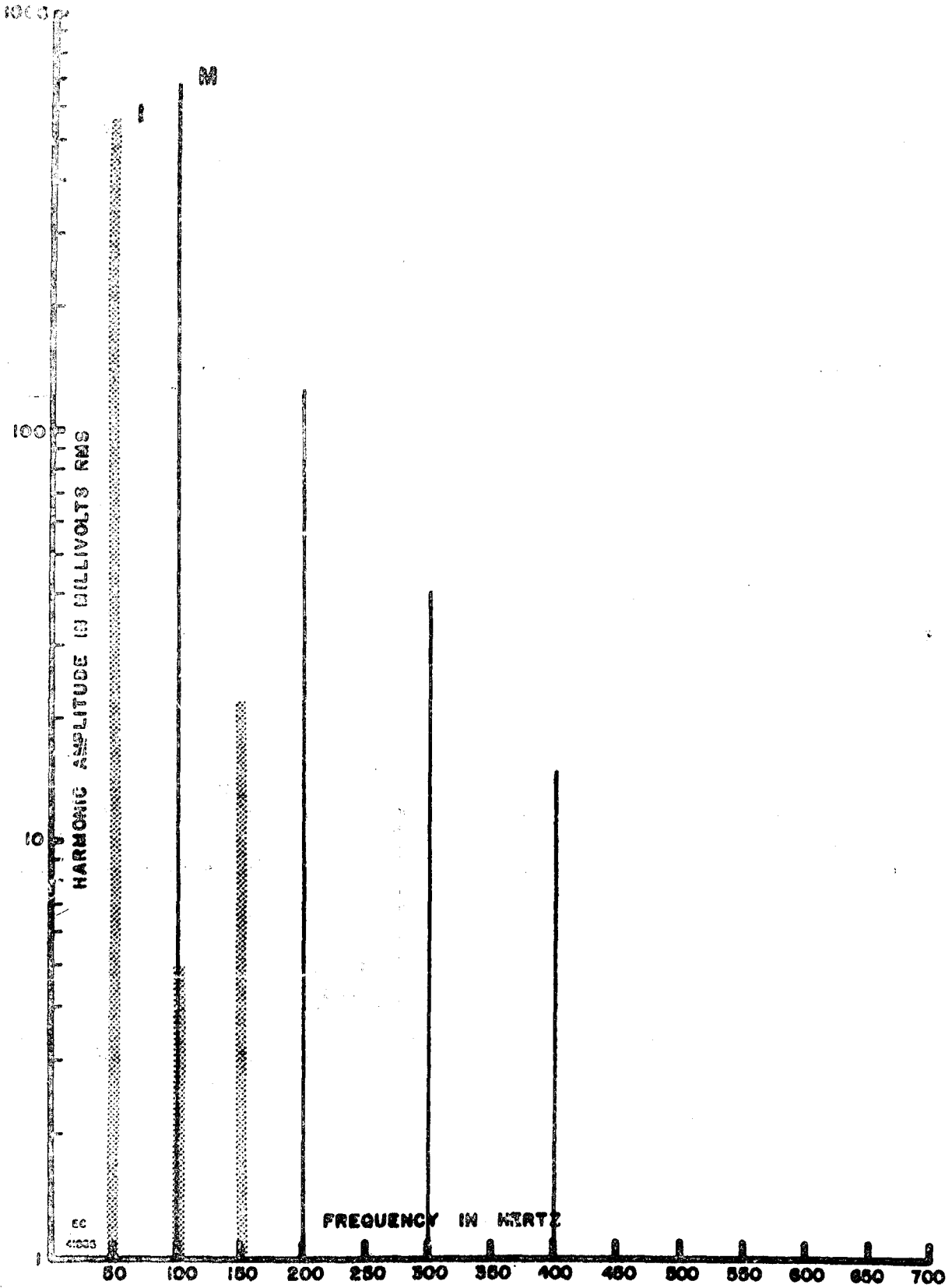
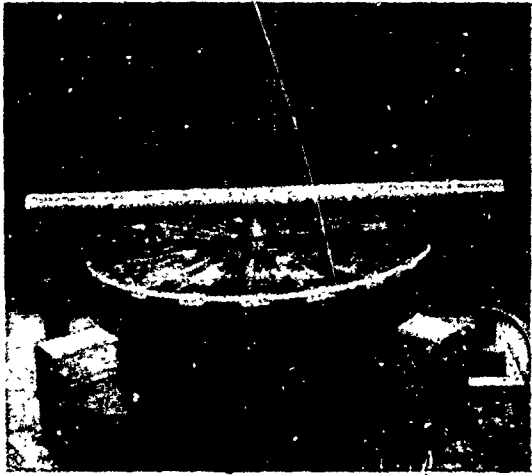


FIGURE 16b. HARMONIC AMPLITUDES FROM TYPE BX ELECTRICAL CONDUIT

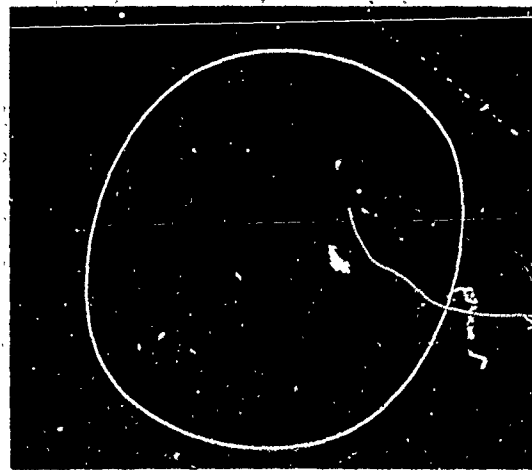
**MAGNETOABSORPTION SIGNAL**



**OBJECT LOCATION:** 1"

**VERTICAL SEN:** 0.5 V/cm  
2.4 vpp

**INDUCTION SIGNAL**



**OBJECT LOCATION:** 4-3/4"

**PHASE INDICATION**

**OBJECT DESCRIPTION:** THIN WALL ELECTRIC CONDUIT

**CHARACTERISTIC DIMENSIONS:** 1" O.D. x 18"

**FIGURE 17a**

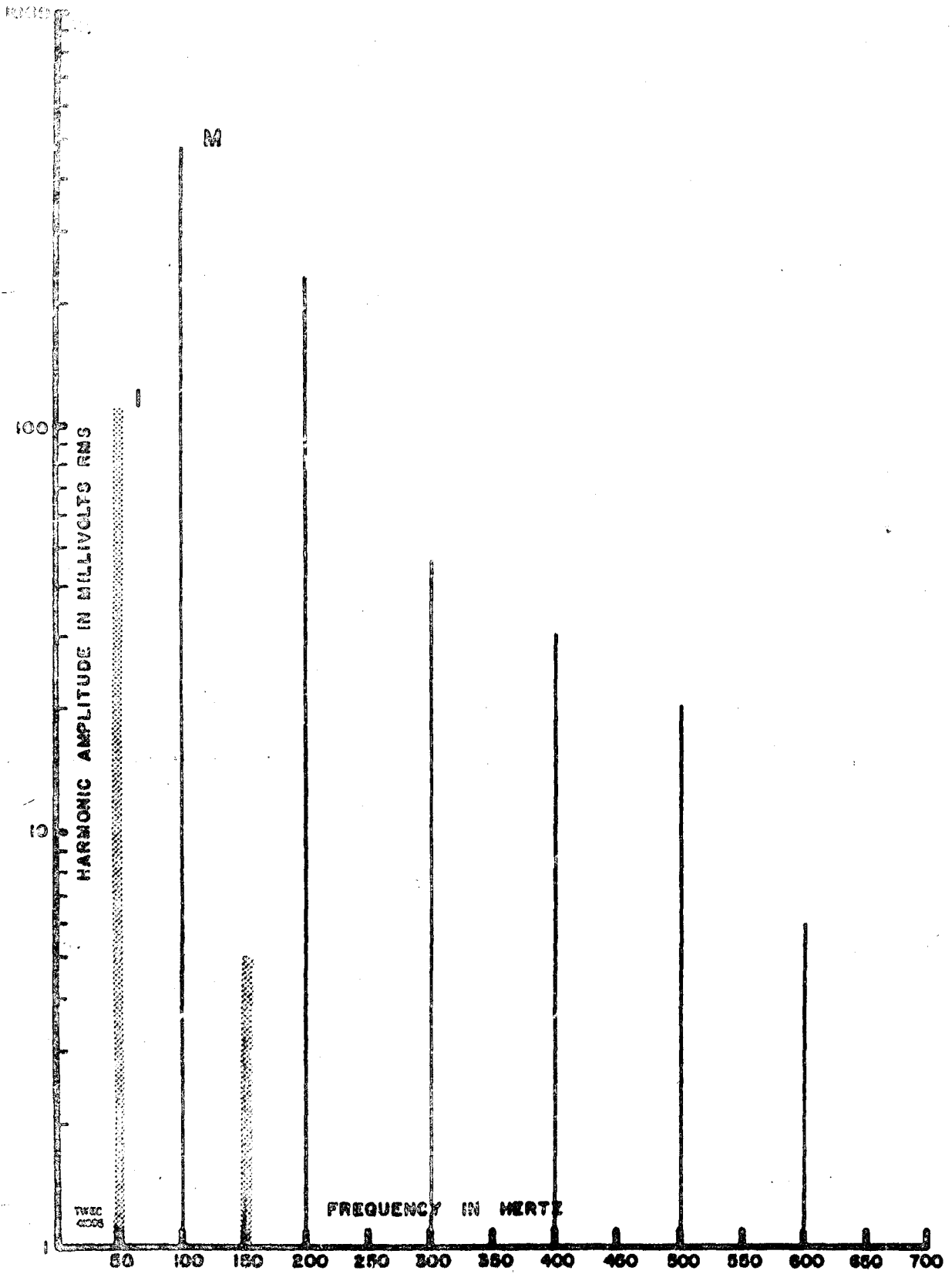


FIGURE 176. HARMONIC AMPLITUDES FOR THIN-WALL ELECTRICAL CONDUIT

amplitudes, Figure 17b, of the induction signal show the third harmonic to be expected but essentially no second-harmonic amplitude.

f. Electrical Outlet Box

The electrical outlet box gives a magnetoabsorption signal, Figure 18a, whose shape is similar to that from the type BX conduit. The magnetoabsorption signal also has a high amplitude of the higher harmonics, Figure 18b, indicating that it is either cold-worked or made from a hardened steel. The induction signal, being at a relative angle of nearly  $90^\circ$ , indicates a magnetic conductor. The induction harmonic analysis, Figure 18b, shows that it has a large third-harmonic component and a smaller second-harmonic amplitude also indicative of a magnetic conductor.

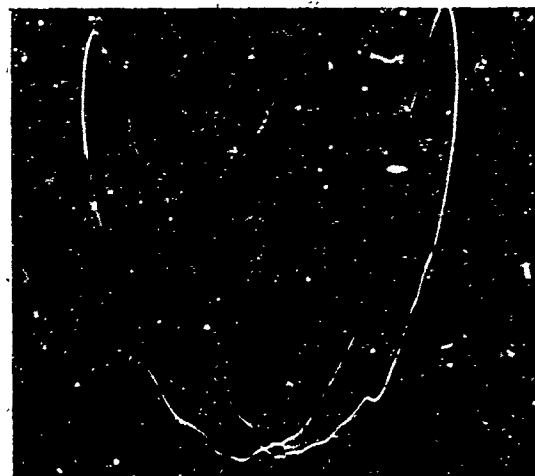
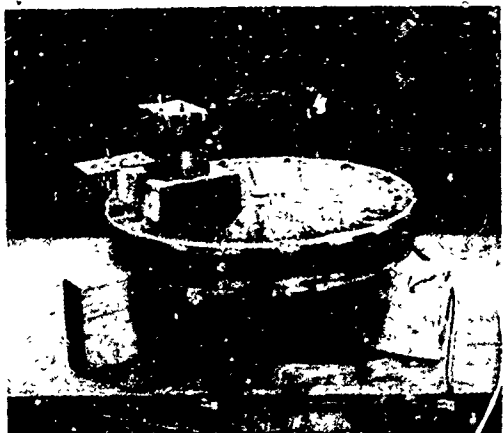
g. Toggle Bolt

The magnetoabsorption signal, Figure 19a, from a toggle bolt indicates that it is a magnetic conductor made from cold-worked steel. The harmonic amplitudes of Figure 19b also indicate the presence of cold-worked or hardened steel. The induction signal of Figure 19a is nearly at a  $90^\circ$  relative angle indicating a magnetic material of low conductivity. The harmonic analysis of the induction signal, Figure 19b, also indicates the large third-harmonic component for hardened steel.

h. Standard Electrical Switch

The shape of the magnetoabsorption signal, Figure 20a, is characteristic of a work-hardened magnetic conductor, and the harmonic

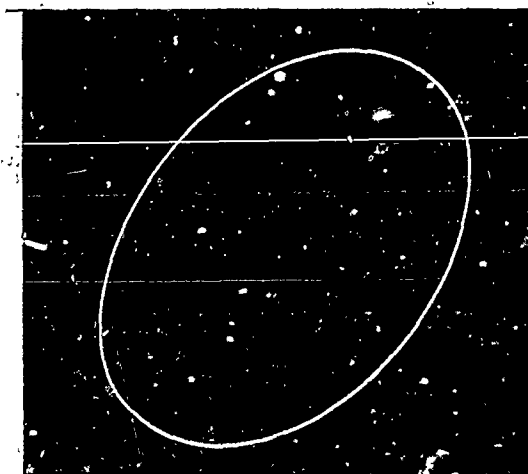
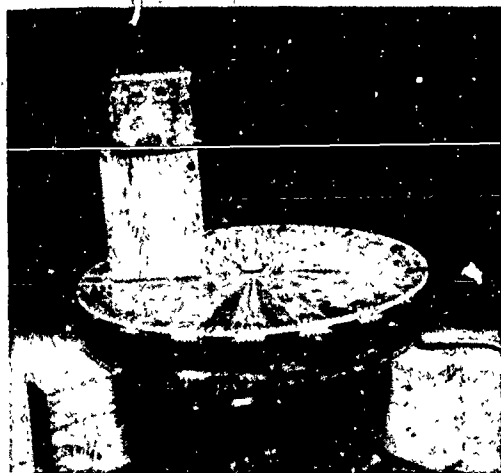
### MAGNETOABSORPTION SIGNAL



**OBJECT LOCATION:** 1-3/4"

**VERTICAL SEN:** 0.5 V/cm  
3.5 vpp

### INDUCTION SIGNAL



**OBJECT LOCATION:** 4-3/4"

**PHASE INDICATION**

**OBJECT DESCRIPTION:** STANDARD ELECTRICAL OUTLET BOX SWITCH

**CHARACTERISTIC DIMENSIONS:** 2" x 3" x 2-1/2"

FIGURE 18a

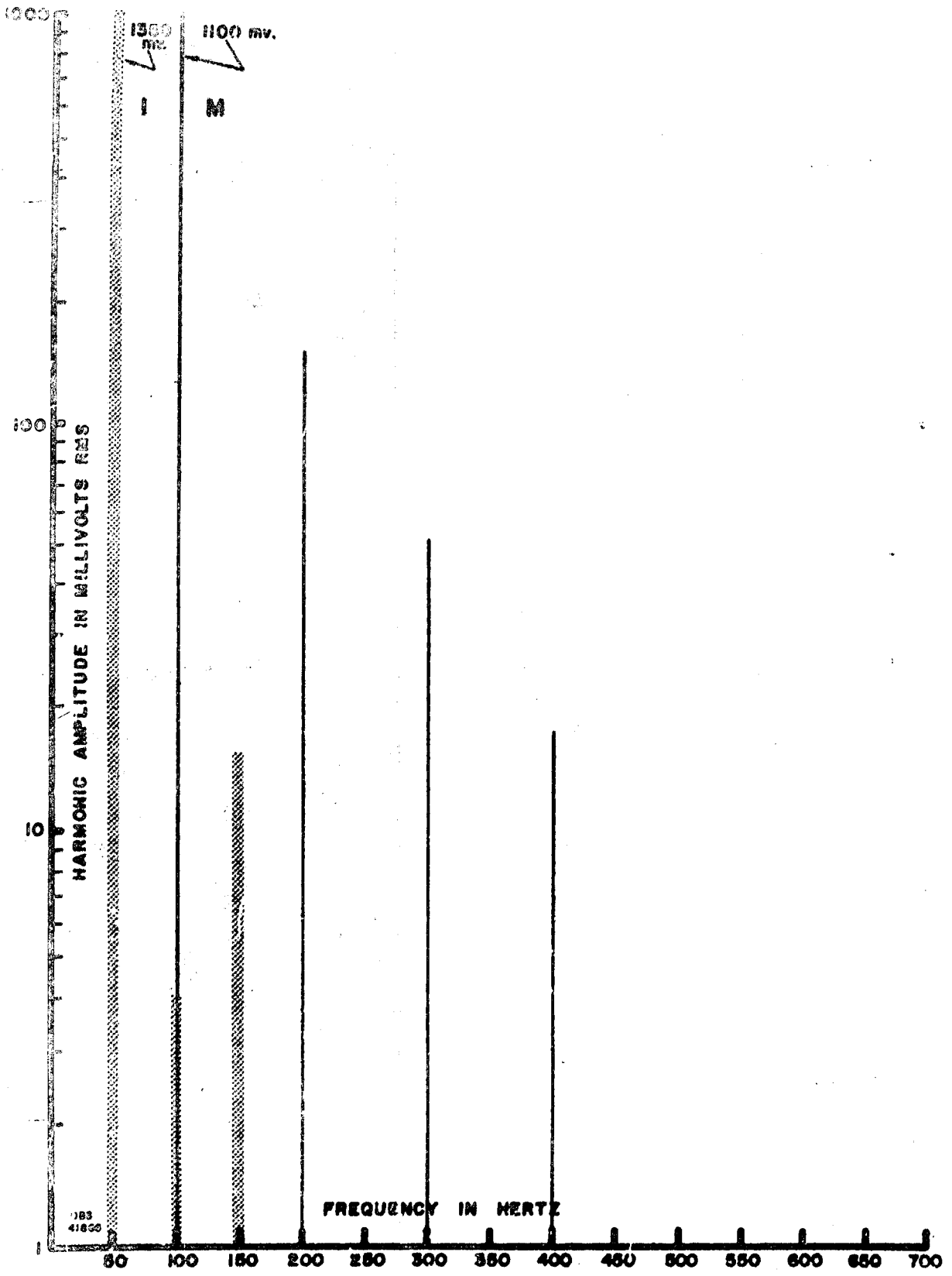
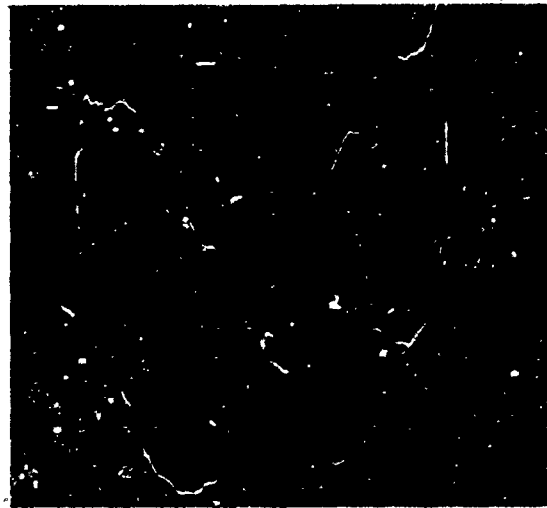


FIGURE 18b. HARMONIC AMPLITUDES FOR AN ELECTRICAL OUTLET BOX



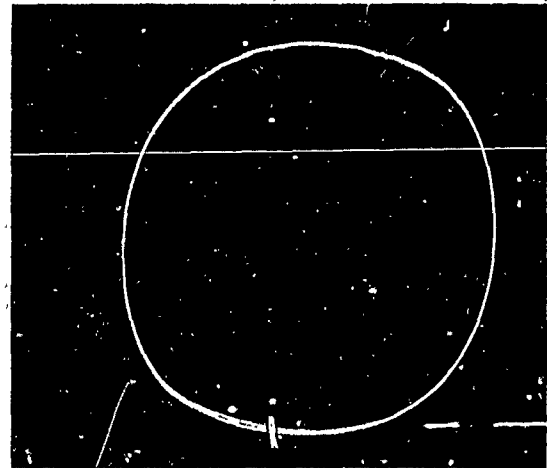
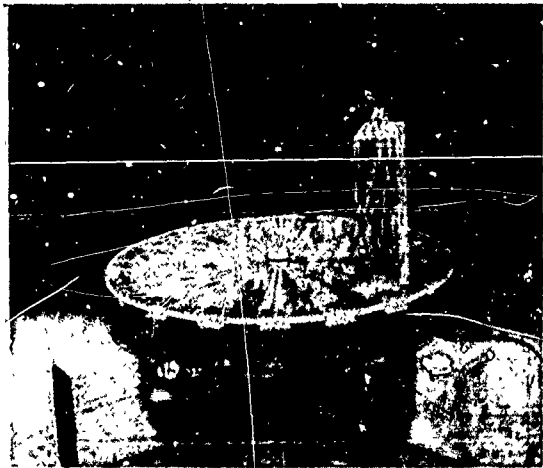
# MAGNETOABSORPTION SIGNAL



OBJECT LOCATION: 1/2"

VERTICAL SEN: 0.2 V/cm  
1.2 Vpp

# INDUCTION SIGNAL



OBJECT LOCATION: 4-3/4"

PHASE INDICATION

OBJECT DESCRIPTION: POGGLE BOLT

CHARACTERISTIC DIMENSIONS: 3/16" x 4"

FIGURE 19a

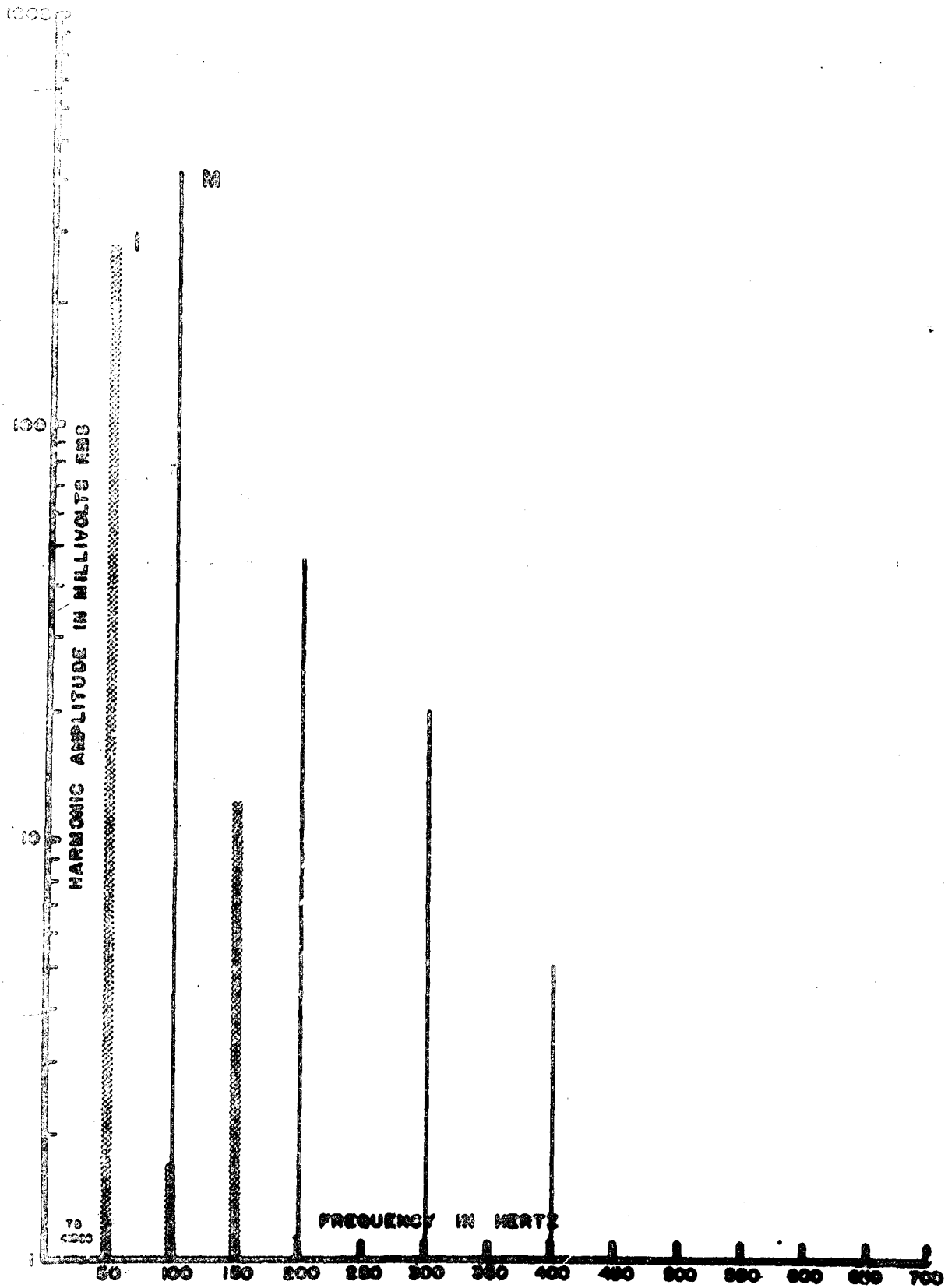


FIGURE 19b. HARMONIC AMPLITUDES FOR A TOGGLE BOLT

amplitudes of Figure 20b also indicate this same material. The induction signal, Figure 20a, also indicates a magnetic conductor with a fair conductivity. The harmonic amplitudes, of Figure 20a, show the large third-harmonic component in the induction as expected from magnetic conductors.

i. Star Bolt

The Star bolt is a brass bolt in a lead sheath. It gave no magnetoabsorption signal and only 5 millivolts of induction signal as shown in Figure 21 which is typical of a nonmagnetic poor-conductor.

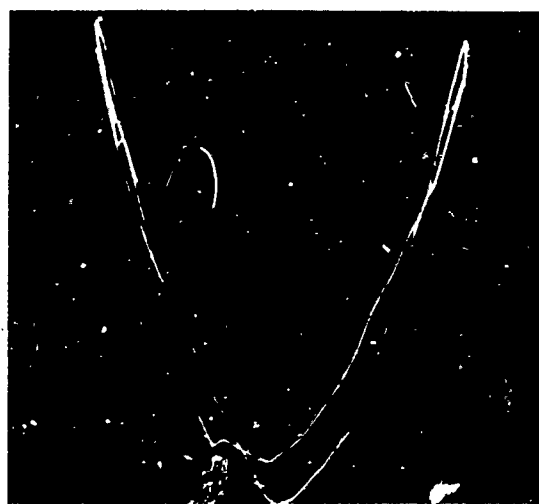
j. Lead Tubing

Lead tubing also gave no magnetoabsorption signal and only 1.5 millivolts of induction as shown in Figure 22. This again is characteristic of nonmagnetic poor-conductors.

k. Metal Plaster Lath

The expanded metal used for plastering gave the strong magnetoabsorption signal of Figure 23a. This signal indicates that the material is soft steel. The amplitudes of the higher harmonics indicate that it is mildly cold-worked. The induction signal in Figure 23a was different from any others, and the harmonic analysis of Figure 23b showed a large fourth-harmonic component as well as large third- and second-harmonic components. These characteristics may be caused by the large area of the material and the number of shorted loops in it.

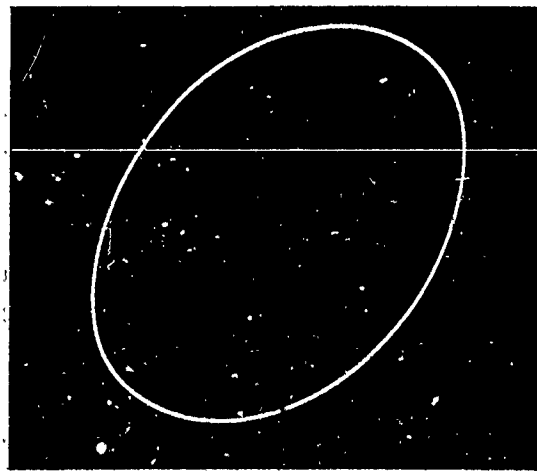
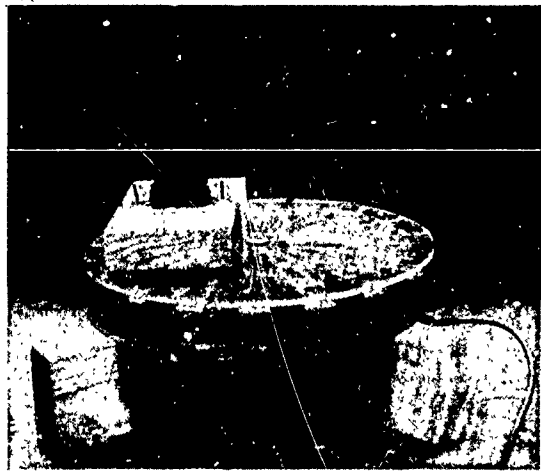
## MAGNETOABSORPTION SIGNAL



OBJECT LOCATION: 1/2"

VERTICAL SEN: 0.5 V/cm  
3.5 vpp

## INDUCTION SIGNAL



OBJECT LOCATION: 1-3/4"

PHASE INDICATION

OBJECT DESCRIPTION: STANDARD SINGLE POLE SWITCH

CHARACTERISTIC DIMENSIONS: \_\_\_\_\_

FIGURE 20a

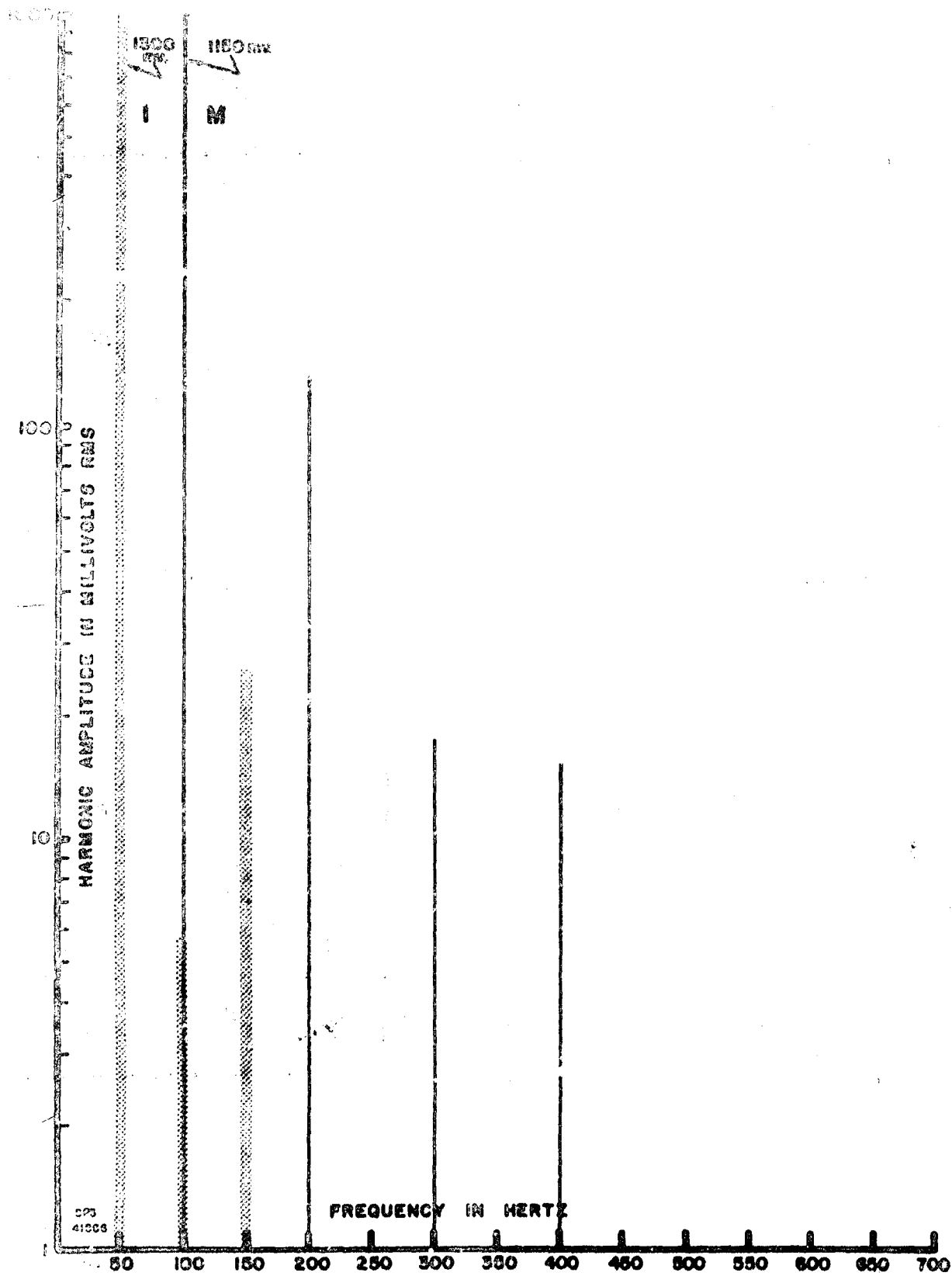
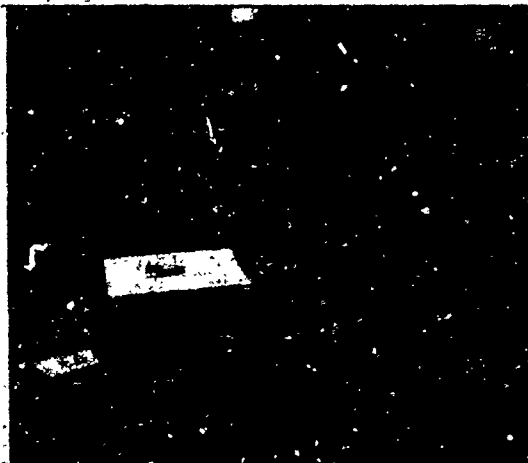


FIGURE 201. HARMONIC AMPLITUDES FOR A STANDARD ELECTRICAL SWITCH

**INDUCTION SIGNAL**



50 Hertz: 5 mvrms

**OBJECT LOCATION:**         ○        

**PHASE INDICATION**

**OBJECT DESCRIPTION:**         STAR BOLT (BRASS BOLT, LEAD SHEATH)        

**CHARACTERISTIC DIMENSIONS:**                         1/4"-20        

FIGURE 21

**INDUCTION SIGNAL**



50 Hertz: 1.5 mvrms

**OBJECT LOCATION:**         1/2"        

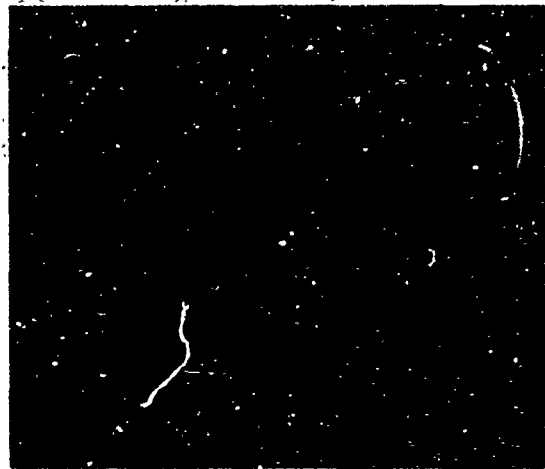
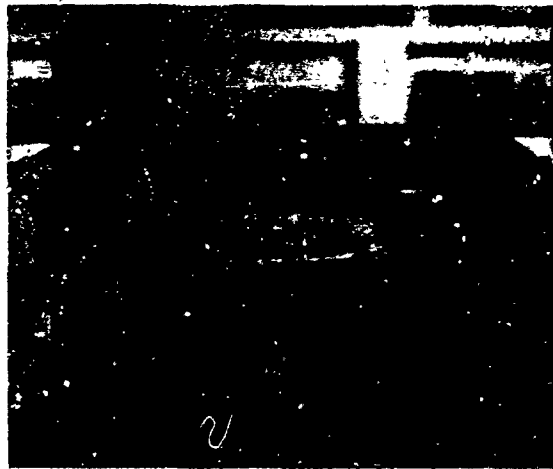
**PHASE INDICATION**  
        Fundamental measurement        

**OBJECT DESCRIPTION:**         LEAD TUBING        

**CHARACTERISTIC DIMENSIONS:**                         3/8" x 5/8"        

FIGURE 22

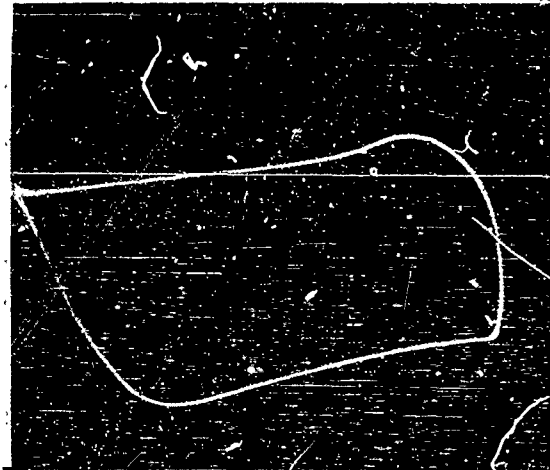
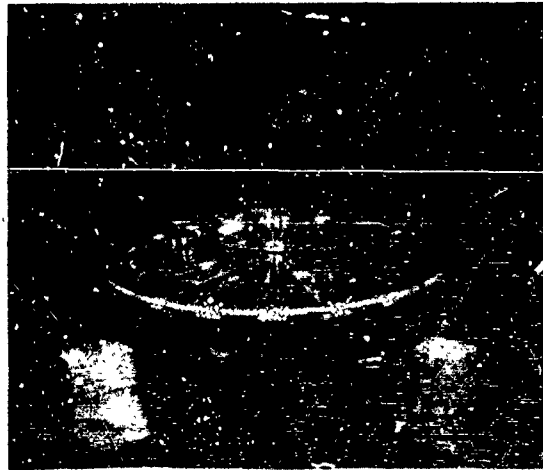
**MAGNETOABSORPTION SIGNAL**



**OBJECT LOCATION:** 3-3/4"

**VERTICAL SEN:** 0.5 V/cm  
2.4 vpp

**INDUCTION SIGNAL**



**OBJECT LOCATION:** 3-3/4"

**PHASE INDICATION**

**OBJECT DESCRIPTION:** PLASTER METAL LATH

**CHARACTERISTIC DIMENSIONS:** 20" x 27"

FIGURE 23a

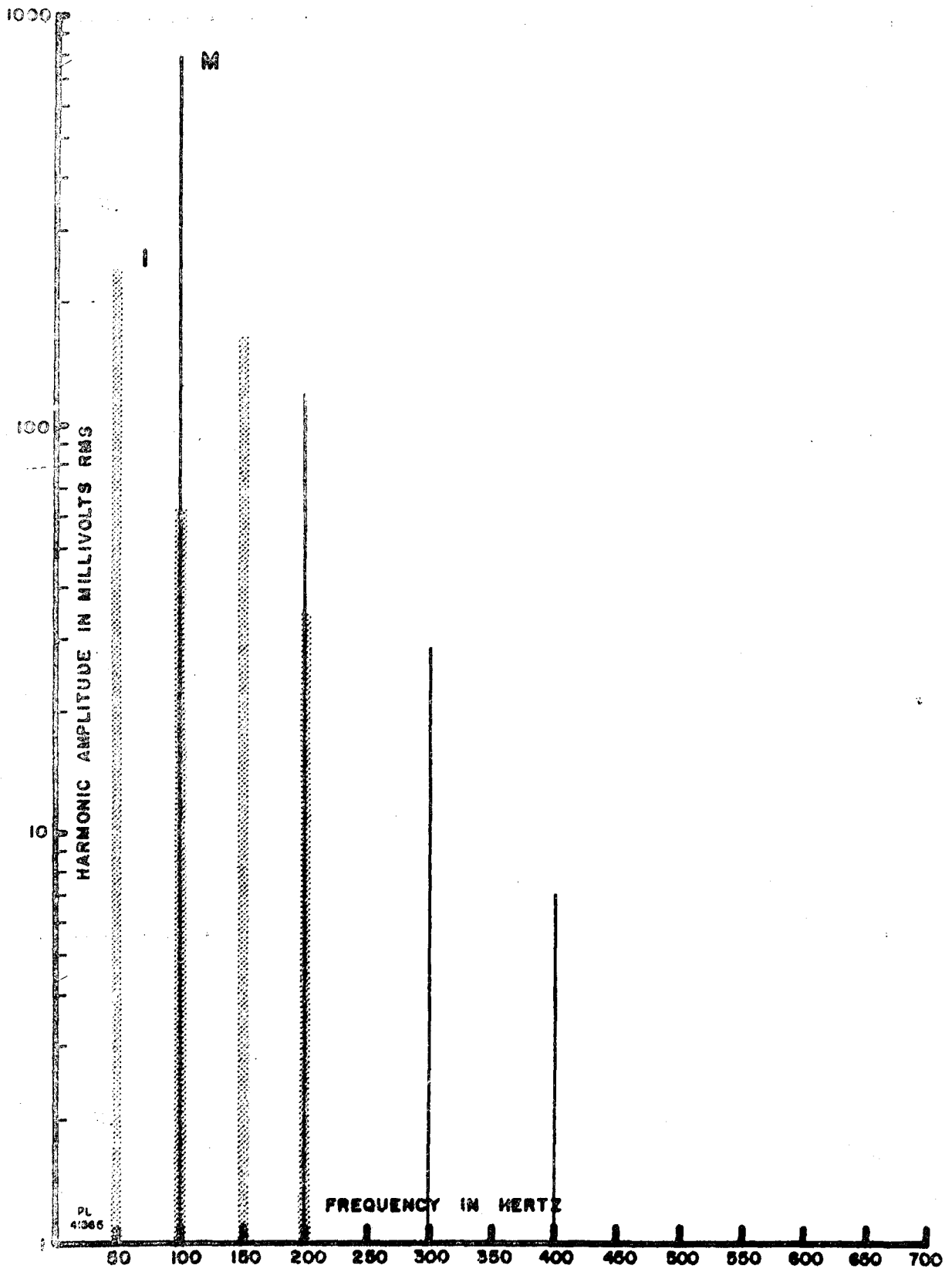


FIGURE 23b. HARMONIC AMPLITUDES FOR METAL LATH



## 2. Electronic Components

### a. Electronic Cables

No oscilloscope presentation could be obtained with either the magnetoabsorption or the induction signals. With a very narrow-band amplifier and a magnetic bias frequency of 1000 cycles, direct induction signals of between 25 and 100 microvolts were obtained. The cables used were regular microphone and two conductor cables 3 to 4 feet long such as Belden 1710, 1450 and 1709.

### b. Aluminum-Encased Microphone

This microphone, although it contained a permanent magnet, gave no magnetoabsorption signal probably because of the radio-frequency shielding effect of the aluminum case. A large induction signal, Figure 24a, was obtained which did show that it came from a magnetic conductor because of its nearly 90° relative phase. The magnetic conductor character of the induction signal was also shown by the third-harmonic amplitude of Figure 24b.

### c. Knowles Microphone

The Knowles Model BE-1530, a very small microphone, also contained a permanent magnet and a metal case. However, this case was an incomplete shield, and the magnetoabsorption signal of Figure 25a was obtained. This shape of magnetoabsorption curve is as predicted for a magnetized material. That is, it contains both a 50-cycle and a 100-cycle component in its magnetoabsorption signal. The harmonic amplitudes of

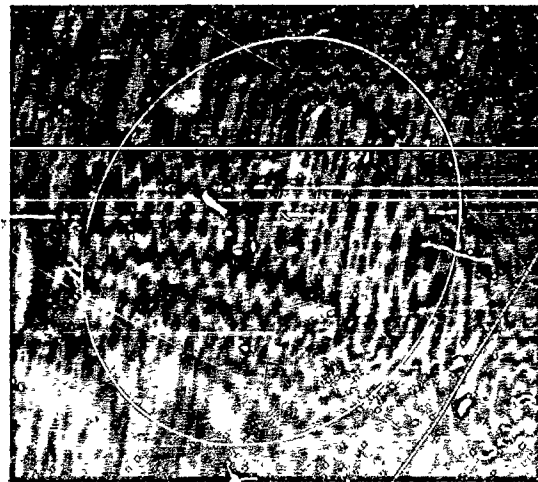
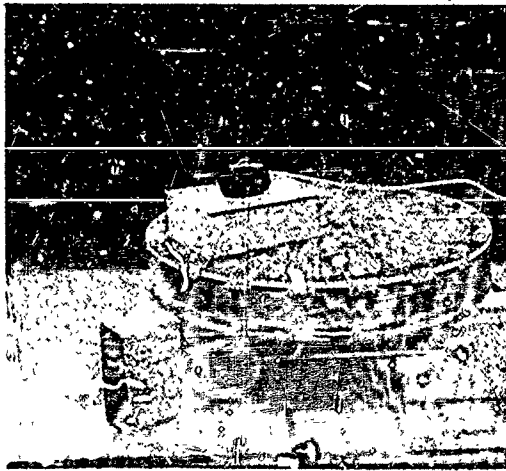
**MAGNETOABSORPTION SIGNAL**

NONE

**OBJECT LOCATION:** \_\_\_\_\_

**VERTICAL SEN:** \_\_\_\_\_

**INDUCTION SIGNAL**



**OBJECT LOCATION:** 1-3/4"

**PHASE INDICATION**

**OBJECT DESCRIPTION:** MICROPHONE (ALUMINUM ENCASED)

**CHARACTERISTIC DIMENSIONS:** 1-3/4" O.D. x 1"

FIGURE 24a

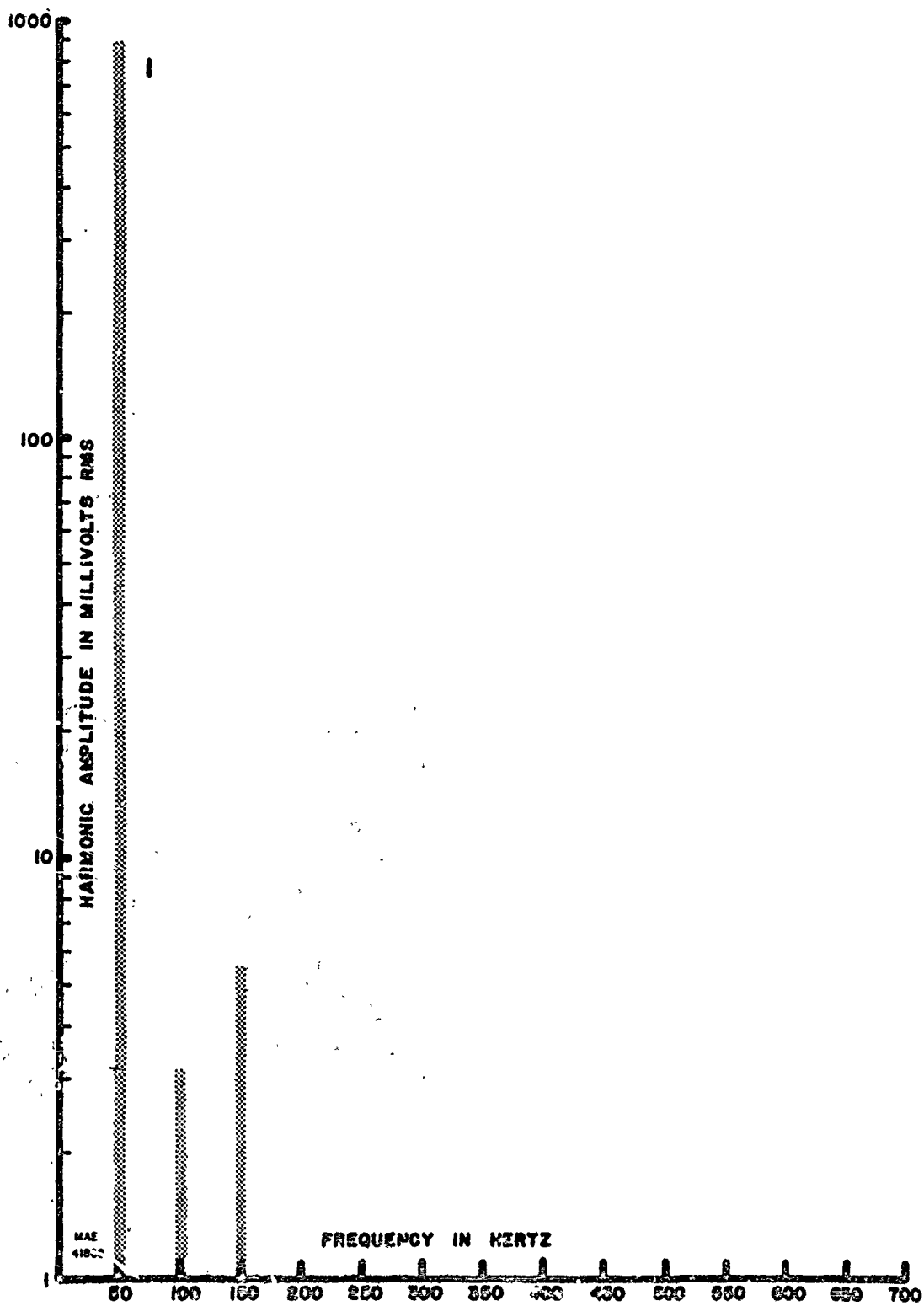


FIGURE 24b. HARMONIC AMPLITUDES FOR AN ALUMINUM-ENCASED MICROPHONE

Figure 25b show that the magnetoabsorption signal from this magnet is composed of a strong 50-cycle component and a weak 100-cycle component. The induction signal is that which would be obtained from a conducting magnetic material as shown by the oscilloscope picture of Figure 25a and the harmonic analysis of Figure 25b.

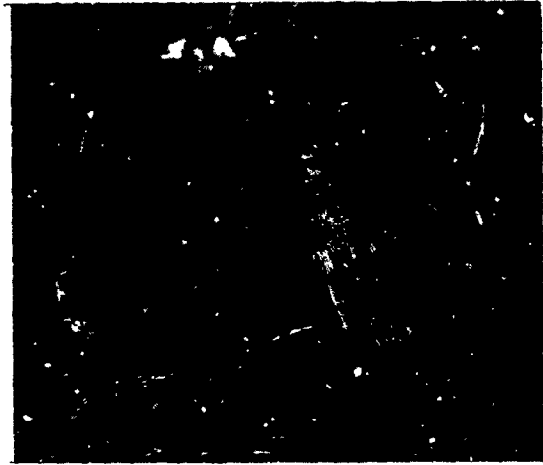
d. Ferrite Rod

A type H Ferramic rod gave a magnetoabsorption signal, Figure 26a, which contained only the fundamental or 100-cycle component as shown by Figure 26b. The induction signal of Figure 26a showed that it was from a magnetic material by its nearly  $90^\circ$  phase angle and that the material had a low conductivity from the absence of a third-harmonic component at 150 cps.

e. Iron Core Choke

The magnetoabsorption signal from a Miller series 4200 radiofrequency choke coil was too small to be photographed on the oscilloscope and so no Lissajous figure is shown in Figure 27a. The harmonic analysis of the magnetoabsorption signal could be measured as shown by Figure 27b. Only the 100-cycle fundamental component of the magnetoabsorption signal could be measured. The induction signal from the choke of Figure 27a showed that it came from a magnetic material, and the small third-harmonic component indicated that it had a very small conductivity. Thus, it had similar characteristics to the ferrite rod except at a much lower level.

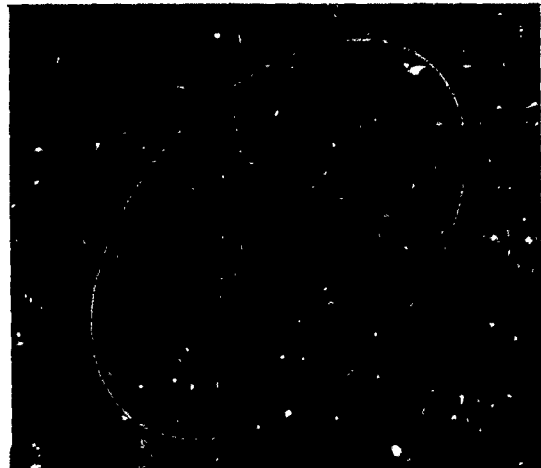
MAGNETOABSORPTION SIGNAL



OBJECT LOCATION: 0"

VERTICAL SEN: 0.2 V/cm  
0.2 vpp

INDUCTION SIGNAL



OBJECT LOCATION: 0"

PHASE INDICATION

OBJECT DESCRIPTION: MICROPHONE (KNOWLES ELECTRONIC MODEL BE 1530)

CHARACTERISTIC DIMENSIONS: 14/32" x 7/32" x 5/32"

FIGURE 25a

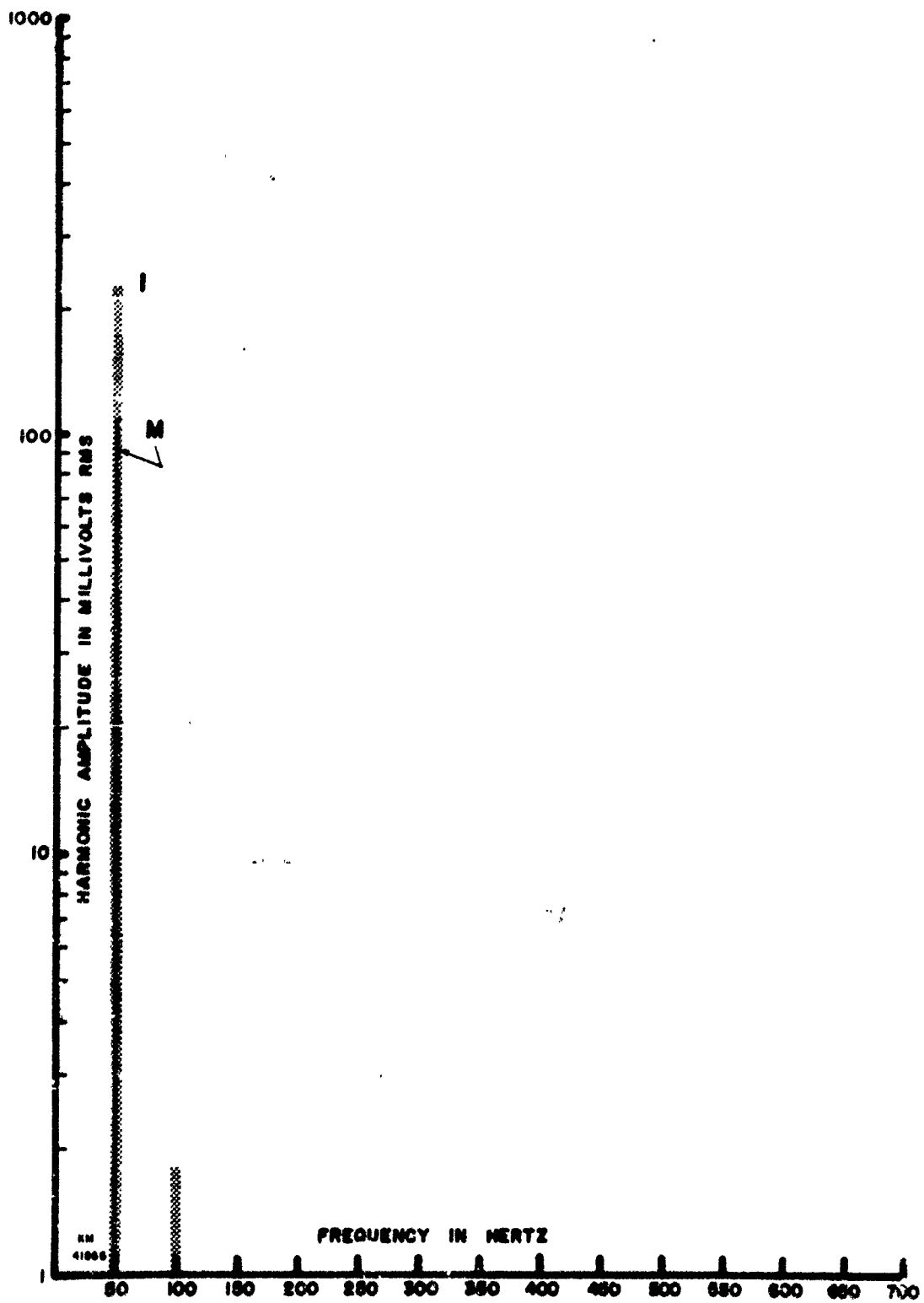
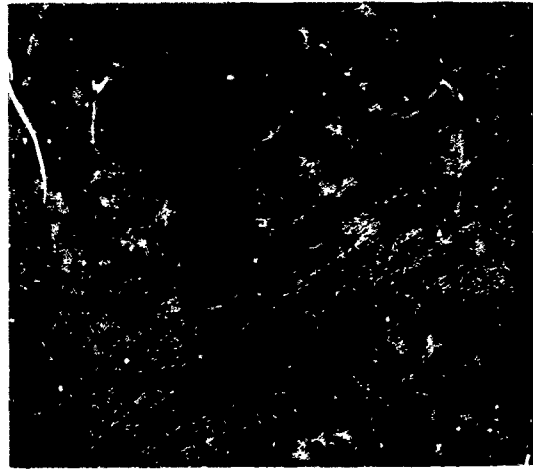


FIGURE 25b. HARMONIC AMPLITUDES FOR A KNOWLES MICROPHONE

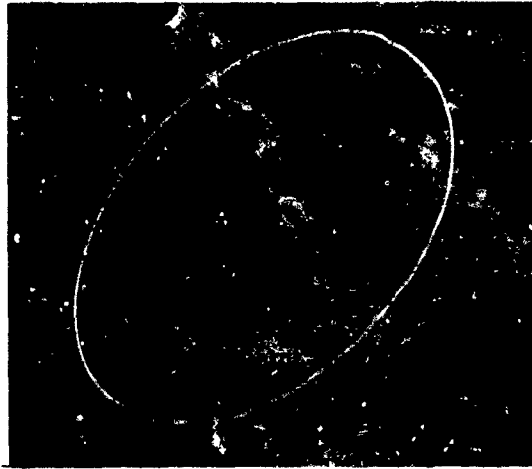
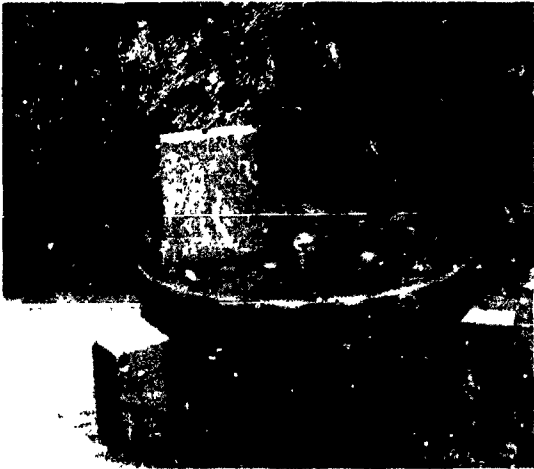
MAGNETOABSORPTION SIGNAL



OBJECT LOCATION: 0

VERTICAL SEN: 0,5 V/cm  
1.0 vpp

INDUCTION SIGNAL



OBJECT LOCATION: 4-3/4"

PHASE INDICATION

OBJECT DESCRIPTION: FERRITE ROD

CHARACTERISTIC DIMENSIONS: 5/16" x 1-3/4"

FIGURE 26a

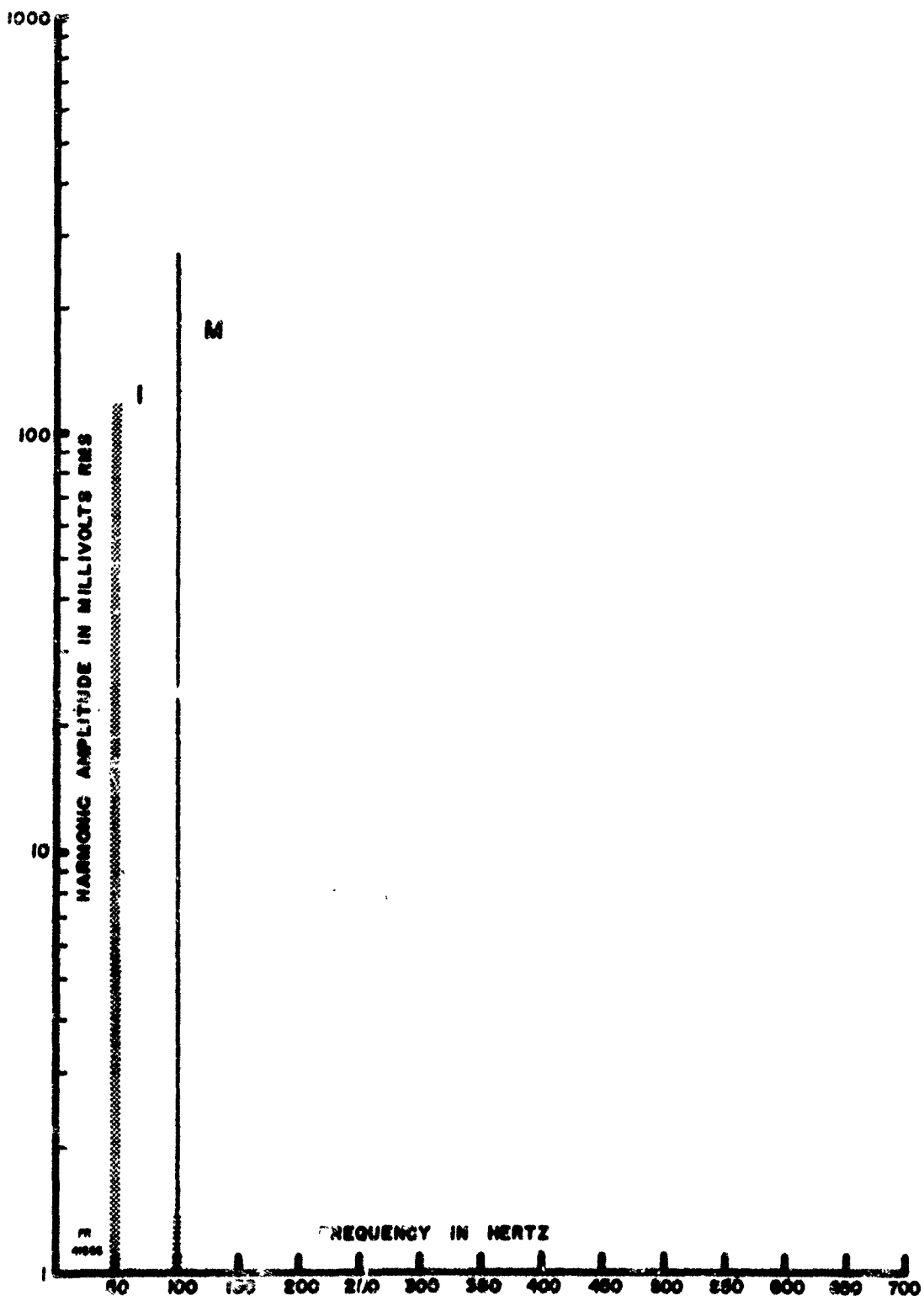


FIGURE 26b. HARMONIC AMPLITUDE FOR A FERRITE ROD



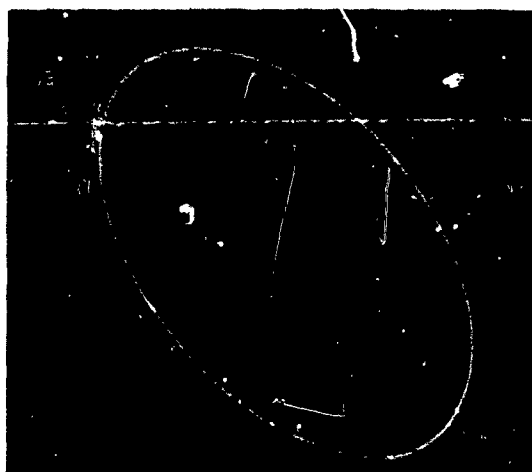
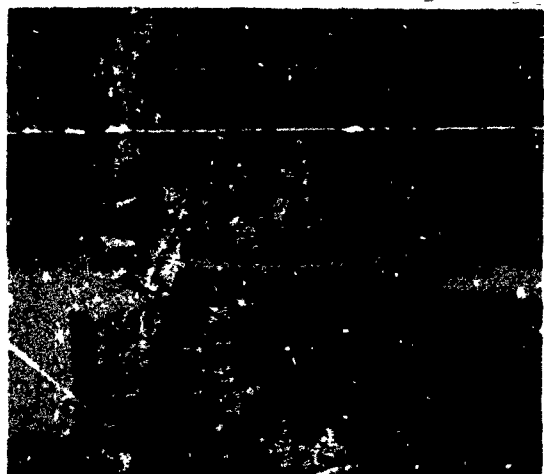
**MAGNETOABSORPTION SIGNAL**

NONE

OBJECT LOCATION: \_\_\_\_\_  
\_\_\_\_\_

VERTICAL SEN: \_\_\_\_\_  
\_\_\_\_\_

**INDUCTION SIGNAL**



OBJECT LOCATION: \_\_\_\_\_  
\_\_\_\_\_

PHASE INDICATION  
\_\_\_\_\_

OBJECT DESCRIPTION: MILLER CHOKE FERRITE CORE (4200 SERIES)

CHARACTERISTIC DIMENSIONS: \_\_\_\_\_

FIGURE 27a

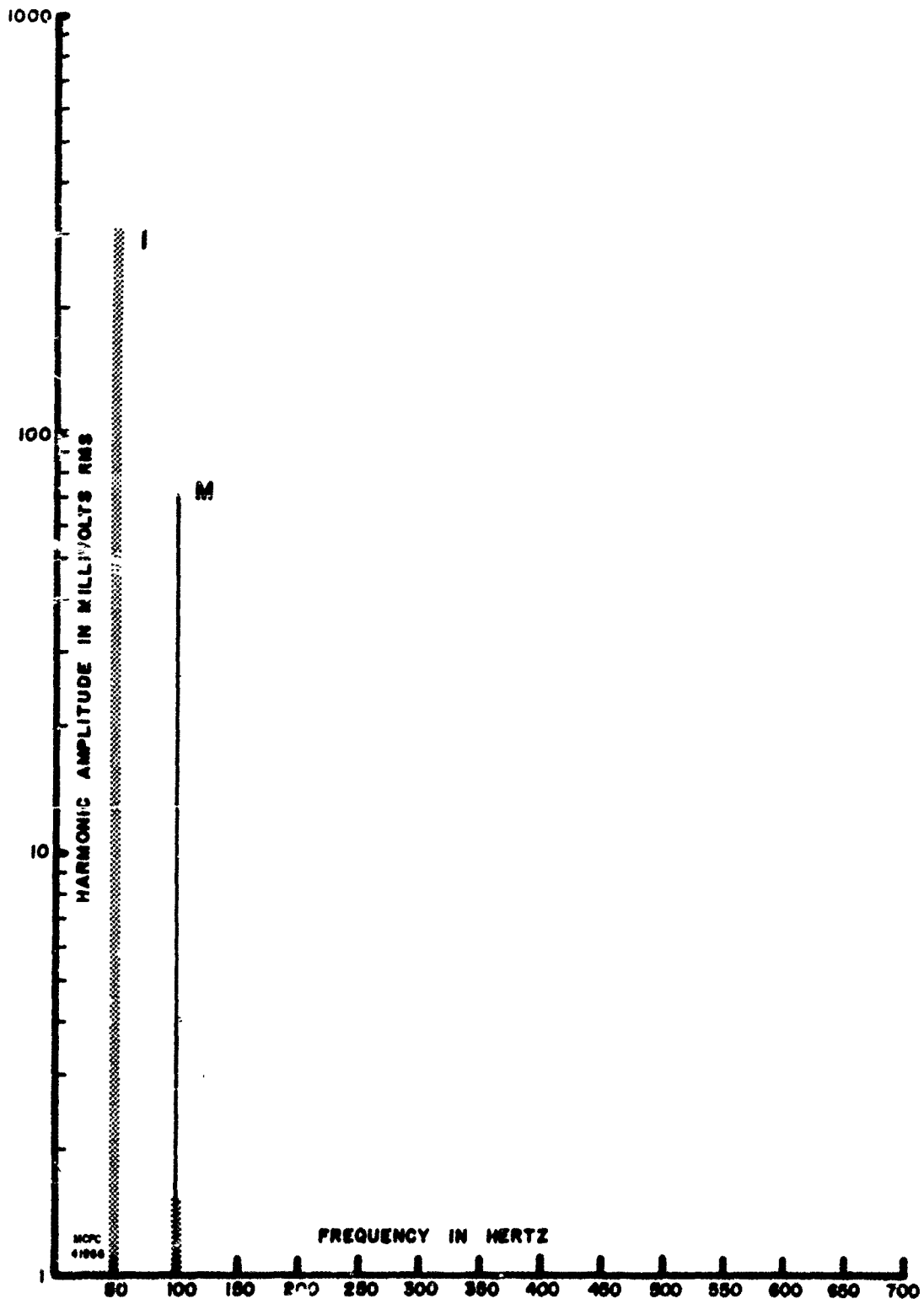


FIGURE 27b. HARMONIC AMPLITUDES FOR AN IRON CORE CHOKE

f. Transistorized Preamplifier

The small audio amplifier used was constructed of standard transistors, resistors and condensers. No magnetoabsorption signal was obtained as shown by Figures 28a and 28b. The induction signal was that which would be obtained from a magnetic conductor. However, the signal was too weak to analyze properly, and the harmonic amplitude graph of Figure 28b shows only the fundamental at 50 cycles.

g. Mercury Cell

The mercury battery used was about 1/4 inch in diameter and 3/16 inch high. It gave a very noisy magnetoabsorption signal as shown by Figure 29. It also gave a very small induction signal as shown also in Figure 29. Both of the signals were too small for a useful harmonic analysis. The magnetoabsorption signal showed a single 100-cycle component and the induction a single 50-cycle component. The signals indicate that they come from a magnetic conductor which may be the nickel case.

h. Printed-Circuit Oscillator

One of the International Crystal, 27-megacycle, crystal oscillators gave a magnetoabsorption signal too small to photograph and display in Figure 30a. The magnetoabsorption signal did have a single 100-cycle component as shown in Figure 30b. The induction signal was quite strong as shown in Figure 30a, and it had both a fundamental at 50 cycles and a third harmonic at 150 cycles. Therefore, the detection head was giving signals from some magnetic conductor on or in some electronic component.

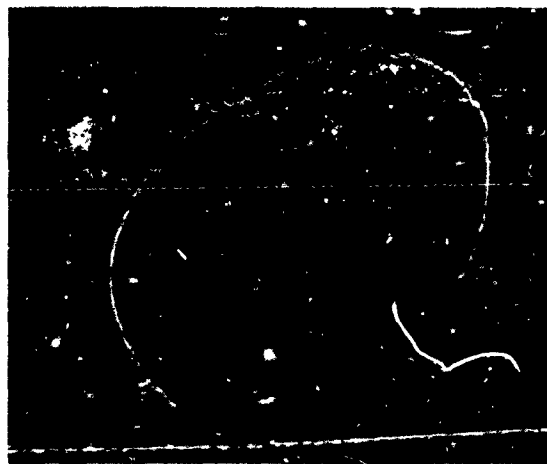
MAGNETOABSORPTION SIGNAL

NONE

OBJECT LOCATION: \_\_\_\_\_  
\_\_\_\_\_

VERTICAL SEN: \_\_\_\_\_  
\_\_\_\_\_

INDUCTION SIGNAL



OBJECT LOCATION: 1-3/4"  
\_\_\_\_\_

PHASE INDICATION  
\_\_\_\_\_

OBJECT DESCRIPTION: SOLID-STATE PREAMPLIFIER  
\_\_\_\_\_

CHARACTERISTIC DIMENSIONS: 3/4" O. D.  
\_\_\_\_\_

FIGURE 28a

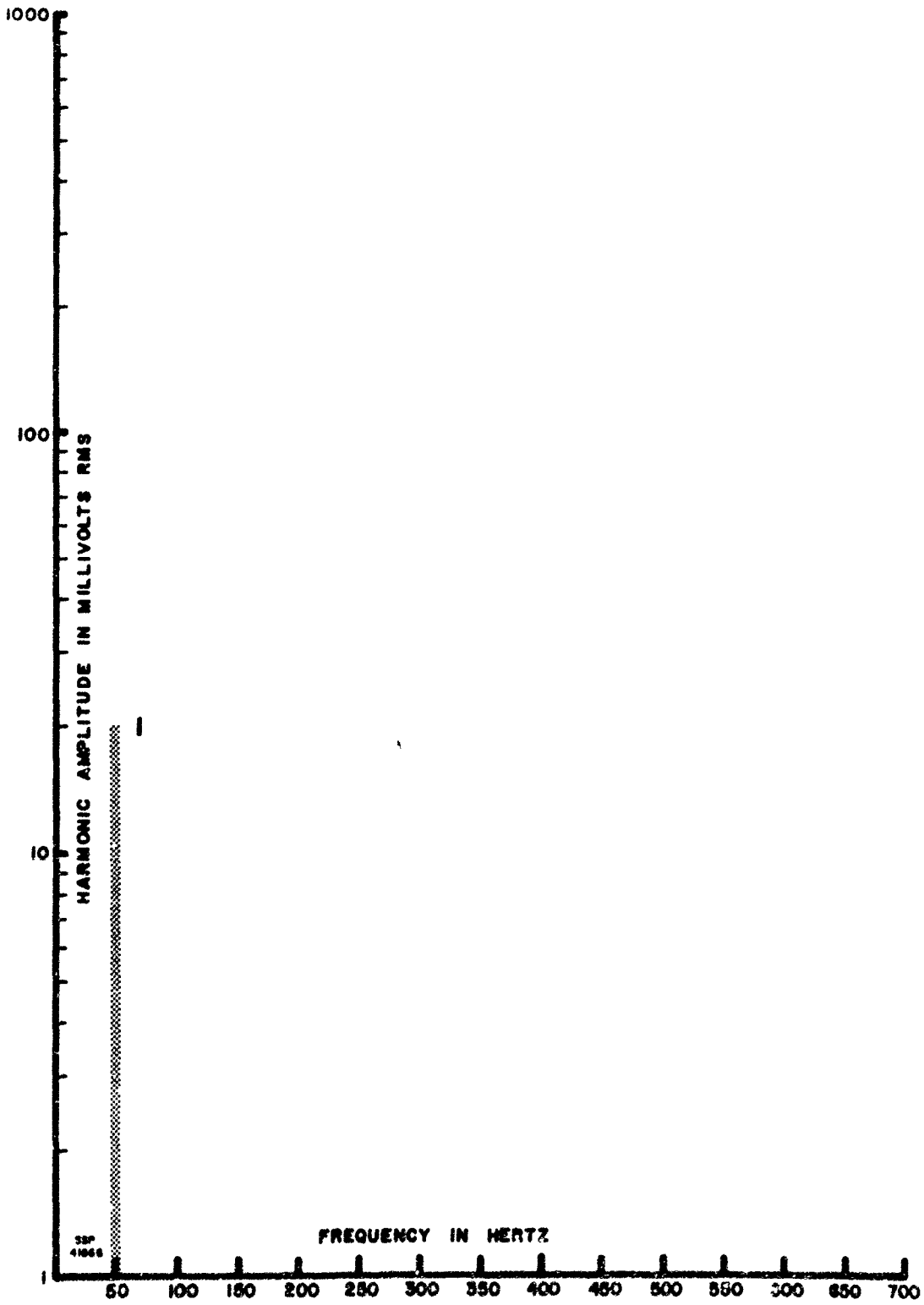
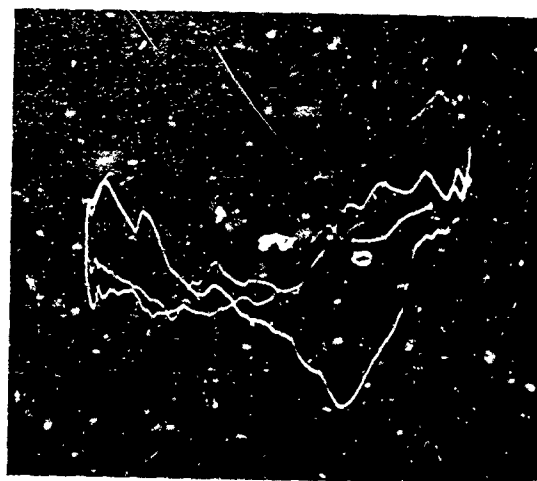
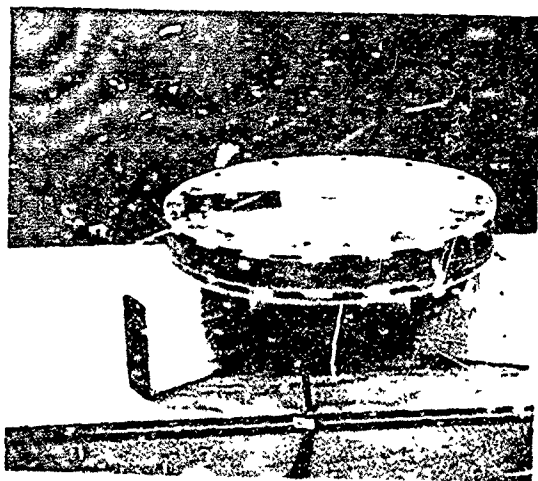


FIGURE 28b. HARMONIC AMPLITUDES FOR A TRANSISTORIZER PREAMPLIFIER

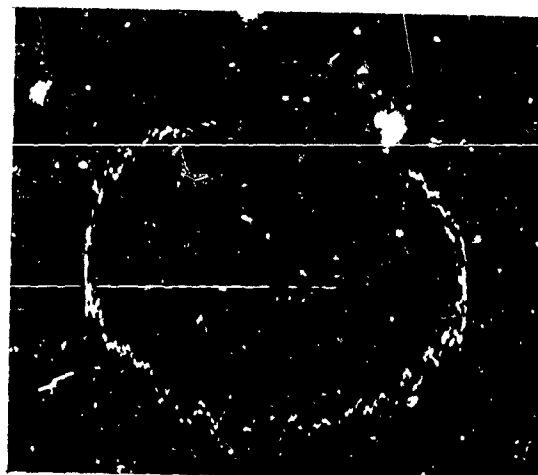
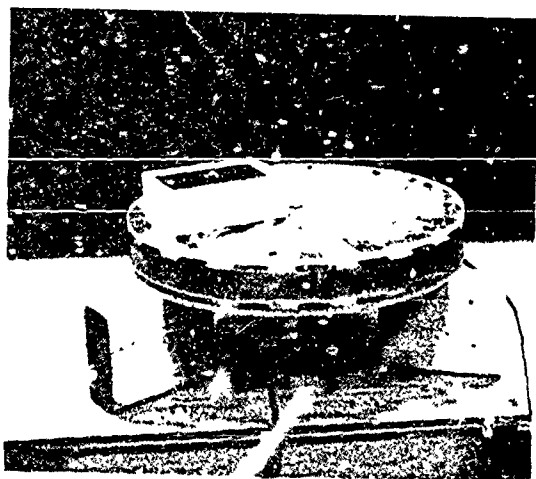
## MAGNETOABSORPTION SIGNAL



OBJECT LOCATION: 0"

VERTICAL SEN: 50 MV/in

## INDUCTION SIGNAL



OBJECT LOCATION: 1-3/4"

PHASE INDICATION

OBJECT DESCRIPTION: MERCURY CELL

CHARACTERISTIC DIMENSIONS: 1/4" O.D. x 1/8"

FIGURE 29

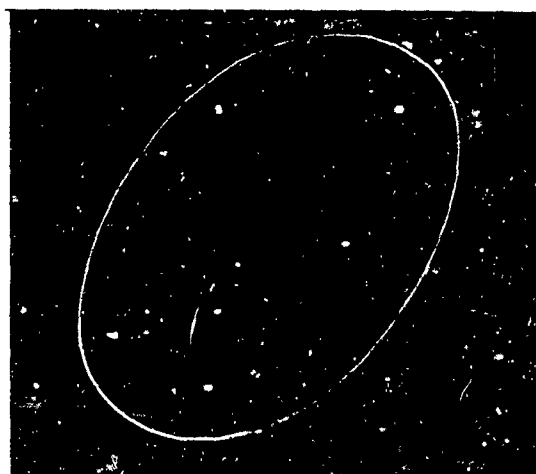
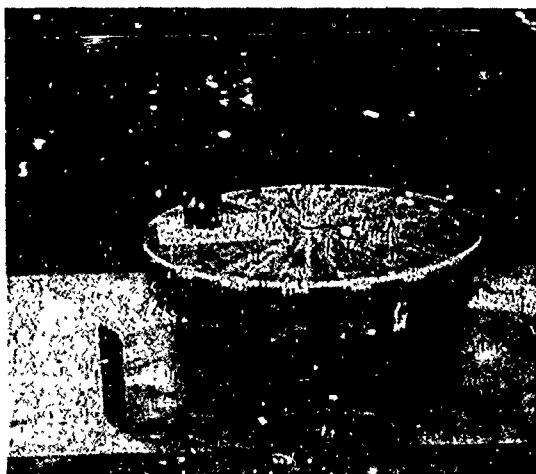
MAGNETOABSORPTION SIGNAL

NONE

OBJECT LOCATION: \_\_\_\_\_  
\_\_\_\_\_

VERTICAL SEN: \_\_\_\_\_  
\_\_\_\_\_

INDUCTION SIGNAL



OBJECT LOCATION:   C    
\_\_\_\_\_

PHASE INDICATION  
\_\_\_\_\_

OBJECT DESCRIPTION:   PC OSCILLATOR  

CHARACTERISTIC DIMENSIONS:   1-1/2" x 1-1/2" x 1-1/4"  

FIGURE 30a

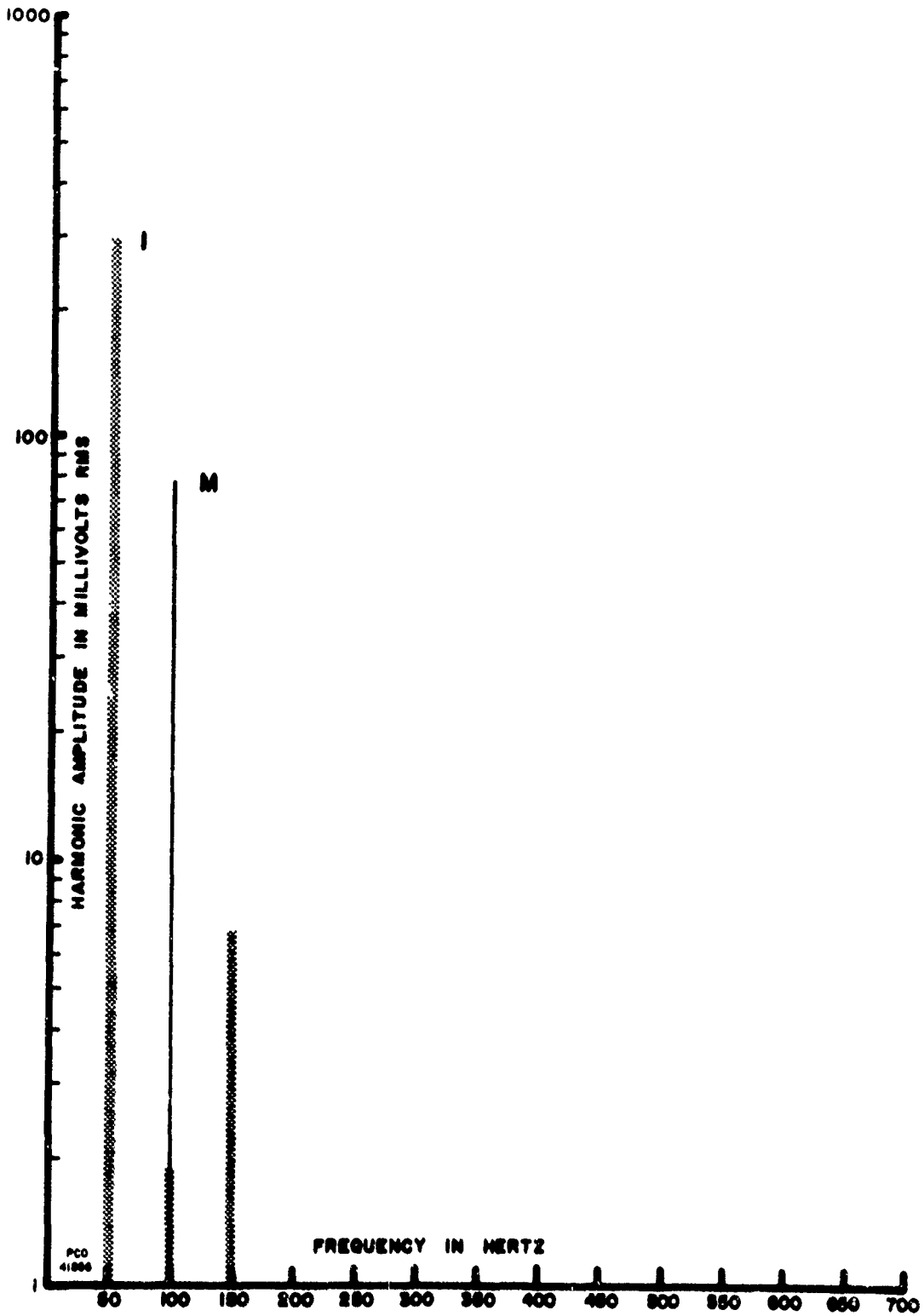


FIGURE 30E. HARMONIC AMPLITUDES FOR A PRINTED CIRCUIT OSCILLATOR



### 3. Summary of Results on Discrete Objects

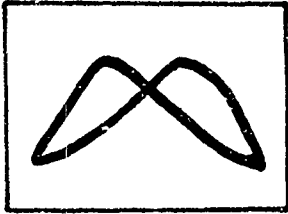
The data presented in Figures 13 through 30 have indicated that a combination of the direct induction and magnetoabsorption detectors into one detection head will permit the detection of discrete objects and the identification of the material from which they are made. The magnetic conductors give a magnetoabsorption signal with higher harmonics and an induction signal with a large third-harmonic component. Magnetic nonconductors give a magnetoabsorption signal with few higher harmonics and an induction signal with a low or no third-harmonic component. In addition, all magnetic materials give an induction signal nearly  $90^\circ$  out of phase with the bias field reference signal. Magnetized materials, unless shielded from radiofrequencies, give a magnetoabsorption signal which contains both a 50-cycle and a 100-cycle signal as well as harmonics of the 100 cycles. A magnet will also give an induction signal with the  $90^\circ$  magnetic phase shift, but it should also contain a third-harmonic component. Nonmagnetic conductors do not give a magnetoabsorption signal but do give an induction signal nearly in phase with the magnetic bias reference.

#### D. Influence of Object to Detector Distance

In order to obtain the greatest utilization of the magnetoabsorption signal as a signature of a material, the shape of the signal should retain its essential characteristics for large changes in the object to detection head distance. It has been found that this condition is met for two materials whose distance was changed from less than an inch to over 2 inches

Figure 31 shows the magnetoabsorption signals for two distances from two materials - one of relatively low permeability and one of high permeability. Figures 31 (a) and (b) show the magnetoabsorption signals from iron at 11/16 inch and at 2 inches. The shapes appear very similar and have retained all of their essential characteristics.

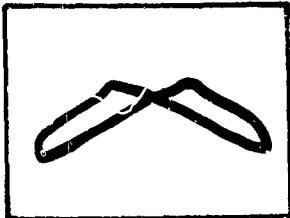
A similar indication is found for the Genetic sample at 11/16 and 2 inches as shown by Figures 31 (c) and (d). If the harmonic analyses of the four magnetoabsorption signals were made, they would show a large variation but they would still retain their essential characteristics. That is, the signals of Figures 31 (a) and (b) each have a large fundamental amplitude at 100 cycles with the higher harmonics having a low amplitude. Similarly, the signals of Figures 31 (c) and (d) have essentially the same harmonic character; that is, high amplitude fundamental at 100 cycles and a high amplitude of higher harmonics.



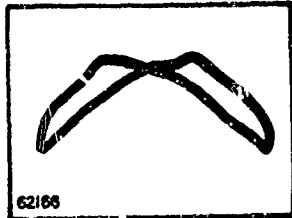
a. Magnetoabsorption Lissajous for an iron sample at 11/16 inch.



b. Magnetoabsorption Lissajous for an iron sample at 2 inches.



c. Magnetoabsorption Lissajous for a conetic sample at 11/16 inch.



d. Magnetoabsorption Lissajous for a conetic sample at 2 inches.

FIGURE 31. THE VARIATIONS OF THE MAGNETOABSORPTION SIGNAL WITH OBJECT HEIGHT

### III. DISCUSSION

#### A. Electromagnetic Studies on Magnetic Void and Discrete Object Detection

A search of the literature was conducted to find a suitable electromagnetic model for the magnetoabsorption mine detection scheme. It is envisioned that the configuration may be represented by a current carrying radiofrequency coil laying parallel to a finitely conducting half-space (the earth) with electrical parameters  $\mu_2$ ,  $\epsilon_2$  and  $\sigma_2$ . Induced eddy currents in conducting half-space modify the magnetic field above the interface and so change the flux distribution around the radiofrequency coil. The change in flux distribution appears as an impedance change in the radiofrequency coil compared to the free space impedance of the coil. A buried mine may now be represented by a cylindrical cavity with electrical parameters,  $\mu_1$ ,  $\epsilon_1$  and  $\sigma_1 = 0^*$  embedded in the conducting media laying coaxially beneath the radiofrequency coil. This cavity then further alters the flux distribution and decreases the effect of the media on the impedance of the radiofrequency coil. The influence of magnetic bias coils may be represented by a slowly varying magnetic bias field that alters uniformly the permeability of the conducting half-space. The variation in permeability of the media caused by the bias field also causes changes in the impedance of the radiofrequency coil and results in a magnetoabsorption signal when suitably detected. From

---

\*In general, the conductivity of a mine may be other than zero.

the above discussion, it is understood that the impedance change in the radio-frequency coil caused by the cavity arises from two sources. These sources are identified as a decrease in eddy current losses caused by the presence of the cavity under static bias field conditions and by a decrease in the effective permeability resulting from the presence of the cavity under varying bias field conditions. Both will decrease the magnetoabsorption signal whenever a cavity occurs beneath the radiofrequency coil. It is in this manner that a buried magnetic void is located.

The literature search indicated that many have treated the problem of the impedance of a filamentary coil placed near a conducting sheet of half-space [1 - 5]. However, the solution of the case with the imbedded cavity was found to have not been treated.

The magnetic vector potential for the case with a cylindrical cavity can be readily established. However, the numerical calculations would have required involved computer methods and were not attempted. Changes in impedance caused by the cavity and the permeability, for example, could have been determined by numerically comparing the cases with and without a cavity. Had time permitted, such an analysis could have yielded design guidance to determine the influence of coil diameter, detection height, frequency of the driving current, and mine depth and to determine whether amplitude or frequency demodulation would have been best. However, since such information was not readily available, experimental techniques were used to obtain design information.

A similar search of the literature was conducted for an electromagnetic model suitable to discrete object detection and discrimination. Two approaches are required, one for the induction technique and the other for the magnetoabsorption technique. The induction method encountered in geophysical exploration and metallic mine detection is well described in technical publications [6 - 10]. In this method, an alternating magnetic field produced by a transmitter induces a magnetic dipole moment in metallic objects in the field of the detector head. The external field of the magnetic dipole moment in turn induces a small voltage in the transmitter coil or in a passive secondary receiver coil. The phase of the induced voltage serves as an indication of the electrical properties of the object, and the amplitude of the induced signal serves as an indication of the distance of the object. This induced voltage may be related to a change in impedance of the transmitter coil or a passive receiver coil. When a passive receiver coil is employed, it is normally designed to achieve a null condition to the induction field of the transmitter coil. When an object is present, the field configuration is perturbed, and a voltage in the receiver coil is produced. In this manner, the induction system can be considered as a changing mutual inductance, caused by the object, between the transmitter and receiver coils.

The magnetoabsorption principle for ferromagnetic or ferrimagnetic objects differs from the induction principle. In this method, a ferromagnetic or ferrimagnetic object is placed within the fields: (1) of a radiofrequency

coil which is the inductance of the tuned circuit for a marginal-oscillator, and (2) of a slowly varying magnetic bias coil. The object will absorb energy from the radiofrequency field at a rate twice that of the frequency of the bias field. Therefore, these absorptions change both the oscillation amplitude and the frequency of the marginal-oscillator. That is, the changes in absorption are a consequence of the changing magnetic moment of the object which may be regarded as a small current loop whose impedance is a function of bias field intensity since its magnetic permeability is a function of this magnetic bias. If the frequency of radiofrequency field is entirely controlled by the radiofrequency coil, then not only amplitude modulations will occur but frequency modulations will be present as the objects equivalent reactance changes because the effective permeability of its material changes as a function of the strength of the bias field. The amplitude modulation, called the magnetoabsorption amplitude signal, can be stripped off by an amplitude detector. The frequency modulation, called the magnetoabsorption frequency signal, is obtained by using a frequency discriminator. In the marginal-oscillator, the frequency modulation causes negligible amplitude modulation and vice versa because the oscillator is operating in its most linear region.

The amplitude modulations and the frequency modulations are uniquely related to the magnetic properties of the object. Objects having different properties will demonstrate different magnetoabsorption waveforms which can be used as signatures. Thus, these signatures can be related to the kind

of material from which the object is constructed. Further, knowledge of the kind of material will help identify the type of object.

Magnetoabsorption, as related to discrete object detection, exhibits different characteristics from the induction type of detector. A similarity exists only in the fact that the same coils can be used for both methods. A subtle difference occurs in the effective impedance of the object as it is influenced by the intensity of the bias field. The reflected impedance in the receiver coil for the induction case is a function of the conductivity and the permeability at the frequency of the magnetic bias field or 50 cycles. For magnetoabsorption, the impedance reflected into the radiofrequency coil depends upon the permeability at the radiofrequency (500 kcs) and how this permeability changes with the magnetic bias field. For strong magnetic bias fields and conducting nonmagnetic materials, the permeability may be regarded as constant; in which case, the received induction signal is composed of the frequency of the bias field with negligible harmonics. For the case of magnetic conductors, the induction signal will have a much larger amount of the odd harmonics of the transmitter frequency. If the object is magnetized, the even harmonics will also exist. This would mean that 50, 100, and 150-cycle components would be present in the induction signal in varying amounts, depending upon the object.

In the magnetoabsorption detection, which depends upon both the magnetic bias field and the field of the radiofrequency coil, the radiofrequency



field is kept at a low level so that negligible harmonics are developed by the influence of the object. The magnetic bias field is made very large so that the major portion of the hysteresis loop of the object is traversed each cycle. Since this magnetic bias field causes a change in the radiofrequency permeability of the object, it also causes a change in its reflected impedance in the radiofrequency coil. Since the change in permeability is the same for positive magnetic bias as it is for negative values, the permeability changes at twice the frequency of the magnetic bias field. Thus, the fundamental frequency for the magnetoabsorption is 100 cycles for a 50-cycle bias field. Since the permeability change is very nonlinear, harmonics at 200, 300, 400, 500 and 600 cycles will be present in varying amounts, depending upon the type of material in the object. Thus, the magnetoabsorption signal contains only even harmonics of the magnetic bias frequency. An object having a straight line B/H curve (no hysteresis) would have only 100 cycles in its magnetoabsorption signal, whereas an object having a square-loop configuration to its hysteresis may have the harmonics of a 100-cycle square wave.

Thus, the two detection systems, magnetoabsorption and induction, can be used together in one detector to both detect the presence and describe the materials in a hidden discrete object. The different signals obtained in the two manners should provide a means for reducing ambiguity. For the magnetic-void detection, the buried object will cause a decrease in the

magnetoabsorption signals from the magnetic materials in the soil. This decrease can be measured by using the magnitude of one or more of the even harmonics of the bias frequency in the magnetoabsorption signal.

Therefore, both the magnetoabsorption system alone for the detection of magnetic voids in soil as well as the combination of magnetoabsorption and direct induction for the detection of discrete objects can use a detection head which contains a magnetic bias coil driven at a low frequency of around 50 cycles and a radiofrequency coil at 500 kilocycles. In both cases, the direct induction at 50 cycles is reduced to null in the radiofrequency coil by shaping the coil in the double-D fashion. For both measurements, the radiofrequency coil is made the inductance of the tuned circuit of an oscillator. The magnetoabsorption signal is an amplitude or a frequency modulation of the voltage across the coil. The direct-induction signal is a 50-cycle signal added directly to the voltage in the coil. Therefore, the two signals can be separated by filters and detected. The magnetoabsorption amplitude signal is selected by a high-pass filter and obtained by means of an amplitude detector. The magnetoabsorption frequency signal is obtained by means of a frequency discriminator. Since each should contain nearly the same information, only the amplitude signal has been used. The direct-induction signal is selected through a low-pass filter and requires no further processing. The following paragraphs will describe the components developed to produce the equipment required to simultaneously measure these two signals.

## B. Detection Head Assembly

The detection head consists of two parts:

- (1) The bias field coil which produces a strong magnetic field to modulate the permeability of the soil or the discrete object.
- (2) The radiofrequency coil which produces a radiofrequency field from which energy is absorbed at a rate twice the frequency of the bias field and which causes a modulation of the frequency if the radiofrequency coil is the frequency controlling element of a marginal-oscillator.

In the consideration of the proper probe geometry, the following design considerations were made:

- (1) The radius of both coils should be comparable to the depth of the buried object, and its area should be comparable to its cross-sectional area. As derived from considerations of Biot-Savart's law, the field\* of a current loop is expressed as

$$H(z) = \frac{NIa^2}{2(z^2 + a^2)^{3/2}}$$

along the axis of the loop where  $a$  is its radius and  $z$  is the distance along the axis. From this expression, it is understood that the field intensity falls off as  $1/z^3$  and is inversely proportional to  $a$  at the center. From the nature of the formula, it is further understood that the field varies rather slowly until  $z$  approaches  $a$ . Thus, if the object is to present a large filling factor to the probe, it is important that the object be within a distance equal to the radius of the coil.

- (2) Since the radiofrequency detector coil will be placed directly in the magnetic field of a bias coil, the geometry of the radiofrequency coil must be such as to eliminate the induction from

---

\*The validity of this expression at the frequencies of interest is supported by experiment and by the fact that the period of the operating frequencies is much less than the propagation time in the region of greatest influence.

the bias field directly into the radiofrequency detection coil since large bias field voltages in the detector would greatly reduce the sensitivity level of the detection system. Further, for experimental flexibility, provisions for cancellation adjustments should be made since the bias field is not uniform over the entire area of the radiofrequency coil.

- (3) The radiofrequency coil should be designed to provide shielding from outside radiofrequency sources without degrading the sensitivity of the magnetoabsorption detection which is proportional to  $Q$ .
- (4) To avoid microphonics, the shielding, windings, and supports for the coil should be rigidly constructed.

The field of the bias coil, which modulates the permeability of the soil, was designed to serve as the main structural member of the detector head assembly. The Lucite coil form, designed to accept 176 turns of #16 AWG Formvar-clad copper wire, is shown in Figure 32. The form has a radius of 6.5 inches which is comparable to the anticipated object's 6-inch depth. The windings were packed tightly on the bobbin to avoid vibrations resulting from Lorentz-type forces between current carrying conductors. The outer windings were impregnated with epoxy cement and a fiber glass cover was applied to reinforce the Lucite-form, to seal the coil, and to assure additional winding rigidity. The designed and measured characteristics of the magnetic bias field coil are shown in Table I.

The radiofrequency coil was designed to fit concentrically within the bias field coil. The direct induction into the radiofrequency coil from the bias field is cancelled by a mutual-aiding double-D coil geometry. Early in the work, the necessity of precise geometries and adjustment techniques for

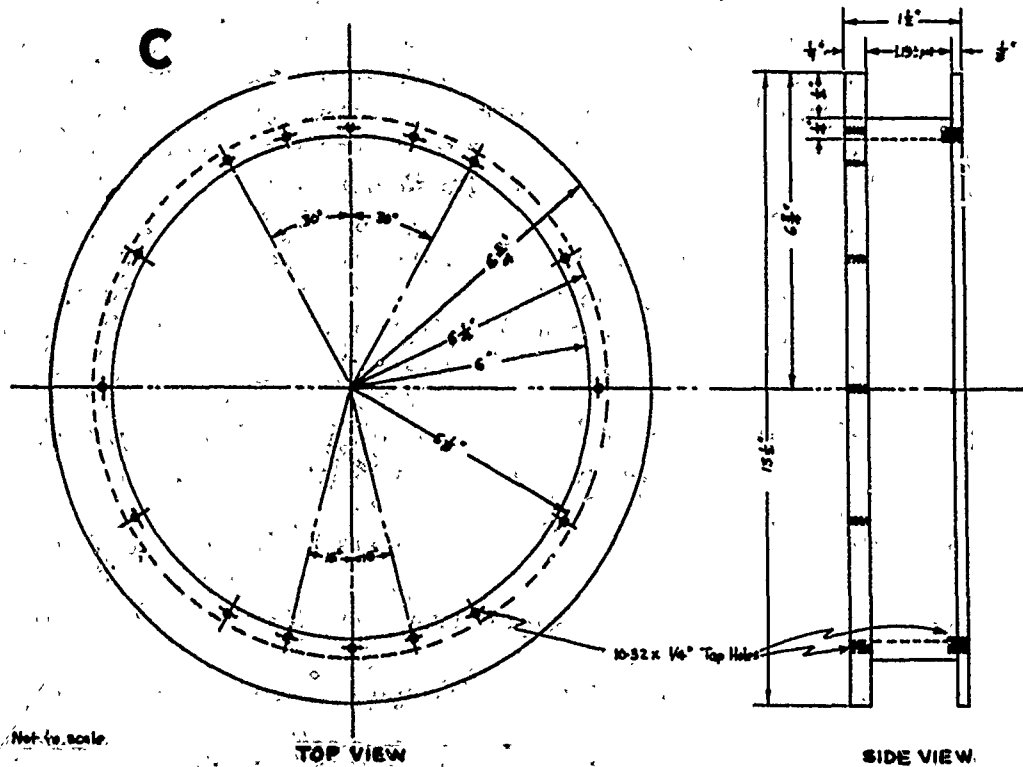


FIGURE 32. MAGNETIC BIAS FIELD COIL FORM

TABLE I. MAGNETIC BIAS COIL CHARACTERISTICS

<u>Parameter</u>	<u>Predicted</u>	<u>Measured</u>
DC resistance	2.58	2.38
Inductance	16.78 mh	18.5 mh
Gauss/ampere at the center of the coil	6	6

improved cancellation became evident. Consequently, the radiofrequency coil bobbin was designed to form a platform having 3 degrees of freedom corresponding to the distance and the two angles of a spherical coordinate system within an assembly supported by the bias coil. Measurements demonstrated that, by this technique, the voltage in the radiofrequency coil from the magnetic bias coil at 50 cycles can be reduced to a value below 1 microvolt with a bias field intensity of 24 gauss.

The first radiofrequency coil constructed and tested is shown in Figure 33. The 11-1/2-inch diameter coil form was threaded to separate the windings thereby reducing interwinding capacitance. The electrical properties of the radiofrequency coil are listed in Table II, and Figure 34 gives the graph of the quality factor\* of the coil as a function of frequency. The Q was measured with a Boonton, Model 260-A, Q meter. A shield of copper-clad flexible laminate was prepared for the coil. The shield was split

TABLE II. ELECTRICAL PROPERTIES OF THE  
11-1/2-INCH RADIOFREQUENCY COIL

Type of wire	=	#30 AWG-enamel
Turns per inch	=	52
Number of turns per "D"	=	24
Inductance	=	1.16 mh
Q at 500 kilocycles	=	85 (without shield)

\*The quality factor, Q, of an inductor is defined as  $Q = \omega L/R_c$

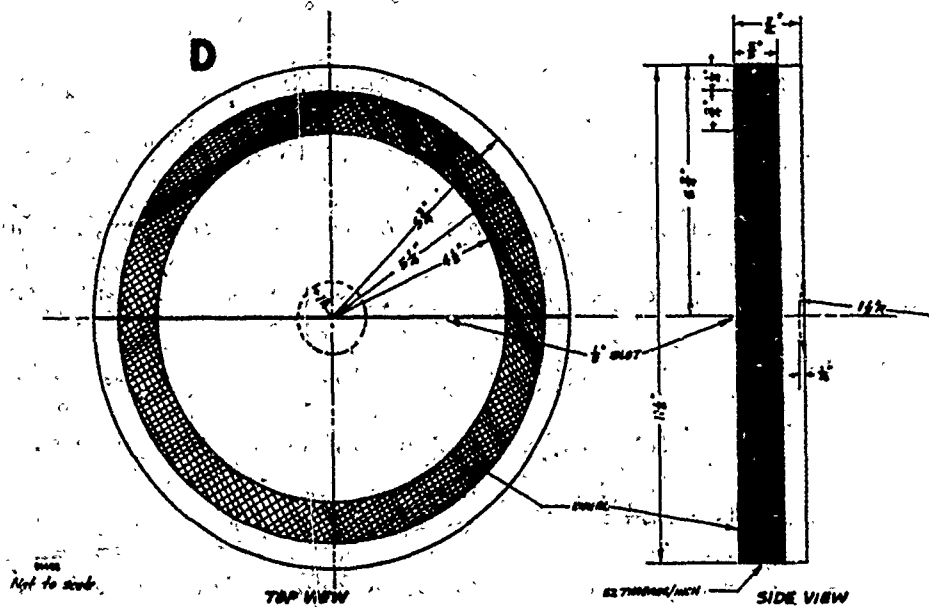


FIGURE 33. 11-1/2-INCH DOUBLE-D RF COIL FORM

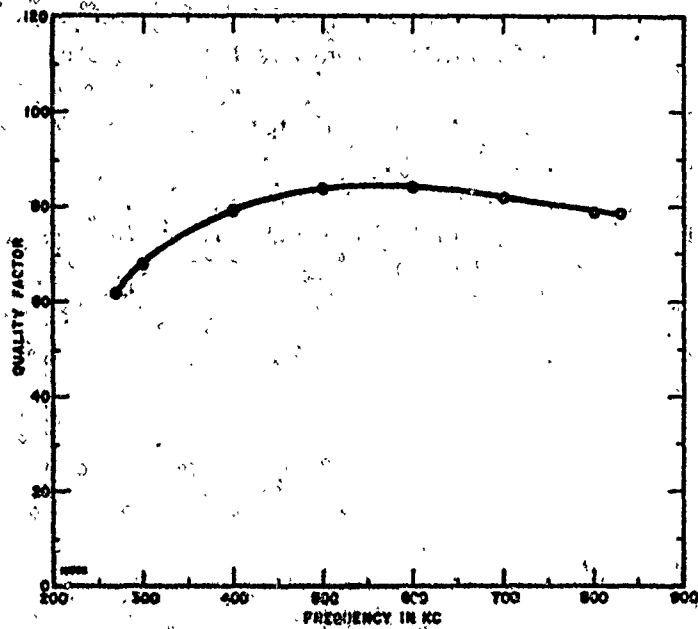


FIGURE 34. QUALITY FACTOR VARIATIONS WITH FREQUENCY FOR 11-1/2-INCH DOUBLE-D COIL

at the transposition and at the outer edge of the double-D to prevent the effects of eddy currents from either the bias or radiofrequency fields. The shielded radiofrequency coil mounted within the bias coil is shown in Figure 35.

To determine the variations with distance of the radiofrequency field from the coil shown in Figure 35, relative field measurements were performed with a small search coil at the surface of the coil form and 2 inches from the mean center of the windings. The relative intensities of the vertical and horizontal components along a diameter perpendicular to the center conductors are shown in Figure 36. The solid curves were obtained with the shield on the coil. When the shield was removed, the dashed-line curves were obtained. At a distance of 2 inches, there was less change in the field caused by the shield than close on the coil. Further away from the coil, the field distribution becomes more like that of two identical isolated loops, except for the increase in the horizontal component at the center. If it were assumed that the double-D were composed of two identical loops, then, from a comparison of the relative vertical amplitudes at the center of each D shaped coil, it is estimated that each coil has an effective loop radius of 3 inches. This estimate appears to be a reasonable value when the actual geometry is considered.

Since the field measurement of the bias coil indicated that the shielding was severely influencing the field distribution at the coil surface and since the shielding capacitance adversely affects the quality and performance of the coil, a second radiofrequency coil was designed, constructed, and tested. The



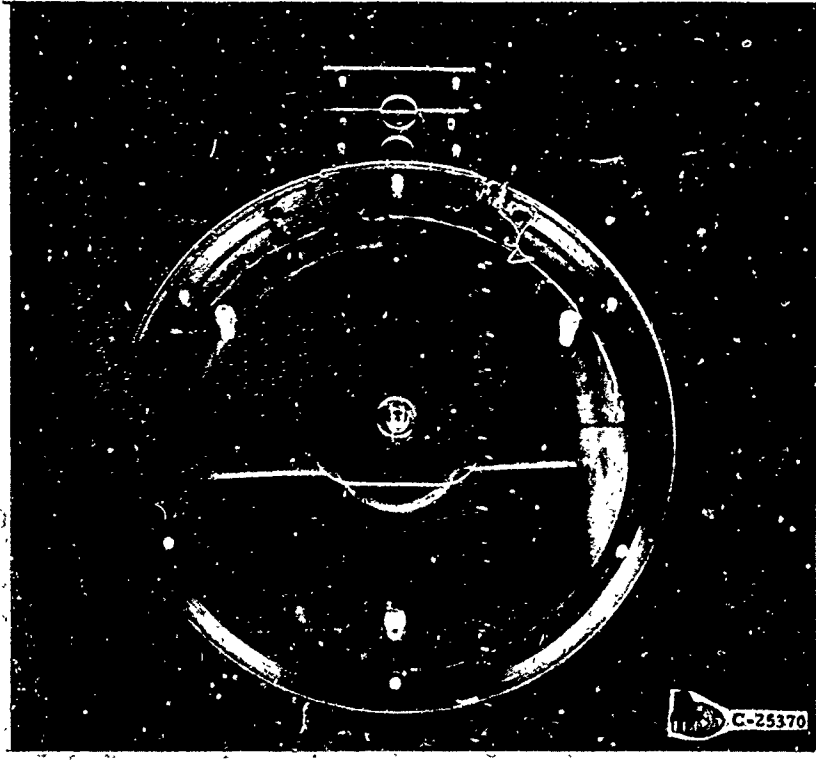


FIGURE 35. A DEMONSTRATION MODEL MINE DETECTOR HEAD WITH MOUNTING BRACKET

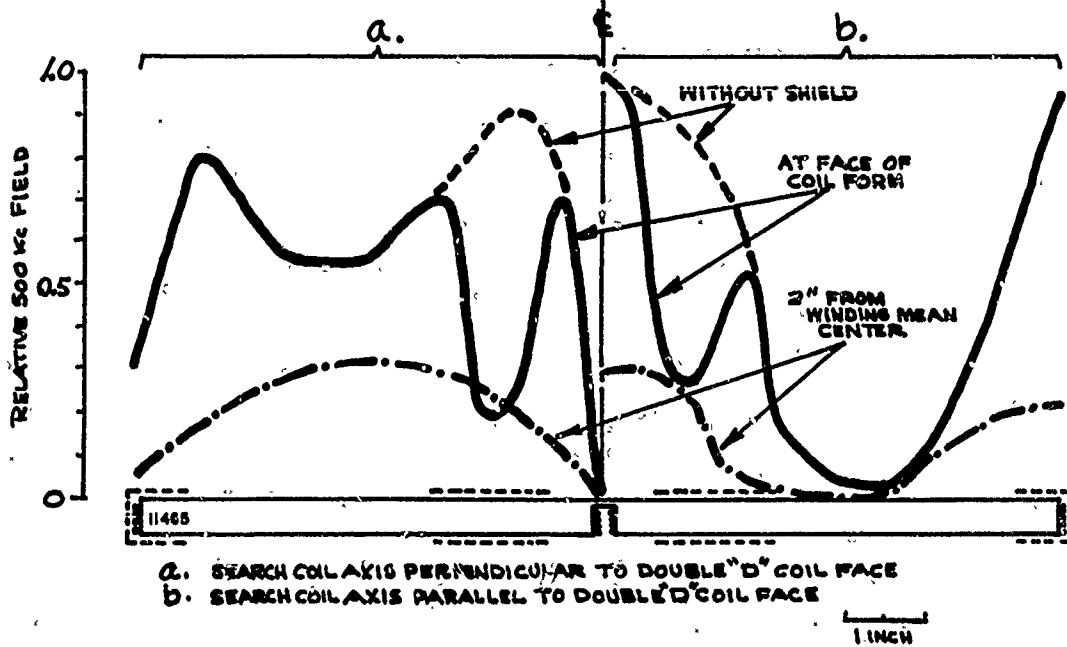


FIGURE 36. THE RELATIVE FIELD VARIATION OF HORIZONTAL AND VERTICAL COMPONENTS AT AND ABOVE 11-1/2-INCH DOUBLE-D COIL

design required the use of closely wound large diameter litz wire, and the design drawings of the coil form are shown in Figure 37. The electrical parameters are listed in Table III, and variations of Q with frequency are shown in the graph of Figure 38. In laboratory experiments, this coil has shown superior performance to the first coil. The improved performance is attributable first of all to the fact that the larger self-mutual between turns increases its sensitivity to induction variations. Secondly, the coil form pivotal point was placed so that the winding lay closer to the soil. Lastly, the winding is recessed from the outer diameter, and the internal core for material was removed to allow complete shielding without excessive shunt capacitance. It should be noted that radiofrequency leakage to the shield causes a loss of signal since these currents bypass the resonating capacitor and are not applied to the detector. Several shielding schemes have been examined with this coil. The most successful of these shield configurations is shown in Figure 39. A "sunburst" array etched from flexible copper-clad laminate is securely bonded to the interior of the top and bottom cover plates.

TABLE III. ELECTRICAL CHARACTERISTICS OF THE  
10-5/8-INCH RADIOFREQUENCY COIL

Number of turns per "D"	19
Type of wire	20 - #44 litz
Inductance	0.6 mh
Self-resonant frequency	4.1 mc
Q at 600 kcps	92

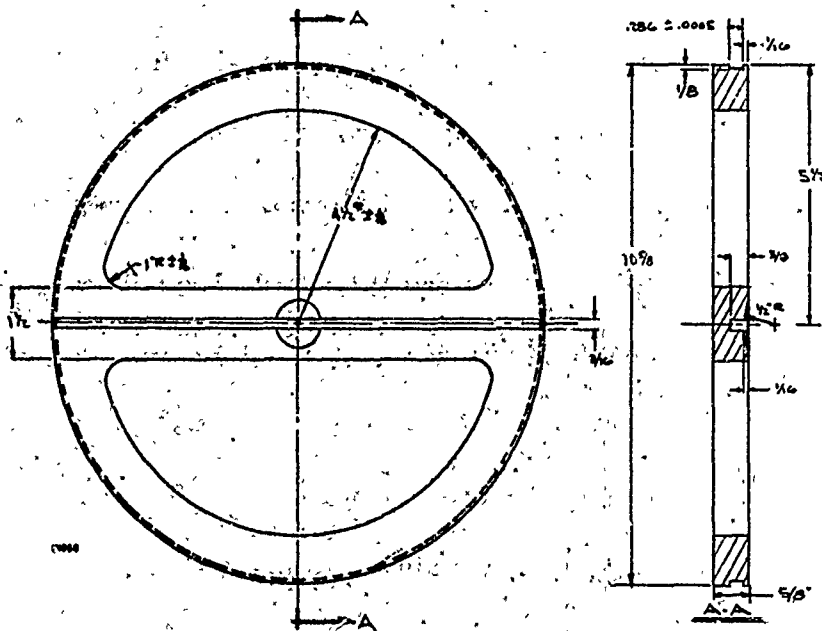


FIGURE 37. 10-5/8-INCH DOUBLE-D RF COIL FORM

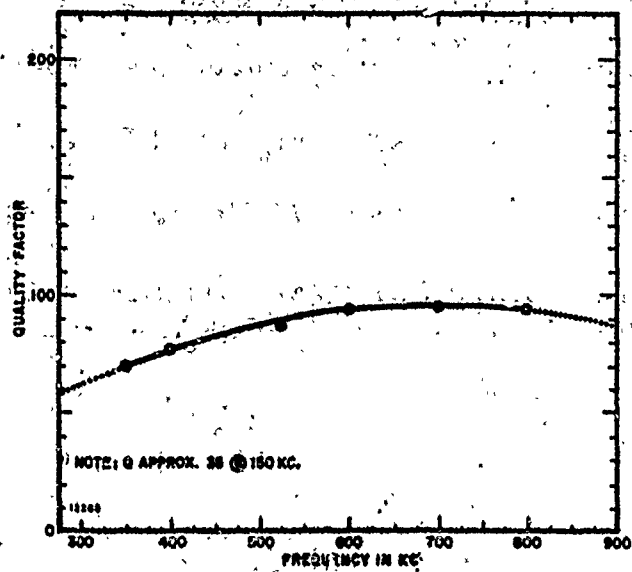


FIGURE 38. QUALITY FACTOR VARIATIONS WITH FREQUENCY FOR 10-5/8-INCH DOUBLE-D COIL

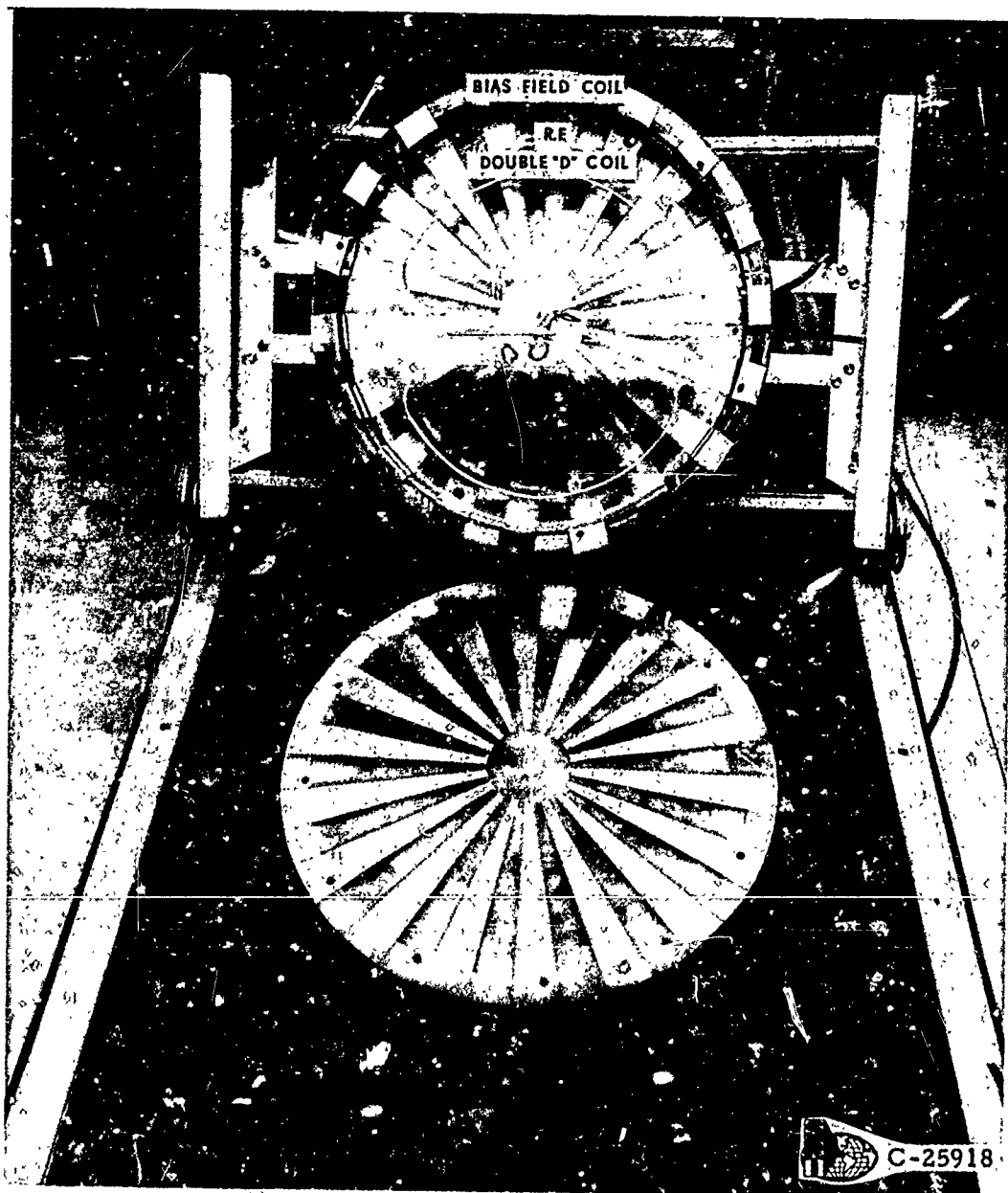


FIGURE 39. DETECTOR HEAD WITH SHIELDING EXPOSED

The legs of the top array are extended along the inner surface of the bias coil to mate with the array at the bottom. With such a design, closure of the eddy current paths from either the bias coil field or the radiofrequency coil is prevented. Therefore, shield reaction to either coil is minimized. A single ground point for the shield occurs at the entrance of the radiofrequency cable to the detector head. It was important that the shield be bonded tightly to avoid microphonic action between shield and radiofrequency detector.

C. Marginal Oscillators

There are a number of methods whereby impedance changes can be detected in the radiofrequency coil caused by permeability changes in the soil or buried object induced by the magnetic bias field. Perhaps the simplest is a circuit described by Rollins [11], wherein a tuned circuit of which the sample coil is the inductive element is driven at its natural frequency by a constant source. It is easily shown in this case that the impedance change of the sample coil is given by

$$\Delta Z = \left( \frac{\omega L_0}{R} \right)^2 [\Delta R + j\omega \Delta L] \quad (1)$$

for a change  $\Delta R + j\omega \Delta L$  in the coil. Each symbol is defined in Figure 40.

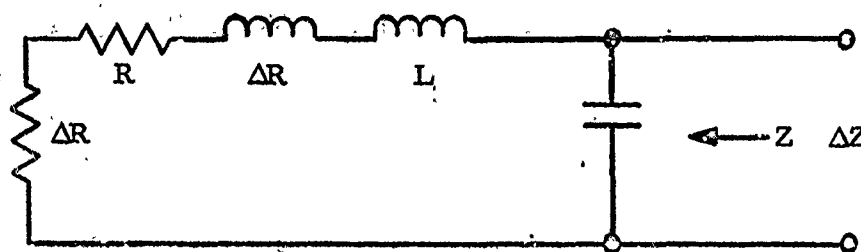


FIGURE 40. THE ROLLINS' CIRCUIT FOR MAGNETOABSORPTION DETECTION

From Eq (1), it is understood that sensitivity to  $\Delta R$  and  $\Delta L$  changes are dependent directly upon the quality factor,  $Q = \omega L/R$ , of the sample coil. This arrangement is, in principle, simple, but it suffers from several disadvantages which limit its use. In particular, the quality of a coil is physically limited and consequently limits the sensitivity. Secondly, it is highly inconvenient to obtain accurate tracking of the frequency of an oscillator with the resonant frequency of the detection coil. Thirdly, it is highly susceptible to microphonics such as changes in cable capacitance. Further, it can be shown that mistuning only enhances the effects of microphonics [12].

An alternative, not having these disadvantages, is the marginal-oscillator\*. It can be shown that the marginal-oscillator is approximately 1/5 as sensitive to microphonics. The sensitivity to impedance changes is not as severely limited by the quality of the coil since the regenerative circuit has a  $Q$  multiplying effect at low oscillation levels [13]. Further, the marginal-oscillator is more convenient to use since the oscillator frequency and the detector frequency are determined by the same resonant circuit, and no tracking is needed.

Among the many types of marginal-oscillators, the Robinson, Colpits, and Pound-Knight-Watkins (PKW) types are the common types. The Robinson

---

\*A marginal-oscillator is a generic term used to describe any oscillator which is maintained at a very low oscillation level where it is operating in its Class A or linear region and where it has great sensitivity to  $\Delta R$  and  $\Delta L$ .

type [12] consists of an amplifier followed by a limiter. The limiter serves to stabilize the amplitude of the oscillator and to reduce the effects of noise through a reduction of the noise figure for the oscillator amplifier. The Colpitts [14], on the other hand, is a commonly employed oscillator of the series resonant type and requires little further description. The PKW type is composed of a buffer stage and noninverting amplifier [13]. For the most part, marginal-oscillators employed in earlier magnetoabsorption measurement and those reported in literature have been vacuum-tube models. Early attempts with vacuum-tube and simple solid-state marginal-oscillators indicated the difficulty and the complexity of their use in extracting magnetoabsorption signals from soil where the concentration of magnetic material is very small, and the filling factors for flat coils are also small. Measurements indicated that typical signal amplitudes would range from the few microvolts to a maximum of 100 microvolts of modulation on the radiofrequency voltage. With respect to the radiofrequency amplitudes, these signal amplitudes represent modulations of one part in  $10^4$  to one part in  $10^6$ . Consequently, solid-state design techniques suitable for low noise, high sensitivity marginal-oscillators had to be investigated since no satisfactory solid-state marginal-oscillators were described in the literature. The following requirements were specified:

- (1) Amplitude stabilization without external circuits
- (2) Freedom from microphonics
- (3) High sensitivity
- (4) High signal/noise ratio
- (5) Low power consumption
- (6) Small volume and weight

Since among the vacuum-tube types the Robinson exhibits some superior qualities, the investigation was confined to circuital applications appropriate to the Robinson concept. Since amplitude limiting by solid-state techniques is not well established at high frequencies, a short literature search on this subject was conducted. The search revealed two types with desirable characteristics. One employed unconventional circuitry to prevent undesirable shifts in operating points with changes in level [15]. The other employed Zener diodes whose frequency range was extended by adding shunt capacitors and series diodes.

In early efforts, the Robinson type of marginal-oscillator with solid-state design shown in Figure 41 was constructed and tested. A low noise, high frequency transistor type 2N3694 was employed for the input buffer-driver stage. The output of the buffer drives a step down autotransformer which in turn drives the limiter. The limiter is composed of a pair of switching transistors which are dc coupled in such a manner as to prevent undesirable shifts in operating points. The first stage of the limiter switches between cutoff and saturation, while the tuned circuit of the second state restores the sinusoidal waveform. The output of the tuned circuit was fed back through  $R_{FB}$  to the sample coil. The output amplitude of the limiter was controlled by adjusting the collector supply voltage for the limiter stages. Although magnetoabsorption signals with a peak-to-peak amplitude as large as 150 millivolts were obtained from ferromagnetic wires, none were observable from soil. The unsatisfactory features in this design are the large number of inductive



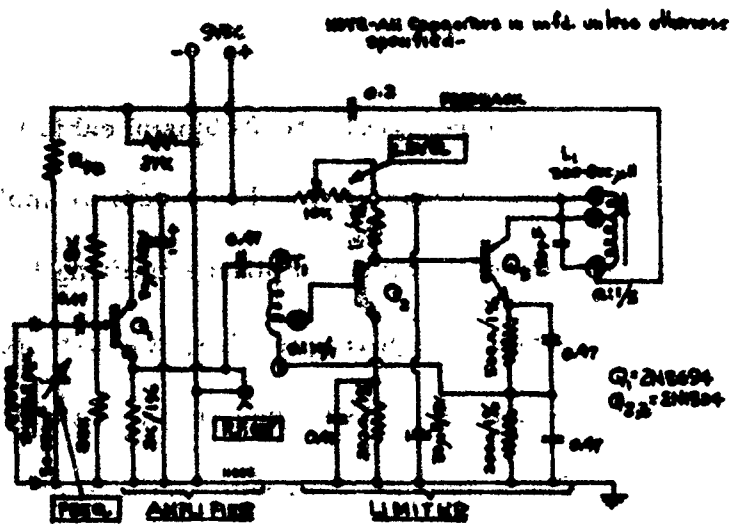


**FIGURE 41. ROBINSON MARGINAL-OSCILLATOR EMPLOYING A BIPOLAR TRANSISTORS LIMITER**

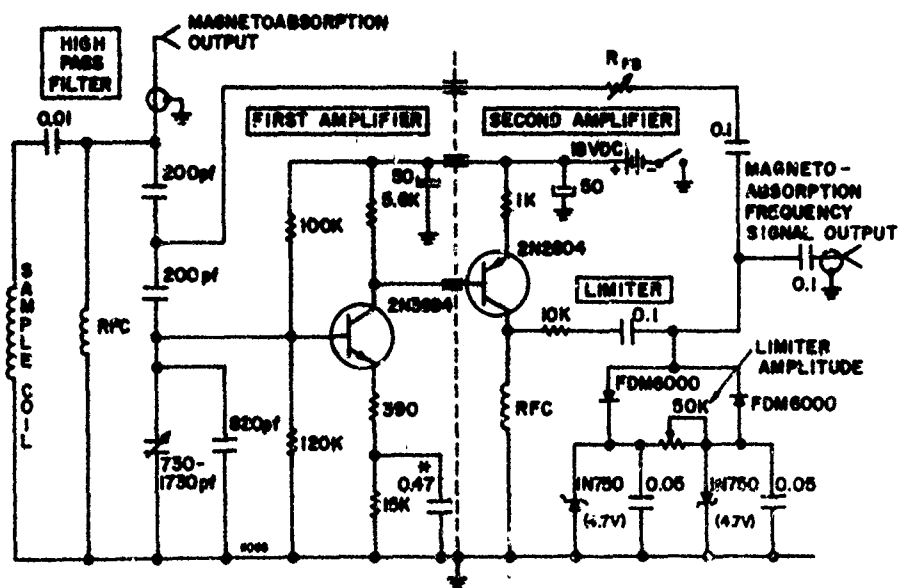


**FIGURE 42. SOLID STATE ROBINSON TYPE MARGINAL-OSCILLATOR EMPLOYING A DIODE LIMITER**

elements in the circuit and the low input impedance of the amplifier  $Q_1$ . The inductive elements are sources of unwanted radiofrequency leakage and pickup. They can also cause undesirable oscillating frequencies to occur. The low input impedance decreases the quality factor of the sample coil, which reduces sensitivity directly in proportion to the reduction in  $Q$ .

Another Robinson-type marginal-oscillator employing solid-state components was designed to eliminate both unsatisfactory conditions. The circuit configuration is shown in Figure 42. The oscillator consists of a sample coil, high-pass filter, amplifier, limiter, and feedback. The low input impedance problem inherent in bipolar transistor amplifiers was overcome by the use of a capacitor impedance matching arrangement, composed of the three capacitors across the coil, from the high impedance of the resonant circuit to the low impedance of the amplifier. The amplifier is based on a complementary transistor design for improved temperature stability with a broadband frequency response. The limiter employs Zener diodes whose frequency response has been extended by adding series diodes and shunt capacitors.

The internal stabilization of the amplitude is achieved by the action of the limiter. As an example, assume that the radiofrequency amplitude at the input to the limiter changes by amount  $\Delta V_{lim}$  due to a change in amplifier gain  $\Delta A$ , i. e.,

$$\Delta V_{lim} = (\Delta A) V_{ri}$$

where  $V_{rf}$  is the amplifier input. The amplitude of the first harmonic of the radiofrequency (not a magnetoabsorption signal harmonic) at the limiter output will be entirely dependent upon the limiting level if the level is better than one-half of the peak radiofrequency amplitude limiter input. Under this condition, the radiofrequency amplitude across the sample coil will not change as demonstrated by the graph of Figure 43. It is evident from this graph that the output voltage is independent of the input when the input exceeds the clipping amplitude by a factor of 2. Consequently, for good amplitude stabilization, the clipping level should be less than one-half of the desired level.

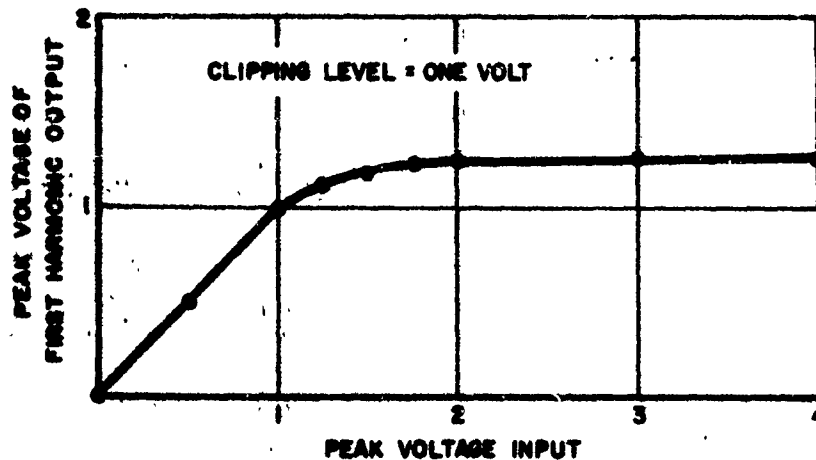


FIGURE 43. FIRST HARMONIC OUTPUT AS A FUNCTION OF INPUT FOR A LIMITER

Freedom from noise and microphonics has been achieved by a number of design features. First, as demonstrated in Robinson's paper, noise figure enhancement results from limiter action. Secondly, since marginal-oscillators have only one frequency to control, spurious signals (microphonics) resulting from capacitance changes are reduced over that of the Rollins

circuit wherein two frequency control elements exist. Microphonics, often a troublesome factor in vacuum tubes, have been reduced further by the use of transistors.

High sensitivity is achieved by selecting a high quality sample coil and by assuring that shunt loading of the sample coil by the feedback and amplifier input impedances has been avoided. The high-pass filter across the sample coil is an additional feature required to retain a high sensitivity for magnetoabsorption detection while reducing the effect of direct induction signals resulting from inhomogeneities in the soil and residual unbalance in the radiofrequency coil. The filter excludes the low frequency induction signals from the oscillator where they would amplitude modulate the oscillator and produce false magnetoabsorption-like signals.

When the amplitude modulation in a marginal-oscillator circuit is small, experience has shown that detection at the sample coil results in better S/N ratios than attempts to detect the signal from a point within the marginal-oscillator amplifier sections when solid-state circuits are used. This is because the solid-state circuits are nonlinear at the high levels required to drive the limiter, and the magnitude of the modulation can be greatly reduced or eliminated entirely in the amplifier.

An FET\* analog of the vacuum-tube infinite-impedance detector was employed to amplitude demodulate the signal at the sample coil because of its

---

\*FET - Field effect transistor

high input impedance and linearity. The impedance of such a device is sufficiently high to prevent loading of the sample coil with subsequent loss in sensitivity. The point at which the detector is connected is shown as the MAGNETOABSORPTION OUTPUT in the schematic of Figure 42. In addition, an output for frequency demodulation is shown as the MAGNETOABSORPTION FREQUENCY SIGNAL OUTPUT also in Figure 42.

The success of this marginal-oscillator together with detector and detection-head assembly was demonstrated by the superior sensitivity and signal-to-noise ratio over other solid-state and vacuum-tube marginal-oscillators examined in these efforts. Signal/noise ratios of 2/1 to 10/1 are readily obtained.

#### D. Equipment for the Magnetic-Void Detection in Soils

The various components that were contemplated for the use of magnetoabsorption signals for the detection of magnetic voids are shown in Figure 44. The system is based on a coherent detection scheme wherein the frequency of the magnetic bias field is locked to the center frequency of the selective amplifier, and an amplitude-sensitive phase detector provides a dc voltage directly proportional to the fundamental of the magnetoabsorption signal in the radiofrequency detection coil. In such a coherent system, extraneous signals of different frequency or phase from the desired signal are suppressed by the selective amplifier and the amplitude-sensitive phase detector. The operation and design of the system is described in the following manner:

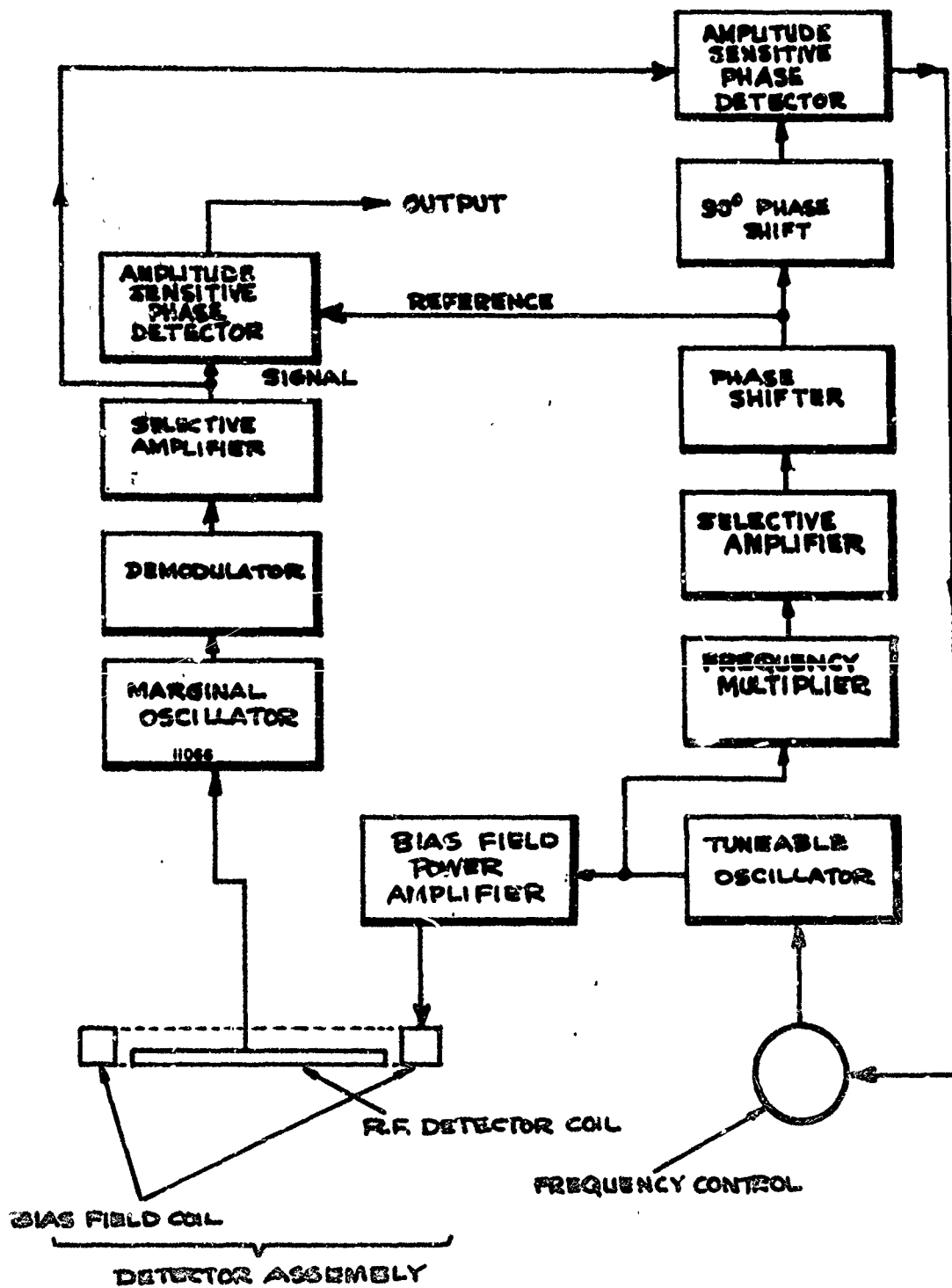


FIGURE 44. BLOCK DIAGRAM OF THE MAGNETOABSORPTION MAGNETIC-VOID DETECTOR

The radiofrequency voltage at the detector coil is both amplitude and frequency modulated at a frequency which is twice that of the magnetic bias field whenever magnetoabsorption occurs beneath the detector assembly. The marginal-oscillator serves both as the source of the radiofrequency field and as the magnetoabsorption detector. The radiofrequency voltage which is modulated by the magnetoabsorption signal is then either amplitude or frequency demodulated. A selective amplifier, tuned to the harmonic of the magnetoabsorption signal most sensitive to the presence of a buried magnetic void, provides the signal source for an amplitude-sensitive phase detector. The reference signal for the phase detector is the appropriate multiple of the bias field frequency derived directly from the same generator which produced the magnetic bias field. When the phase and frequency of the reference is adjusted to that of the selected harmonic, the output is directly proportional to the amplitude of the selected harmonic. To assure that a frequency drift problem is avoided in the system, a frequency control loop operates from an error curve derived from the phase characteristic of the selective amplifier and keeps the frequency of the bias field oscillator at the peak of the selective amplifier.

The magnetic void detection studies were performed with a system similar to that of Figure 44 except that the frequency locking loop was not employed, and tuning was accomplished by hand. A commercial oscillator had sufficient frequency stability so that mistuning was seldom a problem. A simple retuning of the selective amplifier or a resetting of the oscillator frequency was sufficient for the laboratory tests.

#### E. Equipment for Discrete Object Detection and Identification

The basic diagram of the discrete object detector, which is a combination of the magnetoabsorption detector and the induction detector, is shown in Figure 45. It is a combination of two detectors with a common detection head. The balanced feature of the radiofrequency coil to the bias field permits

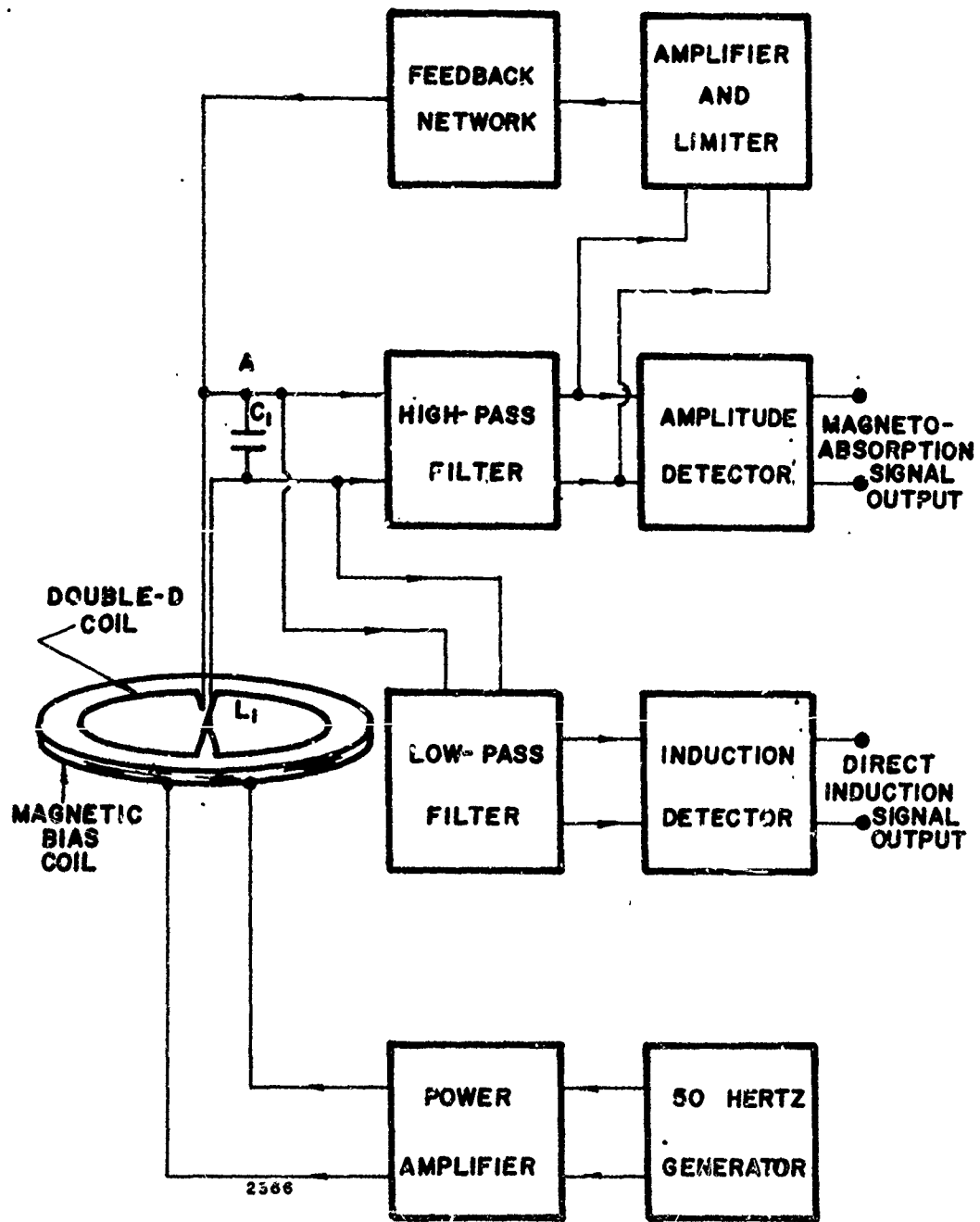


FIGURE 45. BASIC BLOCK DIAGRAM OF THE HIDDEN OBJECT DETECTOR COMPOSED OF A MAGNETOABSORPTION AND AN INDUCTION DETECTOR



the same coil geometry for the magnetoabsorption method to be employed for induction method. With no object in the vicinity of the detection head, there is no magnetoabsorption signal and, because the double-D coil is balanced, there is no induction signal directly from the magnetic bias coil to the double-D coil. When there is a ferromagnetic conductor in the field of the radiofrequency coil, there will be both a magnetoabsorption signal and an induction signal in the radiofrequency double-D coil at point A in Figure 45. The radiofrequency coil is the tuned circuit of a radiofrequency oscillator. The total oscillator is composed of the tuned circuit, the high-pass filter, the amplifier-limiter, and the feedback network. The magnetoabsorption signal appears as a modulation of the radiofrequency voltage at point A. The induction signal also is at point A as a 50-cycle sine wave in addition to the radiofrequency voltage modulated by the magnetoabsorption. Therefore, the high-pass filter will pass the magnetoabsorption signal modulated on the radiofrequency carrier and reject the induction signal by five orders of magnitude. Conversely, the low-pass filter will pass the induction signal and reject the magnetoabsorption signal by several orders of magnitude. Thus, the two signals are separated by filters. The magnetoabsorption signal itself is obtained by means of the amplitude detector. The induction signal requires no more processing beyond the filter except amplification.

Each signal, magnetoabsorption and induction, has more than their fundamental frequency alone as discussed earlier. Each is a complex waveform composed of harmonics of the fundamental. Each of the harmonics bears some amplitude and phase relationship relative to the fundamental.

Thus, the amplitude and phase of the harmonics of each signal, magneto-absorption and induction, are of importance in the identification of objects.

It is of additional importance that the fundamental for the magnetoabsorption signal is twice the frequency in the magnetic bias coil or 100 cycles, while the fundamental for the induction signal is 50 cycles. Therefore, it is possible to have the outputs shown in Figure 46 to use for the identification of objects.

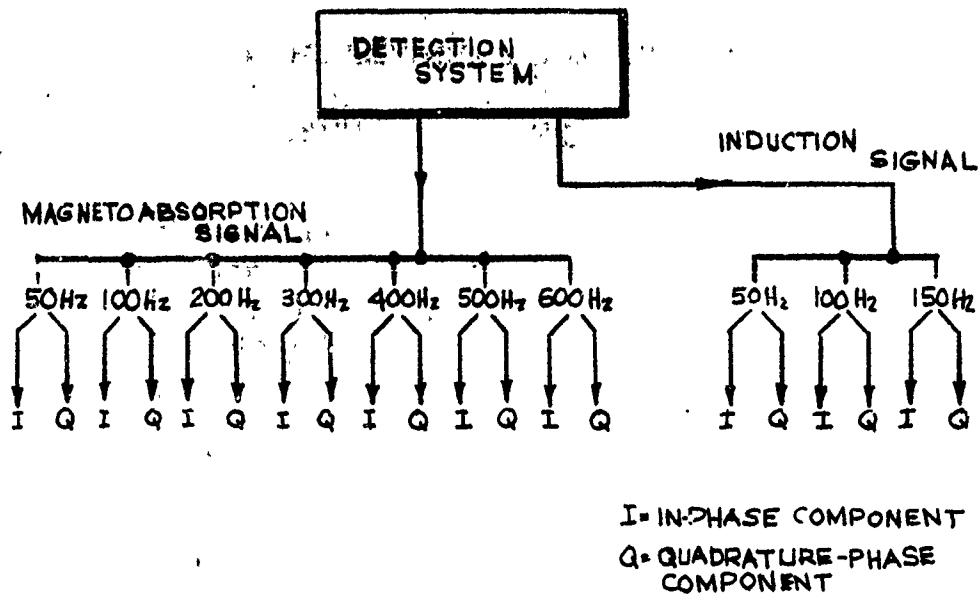


FIGURE 46. SCHEMATIC REPRESENTATION OF THE OUTPUTS AVAILABLE FOR OBTAINING A FINGERPRINT OR IDENTIFYING SIGNAL FOR HIDDEN OBJECTS

F. Equipment Development

The first successful magnetoabsorption signals from soils were obtained with vacuum-tube circuits. For this portable application, solid-state components were designed to replace these vacuum-tube devices. To a large extent, the components are adaptable for either the magnetic-void or the discrete object detection systems. The equipment was constructed to give the three signal channels and one reference channel listed in Table IV.

TABLE IV. EQUIPMENT BY CHANNELS

<u>Magnetoabsorption Amplitude Signal Channel</u>	<u>Direct-Induction Signal Channel</u>
(a) Infinite Impedance Detector	(a) Low-Pass Filter and Amplifier
(b) Selective Amplifier	(b) Amplitude-Sensitive Phase Detector
(c) Combination Narrow or Broadband Amplifier	
(d) Amplitude-Sensitive Phase Detector	
	<u>Magnetoabsorption Frequency Signal Channel</u>
	(a) Frequency Discriminator
	(b) Combination Narrow or Broadband Amplifier
	(c) Selective Amplifier
	(d) Amplitude-Sensitive Phase Detector
<u>Reference Channel</u>	
(a) Frequency Doubler	
(b) Phase Shifter with Buffer	

Where a component occurs in more than one channel, only a single device was constructed to serve in any of the channels. Each component was mounted on its own chassis to facilitate testing and channel interchangeability.

A discussion of the components constructed for the signal channels and the reference channel are briefly described in the following sections.

1. Signal Channel Equipment

a. Detector-Amplifier

Since the amplitude modulations can be exceedingly small, that is  $10^{-4}$  to  $10^{-6}$  of the radiofrequency voltage, not only the amplifiers used but also the detection system must have good signal/noise characteristics and linearity. The broadband noise characteristics of the untuned amplifier sections of the marginal-oscillator gave a noise level which obscured the small amplitude modulations. The limiting action of this amplifier also reduced the modulation and thereby decreased the signal/noise ratio. Detection directly from the sample coil with an "infinite" impedance detector was found to yield better signal/noise ratios and better linearity. The output of the detector is amplified by a system which has a choice of narrow or broadband operations. The schematic for the amplitude detector and amplifier is shown in Figure 47.

b. Combination Narrow or Wideband Amplifier

To monitor the magnetoabsorption signal with an oscilloscope in a broader bandwidth, a high gain amplifier having a bandwidth of either 700 cycles or 100 kilocycles was employed. This amplifier is useful in monitoring the noise characteristic that accompanies the magnetoabsorption. It is anticipated that noise spectrum analysis may be useful in designing an improved selective amplifier. The schematic of this amplifier is shown in

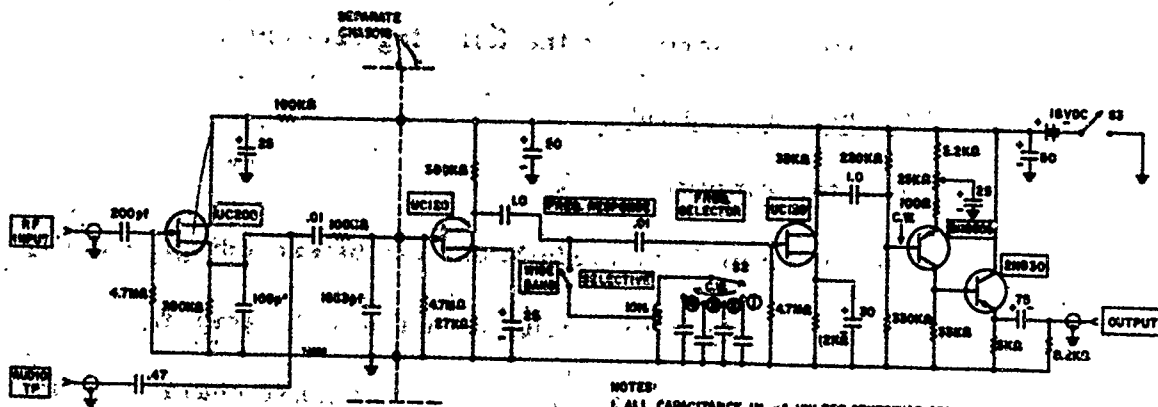


FIGURE 47. DETECTOR-AMPLIFIER

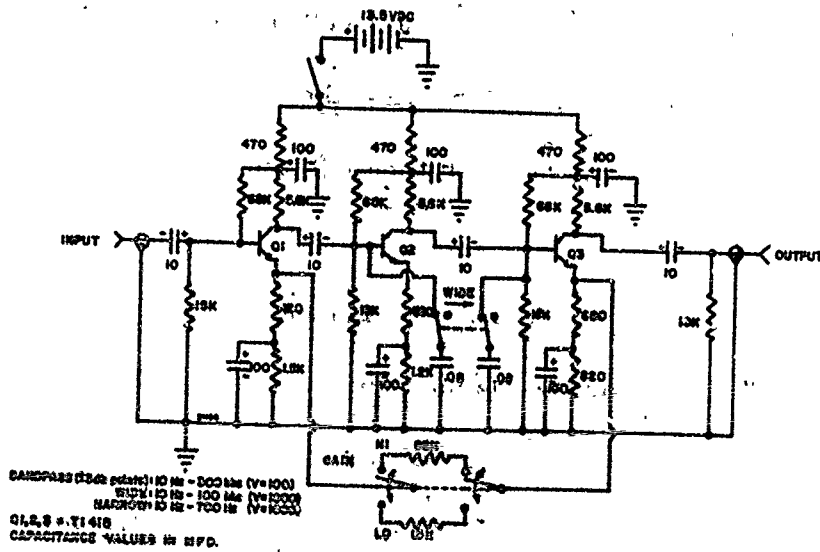


FIGURE 48. AMPLIFIER

c. Low-Pass Filter and Amplifier

To measure the low level induction signal in the radio-frequency detector coil described previously, the low-pass filter and amplifier shown in Figure 49 were used. The design uses a low noise, high frequency FET as the input stage to prevent the filter-amplifier combination from loading the radiofrequency detector coil. The FET drives a low-pass filter having a high frequency cutoff at 10 kilocycles. The output of the filter is amplified by a transformer, another FET amplifier and a bipolar transistor amplifier. A choice of a high or low amplification is given at the output by using the bipolar stage as a common emitter or a common collector amplifier. In the high gain position, induction signals smaller than  $1 \mu\text{v}$  can be observed when a signal is displayed on an oscilloscope having a sensitivity of  $1 \text{ mv per cm}$ .

This filter-amplifier has application primarily in discrete object detection wherein the metallic objects will cause unbalanced bias field inductions in the radiofrequency detector coil. However, it was also employed in magnetic-void detection studies to assist in the balancing of the detection head.

d. Phase Detector

A phase detector was constructed as shown in Figure 50. It is an amplitude-sensitive phase detector using two dual-emitter transistors

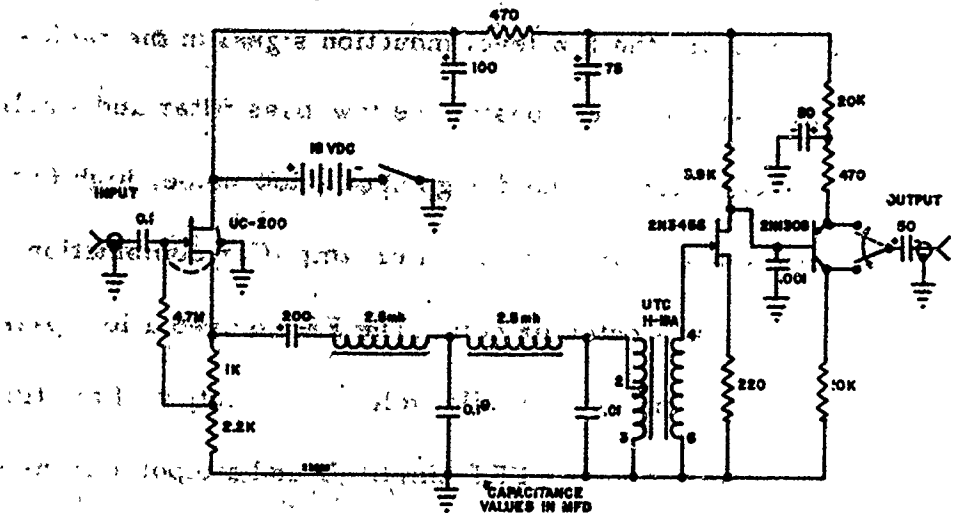


FIGURE 49. LOW-PASS FILTER WITH AMPLIFIER

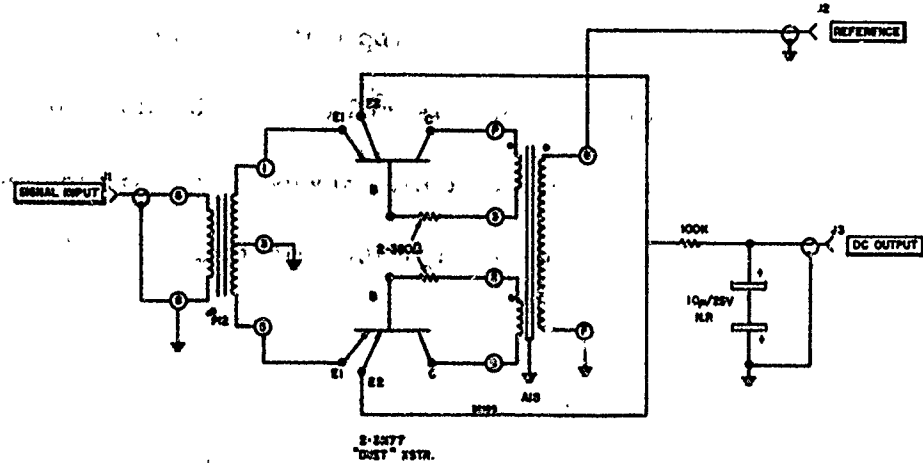


FIGURE 50. PHASE DETECTOR

as the switching elements. The output of the detector is basically given by

$$E_o = kE_s \cos(\phi_s - \phi_r)$$

where

$E_s$  = signal amplitude

$\phi_r$  = phase of reference

$k$  = gain of the detector

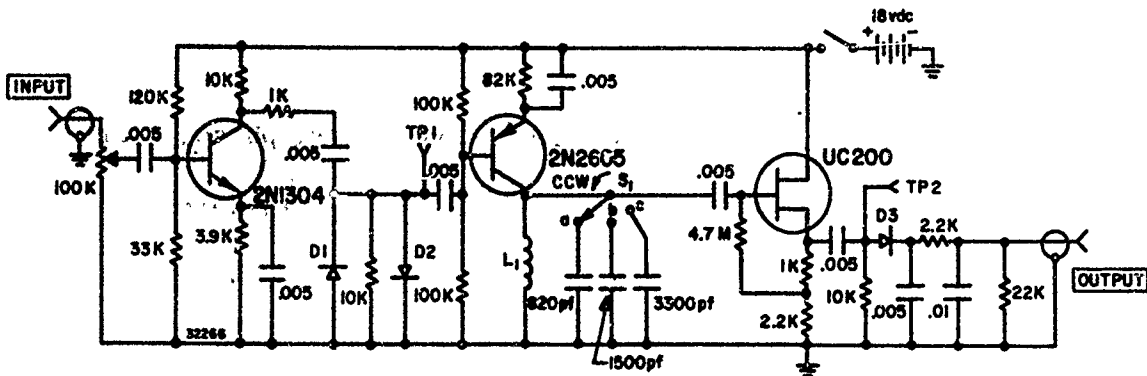
$\phi_s$  = phase of signal

Since the output is sensitive to the amplitude as well as the phase, it can serve as a coherent detector. By exchanging the signal and reference inputs, the detector can be made insensitive to the amplitude of the signal and can be employed to measure only phase angle between two signals of the same frequency. The latter mode could be useful in the harmonic analysis of the magnetoabsorption signal in discrete object studies.

e. Frequency Discriminator

The device to convert the frequency modulation of the marginal-oscillator to the magnetoabsorption frequency signal was the simple frequency discriminator shown in Figure 51. A high-Q resonate circuit tuned above the frequency of the marginal-oscillator changes frequency modulation into amplitude modulation. The diode amplitude detector then converts these to the magnetoabsorption frequency signal. Diode limiters  $D_1$  and  $D_2$  ahead of the resonant circuit eliminate any amplitude modulation present before frequency detection. Tests indicated that the discriminator had a sensitivity of 320 microvolts per cycle. It was found that the signal/





D1,2,3: FDM-6000

L<sub>1</sub> MILLER 4208  
120-330 μh

S<sub>1</sub> a = 400 kHz

b = 300 kHz

c = 200 kHz

ALL CAPACITANCE VALUES IN mfd  
UNLESS OTHERWISE SPECIFIED

Q = 100

Q = 75

Q = 50

FIGURE 51. FREQUENCY DISCRIMINATOR

noise ratio and amplitude of the magnetoabsorption frequency signal were the same as those of the magnetoabsorption amplitude signal, and, therefore, the magnetoabsorption amplitude signal was used.

## 2. The Reference Channel Equipment

### a. Bias Field Oscillator

A Hewlett Packard Model HP-200CD oscillator served as source for the bias field that modulates the reversible permeability of the soil or ferromagnetic discrete object. In a field model, the HP-200CD oscillator should be replaced by a small solid-state oscillator. Several commercial oscillators and conventional circuits that can be frequency controlled would suit this purpose.

### b. The Bias Field Power Amplifier

A 20-watt amplifier served as the power amplifier for the bias field coil. Power consumption in the bias field coil was typically 20 watts. For all measurements, the bias coil was series resonated to decrease the voltage needed for the high current requirement of the bias coil. This tuning also prevented a large phase shift between the bias field and the generator output.

### c. Frequency Doubler

A reference signal for the phase detector mentioned earlier is synthesized from the bias field oscillator output by means of a full-wave rectifier and a passive filter network. The present design allows a choice of

a 25, 50 and 100-cycle bias field frequency through the use of filters at 50, 100 and 200 cycles. The circuit diagram of this frequency doubler appears in Figure 52. The full-wave rectifier output is given by the expression

$$V(\omega) = \frac{2}{\pi} \left( 1 + \frac{2}{3} \cos 2\omega t - \frac{2}{15} \cos 4\omega t + \dots \right)$$

where  $\omega$  is the radial frequency of the bias field. The selective circuit then passes the "2 $\omega$ " or second-harmonic component to form the reference signal. This design features low current, low noise, high impedance FET amplifiers and a low output impedance circuit provided by a hybrid Darlington consisting of an FET and a bipolar emitter follower.

d. Phase Shifter

A phase shifter to compensate for all of the unwanted phase shifts is accomplished in a conventional manner as shown in Figure 53. The output of the phase shifting network is amplified by a Darlington pair of transistors to provide a low impedance output and the power amplification essential for a good reference (switching) signal for the phase detector.

3. Indoor Test Facility

To conveniently make repetitive measurements from a large box of soil having a nonmetallic mine buried at the center, a powered dolly and track were designed and constructed using available materials and components. The dolly and track mounted on the box are shown in Figure 2. The solid-state components assembled into a magnetic void-detection application are shown in the small labeled boxes on the bench behind the box of soil.

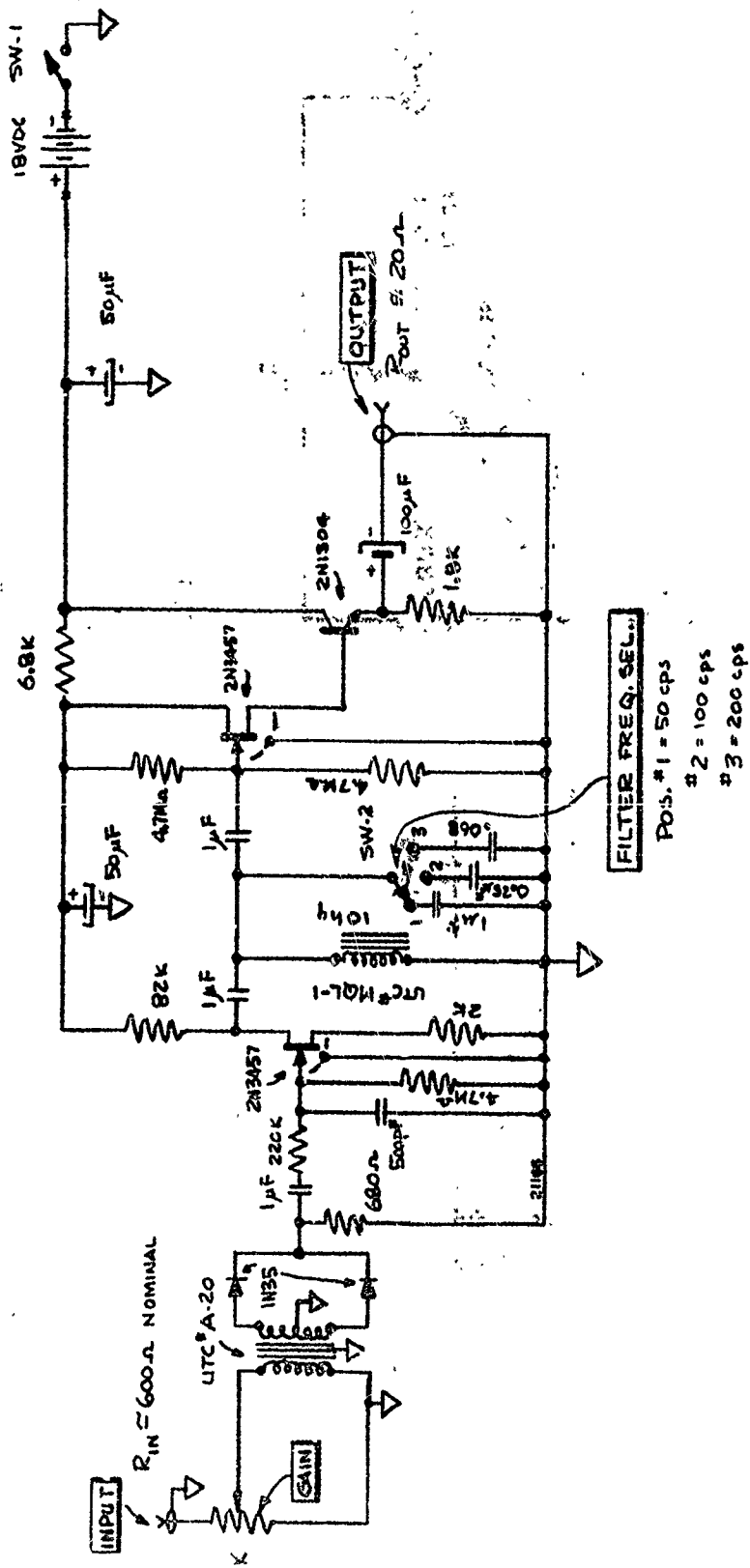


FIGURE 52. FREQUENCY DOUBLER

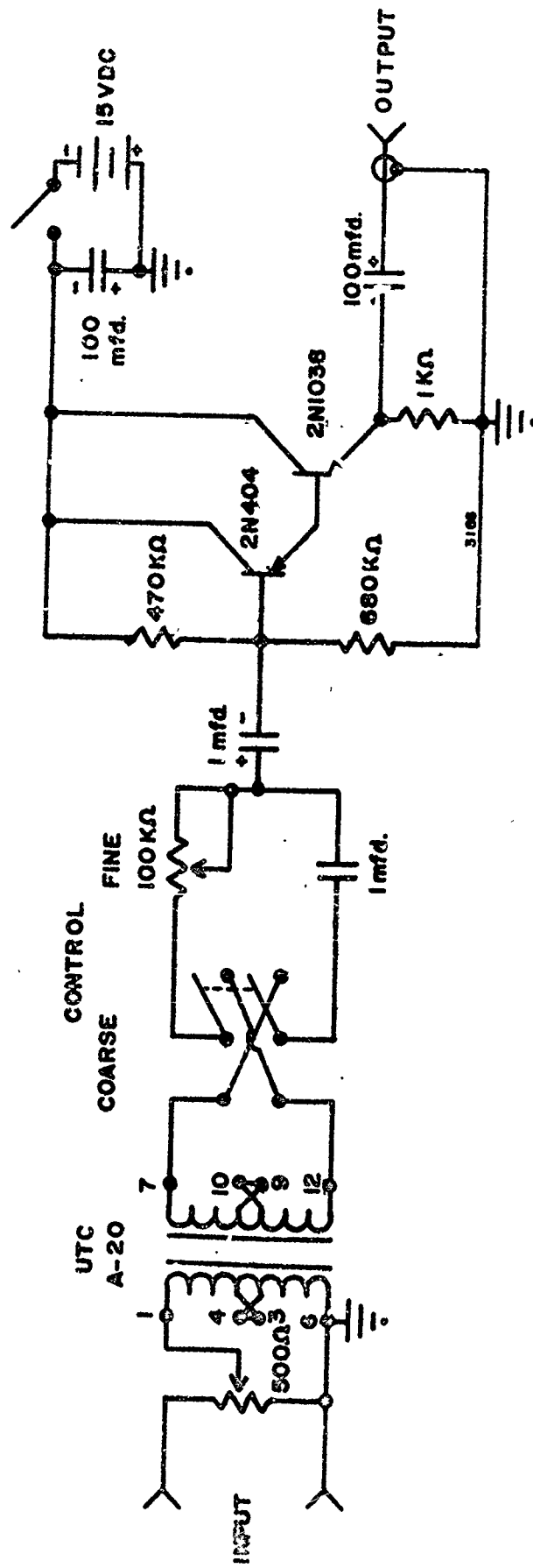


FIGURE 53. PHASE SHIFTER

#### IV. CONCLUSIONS

##### A. Magnetic-Void Detector

The work of this program has given a detection head with a coil for producing the magnetic bias field and a double-D shaped radiofrequency coil which can be used for detection of the direct induction signal with a fundamental at the magnetic bias frequency and a magnetoabsorption signal with its fundamental at twice the magnetic bias frequency. The electronics for the magnetic-void type of detection system using only the magnetoabsorption signal was designed, constructed and tested satisfactorily. The magnetic-void detection system was tested in the laboratory and found to give the expected decrease in magnetoabsorption signal when traversing over a buried magnetic void. The percentage decrease in the magnetoabsorption was 35 percent for a type M-19 mine casing buried with its top 1 inch from the surface of the soil. The percentage change was 15 percent with the casing buried 2 inches. The percent drop in the magnetoabsorption signal caused by the magnetic void was found to be independent of the height of the detection head above the soil and dependent upon the depth of the mine.

Because of these results, it is concluded that: (1) magnetoabsorption signals can be obtained from the magnetic materials within the soil, (2) these magnetoabsorption signals have a useable signal/noise ratio for detection head heights of from 0 to 2 inches and for void depths (to the top of the

void) of 2 inches, (3) the double-D radiofrequency coil and magnetizing coil combination can be made to obtain sufficient sensitivity, rigidity and lightness of weight for a portable field device, (4) that the magnetoabsorption system can find buried magnetic voids with a percentage change in signal of from 15 to 35 percent for a range of void depths of 1 to 2 inches, (5) that the solid-state circuits required for the magnetic-void detection system have all been laboratory tested and found practical for a portable field device, and (6) that the variations in signal caused by changes in the height of the detection head can be made less effective if an automatic gain-control system is used to make the output read the percentage change which is independent of height.

B. Discrete Object Detection and Identification

The same detection head used for the magnetic-void detector was also used for the discrete object detector. The high-pass filter to select the magnetoabsorption signal plus the low-pass filter to select the direct induction signal worked well with the marginal-oscillator used for the magnetic-void detector with no reduction in the sensitivity to the detection of the magnetoabsorption signal. A laboratory model of the discrete object detection and identification system was made from the components of the magnetic-void system. Lissajous patterns and harmonic amplitudes were obtained from twenty-one different discrete objects.

Because of these results with the discrete object detection and identification laboratory tests, it is concluded that: (1) a sensitive detection of

both the magnetoabsorption and the direct induction signals can be obtained with the detection head used; (2) that a marginal-oscillator provides a useable signal/noise ratio with both high-pass and low-pass filters attached to select and separate the magnetoabsorption and direct induction signals, and (3) that the system developed can, with a combination of the Lissajous patterns of magnetoabsorption and direct induction, both detect the presence of all of the discrete objects used and identify the type of material from which they are made. That is, the system can discriminate between nonmagnetic conductors, magnetic nonconductors, magnetic conductors, magnetized magnetic nonconductors and magnetized magnetic conductors.



## RECOMMENDATIONS

### A. Magnetic-Void Detection

On the basis of the successful laboratory tests of the magnetoabsorption magnetic-void detector, it is recommended that the portable field model be constructed using a ruggedized version of the detection head and a miniaturized version of the electronics proven successful by these tests. It is further recommended that the automatic gain system for detection-head-height compensation be designed, developed, tested and included within the field model. Upon the conclusion of these tasks, it is recommended that the field model of the magnetoabsorption magnetic-void detector be given complete field tests with many different types of soil.

### B. Discrete Object Detection and Identification

On the basis of the successful test of the discrete object detection and identification system using only the Lissajous patterns and the harmonic amplitudes, it is recommended that a complete discrete object detection and identification system be designed, developed and tested with amplitude and phase measurements on all necessary harmonics. It is further recommended that the detection head be studied both theoretically and experimentally to obtain the highest sensitivity for both the magnetoabsorption and direct induction signals with discrete objects. It is then recommended that the field test device be constructed and tested and that identification systems be worked out with the greatest simplicity and accuracy.

## REFERENCES

1. Cheng, David, H. S., "The Reflected Impedance of a Circular Coil in the Proximity of a Semi-Infinite Medium," IEEE Transactions on Instrumentation and Measurement, Vol. IM 14, No. 3, p. 107, September 1965.
2. Vine, J., "Impedance of a Coil Placed Near to a Conducting Sheet," Journal of Electronics and Control, Vol. 16, No. 5, p. 569 (1964).
3. Marchant, E. W., and Miller, J. L., "The Loss of Energy in Metal Plates of Finite Thickness, Due to Eddy Currents Produced by Alternating Magnetic Fields," Proceedings of the Royal Society, Vol. 111A, p. 604 (1926).
4. Shmelov, V. P., Shbarlet, Yu. M., "The Electromagnetic Field of a Turn Carrying an Alternating Current above a Conduct Plate," Soviet Physics - Technical Physics, Vol. 9, No. 1, p. 102, July 1964.
5. Pris, G. V., "Electromagnetic Field of a Horizontal Circular Loop Antenna Placed above a Conducting Half-Space," USSR, Physics of the Solid Earth Series, No. 4, p. 263 (1965).
6. Curtis, L. F., "Detectors for Buried Metallic Bodies," Proceedings of the National Electronics Conference, Vol. 2, p. 339, October 1964.
7. Clapp, C. W., "Detection of Tramp Metal," Proceedings of the National Electronics Conference, Vol. 6, p. 194 (1950).
8. Thomas, T. S. E., "Effective Impedance of a Sphere in a Magnetic Fluid," Wireless Engineering, Vol. 23, p. 322, December 1946.
9. Smythe, W. R., Static and Dynamic Electricity, McGraw-Hill Book Company, Inc., p. 397 (1950).
10. Dwornik, S. E. (Editor), Proceedings, Symposium on Detection of Underground Objects, Materials, and Properties, AD 289 531, USERDL, Fort Belvoir, Virginia, p. 27.
11. Rollin, B. V., "Nuclear Magnetic Resonance and Spin Lattice Equilibrium," Nature (London) Vol. 158, p. 669 (1946).

12. Robinson, F. N. H., "Nuclear Resonance Absorption Circuit," Journal of Scientific Instruments, Vol. 36, p. 481 (1959).
13. Watkins, B. D., Ph.D. Thesis, Harvard University (1952).
14. Donnelly, B., and Sanders, T. M., Jr., "Simple Transistor Marginal Oscillator for Magnetic Resonance," The Review of Scientific Instruments, Vol. 31, No. 9, p. 977, September 1960.
15. Schwartz, Samuel A., "Intercarrier Sound Amplifier-Limiter and Discriminator Design for Transistor TV Receiver," Fairchild Application Data, APP-73 (1963).

DOCUMENT CONTROL DATA - R&D		
<i>(Security classification of title, body of abstract and indexing annotation must be entered when the overall report is classified)</i>		
1. ORIGINATING ACTIVITY (Corporate author) Southwest Research Institute 8500 Culebra Road San Antonio, Texas 78206		2a. REPORT SECURITY CLASSIFICATION Unclassified
3. REPORT TITLE Hidden Object Detection by Magnetoabsorption and Induction Method		2b. GROUP
4. DESCRIPTIVE NOTES (Type of report and inclusive dates) Final Technical Report		
5. AUTHOR(S) (Last name, first name, initial) John P. Claassen William L. Rollwitz		
6. REPORT DATE 1 August 1966	7a. TOTAL NO. OF PAGES 110	7b. NO. OF REFS 15
8a. CONTRACT OR GRANT NO. DA-44-009-AMC-1205(T)	9a. ORIGINATOR'S REPORT NUMBER(S)	
b. PROJECT NO.	9b. OTHER REPORT NO(S) (Any other numbers that may be assigned this report)	
c.		
d.		
10. AVAILABILITY/LIMITATION NOTICES Not available without authorization of the sponsoring activity.		
11. SUPPLEMENTARY NOTES	12. SPONSORING MILITARY ACTIVITY Barrier and Intrusion Detection Branch, U.S. Army Engineer Research and Development Lab., Fort Belvoir, Virginia	
13. ABSTRACT The magnetoabsorption signal is shown to be useful for detecting magnetic voids in soils caused by buried objects which are both nonmagnetic and nonconducting. The magnetoabsorption signal from the soil is obtained through the use of a specially constructed detection head, with a radiofrequency double-D coil placed inside of a low frequency magnetizing coil, and a marginal-oscillator type of detection system. The magnetoabsorption signal is separated from the direct induction signal by using a high-pass filter. The magnetoabsorption signal decreases in magnitude by a value which varies from 10 to 40 percent for objects buried with their tops at a depth of from 2.5 inches below the soil surface to just level with the surface. The percentage variation is independent of the height of the detection head above the soil. For the detection and identification of hidden discrete objects, both the magnetoabsorption and the direct induction signals are used. The induction signal is obtained through a low-pass filter while the magnetoabsorption signal comes through a high-pass filter. The Lissajous patterns, using the magnetizing frequency as a horizontal reference, and the harmonic amplitudes for both the magnetoabsorption and the induction signals, obtained from twenty-one different objects show that discrete objects can be both detected and their material makeup identified.		

14. KEY WORDS	LINK A		LINK B		LINK C	
	ROLE	WT	ROLE	WT	ROLE	WT
Detection Induction Magnetoabsorption Mines, nonmetallic Magnetism						

**INSTRUCTIONS**

1. **ORIGINATING ACTIVITY:** Enter the name and address of the contractor, subcontractor, grantee, Department of Defense activity or other organization (*corporate author*) issuing the report.
- 2a. **REPORT SECURITY CLASSIFICATION:** Enter the overall security classification of the report. Indicate whether "Restricted Data" is included. Marking is to be in accordance with appropriate security regulations.
- 2b. **GROUP:** Automatic downgrading is specified in DoD Directive 5200.10 and Armed Forces Industrial Manual. Enter the group number. Also, when applicable, show that optional markings have been used for Group 3 and Group 4 as authorized.
3. **REPORT TITLE:** Enter the complete report title in all capital letters. Titles in all cases should be unclassified. If a meaningful title cannot be selected without classification, show title classification in all capitals in parenthesis immediately following the title.
4. **DESCRIPTIVE NOTES:** If appropriate, enter the type of report, e.g., interim, progress, summary, annual, or final. Give the inclusive dates when a specific reporting period is covered.
5. **AUTHOR(S):** Enter the name(s) of author(s) as shown on or in the report. Enter last name, first name, middle initial. If military, show rank and branch of service. The name of the principal author is an absolute minimum requirement.
6. **REPORT DATE:** Enter the date of the report as day, month, year, or month, year. If more than one date appears on the report, use date of publication.
- 7a. **TOTAL NUMBER OF PAGES:** The total page count should follow normal pagination procedures, i.e., enter the number of pages containing information.
- 7b. **NUMBER OF REFERENCES:** Enter the total number of references cited in the report.
- 8a. **CONTRACT OR GRANT NUMBER:** If appropriate, enter the applicable number of the contract or grant under which the report was written.
- 8b, 8c, & 8d. **PROJECT NUMBER:** Enter the appropriate military department identification, such as project number, sub-project number, system numbers, task number, etc.
- 9a. **ORIGINATOR'S REPORT NUMBER(S):** Enter the official report number by which the document will be identified and controlled by the originating activity. This number must be unique to this report.
- 9b. **OTHER REPORT NUMBER(S):** If the report has been assigned any other report numbers (*either by the originator or by the sponsor*), also enter this number(s).
10. **AVAILABILITY/LIMITATION NOTICES:** Enter any limitations on further dissemination of the report, other than those

imposed by security classification, using standard statements such as:

- (1) "Qualified requesters may obtain copies of this report from DDC."
- (2) "Foreign announcement and dissemination of this report by DDC is not authorized."
- (3) "U. S. Government agencies may obtain copies of this report directly from DDC. Other qualified DDC users shall request through \_\_\_\_\_."
- (4) "U. S. military agencies may obtain copies of this report directly from DDC. Other qualified users shall request through \_\_\_\_\_."
- (5) "All distribution of this report is controlled. Qualified DDC users shall request through \_\_\_\_\_."

If the report has been furnished to the Office of Technical Services, Department of Commerce, for sale to the public, indicate this fact and enter the price, if known.

11. **SUPPLEMENTARY NOTES:** Use for additional explanatory notes.
12. **SPONSORING MILITARY ACTIVITY:** Enter the name of the departmental project office or laboratory sponsoring (*paying for*) the research and development. Include address.
13. **ABSTRACT:** Enter an abstract giving a brief and factual summary of the document indicative of the report, even though it may also appear elsewhere in the body of the technical report. If additional space is required, a continuation sheet shall be attached.

It is highly desirable that the abstract of classified reports be unclassified. Each paragraph of the abstract shall end with an indication of the military security classification of the information in the paragraph, represented as (TS), (S), (C), or (U).

There is no limitation on the length of the abstract. However, the suggested length is from 150 to 225 words.

14. **KEY WORDS:** Key words are technically meaningful terms or short phrases that characterize a report and may be used as index entries for cataloging the report. Key words must be selected so that no security classification is required. Identifiers, such as equipment model designation, trade name, military project code name, geographic location, may be used as key words but will be followed by an indication of technical content. The assignment of links, rules, and weights is optional.